Reproductive Impact of Testosterone Therapy in a Transgender Mouse Model

by

Hadrian M. Kinnear

A dissertation submitted in partial fulfillment
of the requirements for the degree of
Doctor of Philosophy
(Cellular and Molecular Biology)
in the University of Michigan
2022

Doctoral Committee:

Associate Professor Ariella Shikanov, Chair
Professor Gary D. Hammer
Assistant Professor Saher Sue Hammoud
Clinical Associate Professor Molly B. Moravek
Professor Emerita Vasantha Padmanabhan

Hadrian M. Kinnear

hkinnear@umich.edu

ORCID iD: 0000-0003-3563-9296

Dedication

This dissertation is dedicated to my partner, Chelsea, and our cat, Thomas.

Acknowledgements

My deepest gratitude to the many people who supported the work of this dissertation.

Dr. Ariella Shikanov, thank you for making this dissertation possible. You believed in me and in this work and that made all the difference. I have learned so much from your example.

Dr. Molly Moravek, thank you for your vision in launching this project and your guidance throughout the journey. It has been a joy to think and write with you.

Dr. Vasantha Padmanabhan, thank you for championing this project, offering your well-earned wisdom, and always pushing for work of the highest quality.

Dr. Sue Hammoud, thank you for asking such astute questions and giving me the courage to learn new technical approaches.

Dr. Gary Hammer, thank you for helping me to see my work in a broader scientific context and for pushing me to think outside of the box.

To all of the members of the Shikanov laboratory, past and present, thank you for laughing, crying, and learning together. Your hands are all over this work. I could not have done this without you, and I will miss you all so much.

To my mentors and friends from the University of Michigan Medical School, Cellular & Molecular Biology Program, Medical Scientist Training Program, OutMD, and LGBTQ health advisory committee, thank you for believing in me at each step of this journey.

Finally, a huge thank you to my incredible family, who let me restructure all of our lives around the mice.

Table of Contents

Dedication ii

Acknowledgements iii

List of Tables ix

List of Figures x

Abstract xiii

Chapter 1 Introduction 1

1.1 Impact of T on the ovaries 3

1.2 Impact of T on the uterus 6

1.3 Impact of T on the fallopian tubes 7

1.4 Pregnancies after T therapy 7

1.5 Assisted reproductive technology outcomes after T therapy 9

1.6 Animal models for gender-affirming T therapy 11

1.7 Unanswered questions 14

1.8 Contextualizing my dissertation 15

Chapter 2 A Mouse Model to Investigate the Impact of Testosterone Therapy on Reproduction in Transgender Men 16

2.1 Abstract 16

2.1.1 Study question 16

2.1.2 Summary answer 16

2.1.3 What is known already 16

2.1.4 Study design, size, duration 17

2.1.5 Participants/materials, setting, methods 17
2.1.6 Main results and the role of chance 17
2.1.7 Limitations, reasons for caution 18
2.1.8 Wider implications of the findings 18
2.1.9 Study funding/competing interest(s) 18
2.2 Introduction 19
2.3 Materials and Methods 21
2.3.1 Ethical approval 21
2.3.2 Experimental design 21
2.3.3 Vaginal cytology 22
2.3.4 Blood collection and hormone analysis 22
2.3.5 Body weights and measures 23
2.3.6 Histological analysis 23
2.3.7 Follicle distribution analysis 24
2.3.8 Statistical analysis 24
2.4 Results 25
2.4.1 T enanthate caused persistent diestrus in postpubertal adult female mice 25
2.4.2 T enanthate induced elevated serum T levels 26
2.4.3 T Enanthate suppressed LH, minimally changed FSH, and increased AMH 27
2.4.4 T enanthate increased uterine weight and clitoral area 28
2.4.5 T enanthate minimally changed the pre-antral follicle distribution 30
2.4.6 T enanthate increased atretic cyst-like late antral follicles and prevented corpora lutea formation 30
2.5 Discussion 31
2.6 Acknowledgements 34
2.7 Authors' Roles 34

2.8 Funding 34

2.9 Conflict of Interest: 35

Chapter 3 Reversibility of Testosterone-Induced Acyclicity After Testosterone Cessation in a Transgender Mouse Model 36

3.1 Abstract 36

3.1.1 Objective 36

3.1.2 Design 36

3.1.3 Setting 36

3.1.4 Animals 36

3.1.5 Intervention(s) 37

3.1.6 Main outcome measure(s) 37

3.1.7 Result(s) 37

3.1.8 Conclusion(s) 37

3.2 Introduction 38

3.3 Materials and Methods 41

3.3.1 Ethical approval 41

3.3.2 Experimental design 41

3.3.3 Vaginal cytology 42

3.3.4 Weekly blood collection and serum hormone analysis 42

3.3.5 Body weights and measures 43

3.3.6 Histological analysis 43

3.3.7 Ovarian morphometry 43

3.3.8 Statistical analysis 44

3.4 Results 44

3.4.1 T-induced persistent diestrus promptly reverses after the T levels drop 44

3.4.2 Corpora lutea noted with comparable follicle distribution following T cessation 47

3.4.3 Body metrics comparable except for persistent T-induced clitoromegaly 49
3.4.4 Terminal hormone levels comparable following T cessation 50
3.5 Discussion 51
3.6 Conclusion 53
3.7 Authors' Roles 53
3.8 Acknowledgement 53
3.9 Funding 54
3.10 Conflict of Interest 54
Chapter 4 Ovarian Stromal Aberrations Are Present After Testosterone Cessation in a Transgender Mouse Model 55
4.1 Abstract 55
4.2 Introduction 56
4.3 Materials and Methods 59
4.3.1 Ethical approval 59
4.3.2 Experimental design 60
4.3.3 Vaginal cytology 60
4.3.4 Blood collection and hormone analysis 60
4.3.5 Ovarian histological and follicular distribution analysis 61
4.3.6 Ovarian immunohistochemical analysis & periodic acid-Schiff staining 62
4.3.7 Ovarian RNA-sequencing analysis 63
4.3.8 Statistical analysis 64
4.4 Results 65
4.4.1 Mice stop cycling during T therapy and resume cycling as T slowly washes out 65
4.4.2 Reduced corpora lutea On T and Post T with otherwise comparable follicular distributions 68
4.4.3 Stromal changes in ovaries Post T 69

4.4.4 Notable macrophage-associated staining in the ovarian stroma Post T 70
4.4.5 Immune pathway upregulation seen Post T as compared to Control PT and On T 72
4.5 Discussion 72
4.6 Acknowledgements 76
4.7 Authors' Roles 76
4.8 Financial Support 76
Chapter 5 Discussion, Reflections, and Future Directions 78
5.1 Discussion of Findings 78
5.2 Reflections on Experimental Design Choices 80
5.3 Future Directions 83
5.3.1 Emergence of trans science 83
5.3.2 Ovarian stromal physiology 84
Appendix: The Ovarian Stroma as a New Frontier 86
Bibliography 117

List of Tables

Table 1. Comparison of histological ovarian changes with masculinizing T. 5

Table 2. Pregnancies after prior T therapy. 8

Table 3. Assisted reproductive outcomes after initiation of T therapy. 10

Table 4. Comparison of reproductive changes seen in transgender men given T therapy and in our mouse model of postpubertal T therapy. 31

Table 5. General and ovary-specific components of the ovarian stroma. 89

List of Figures

Figure 1. Longitudinal hormonal and cyclic profile. (A) Control mice injected with the sesame oil vehicle progress through the estrous cycle: metestrus (M), diestrus (D), proestrus (P), estrus (E), while mice treated with testosterone (T) show persistent diestrus as determined by the presence of round leukocytes (B) (scale 100 μm). Cyclicity of two representative control mice (C) versus two T-treated mice (D) for several cycles prior to starting injections and then during 6 weeks of T or vehicle injections. (E) Percent cyclicity for mice after starting T treatment at time 0 (control n = 5, T 0.45 mg n = 5, T 0.225 mg n = 5). (F) Longitudinal T levels for mice over 6 weeks of treatment with injections twice per week (mean ± SD). 25

Figure 2. Terminal hormone levels. (A) LH, (B) FSH with open circles for mice in proestrus/estrus not included in calculations, and (C) anti-Müllerian hormone (AMH) levels for control and mice treated with T after 6 weeks of T enanthate at 0.225 and 0.45 mg twice per week (mean ± SD). 26

Figure 3. Terminal body measurements (mean ± SD). (A) Increase in body weight over 6 weeks, (B) terminal liver weight (normalized to terminal average of 22.5 g mouse), (C) terminal uterine weight (normalized to terminal average of 22.5 g mouse), and (D) terminal clitoral area. Increased clitoral size between (E) controls and (F) mice treated with T, with white arrowhead pointing to clitoral structure. 27

Figure 4. Follicle counts for every 10th section for primordial (A), primary (B), secondary (C), total antral (D), atretic cyst-like late antral (E) follicles as well as corpora lutea (F). 29

Figure 5. Perturbed histology in mice treated with T. Hematoxylin and eosin-stained control ovaries with corpora lutea (Row 1) and T-treated ovaries at 0.225 mg (Row 2) and 0.45 mg (Row 3) after 6 weeks of treatment (Columns 1 and 2, x5, scale 500 μm). Antral follicles with oocytes surrounded by several layers of cumulus granulosa cells from control (Row 1) and T-treated mice at 0.225 mg (Row 2) and 0.45 mg (Row 3) doses (Column 3, x20, scale 100 μm). Atretic cyst-like late antral follicles from control (Row 1) and T-treated mice at 0.225 mg (Row 2) and 0.45 mg (Row 3) (Column 4, x20, scale 100 μm). 29

Figure 6. Reversibility of T-induced estrous cycle changes after T cessation. (A) Mice were subcutaneously implanted with a placebo (control) or T enanthate pellet at week 0, which was then removed after 6 weeks. Longitudinal weekly T levels were measured before pellet implantation (week 0), during T therapy (weeks 1–6) and following pellet removal (weeks 7–9) (mean ± SD, error bars shorter than symbol not shown, arrow points to subcutaneously implanted pellet). (B) All mice treated with T pellets at week 0 stopped cycling and demonstrated persistent diestrus until pellet removal at week 6, at which point estrous cyclicity resumed. (C) Two

representative mice implanted with T pellets showed persistent diestrus during T therapy and prompt resumption of cyclicity following pellet removal, while two representative control mice continued cycling throughout the study (E = estrus, M = metestrus, D = diestrus, P = proestrus). The green-shaded rectangle indicates the 6-week T therapy, while the purple-shaded rectangle highlights 3 weeks following T cessation. 47

Figure 7. Comparable ovarian histology. Corpora lutea were noted in the ovaries of control mice (row 1) and post T mice (row 2) (columns 1 and 2; magnification, x5; hematoxylin and eosin stain; scale, 500 μm). Post T mice were sacrificed after T cessation and four estrous cycles. Examples of higher magnification of antral follicles (columns 3 and 4; magnification, x20; scale, 100 μm) and corpora lutea (column 5; magnification, x20; scale, 100 μm) in the ovaries of control mice (row 1) and post T mice (row 2). 47

Figure 8. Comparable follicle counts in every 10th section between placebo (control) and T-treated mice sacrificed four cycles after T cessation (post T) for (A) primordial, (B) primary, (C) secondary, (D) total antral, and (E) atretic late antral follicles in addition to (F) corpora lutea... 48

Figure 9. Terminal body measurements comparable except for persistent clitoromegaly. (A) Body weight increase over approximately 9 weeks, (B) terminal liver weight (normalized to terminal average of 22.9 g mouse), and (C) terminal uterine weight (normalized to terminal average of 22.9 g mouse) (mean ± SD). Increased clitoral area measured at 6 weeks on T remains persistently elevated four estrous cycles following T cessation (D) (mean ± SD). Clitoral size remains enlarged in mice post T (F) compared with that in control mice (E); white arrowheads indicate clitoral structure, while asterisks indicate glands enlarged by T therapy that are not readily visible in the control. 49

Figure 10. Comparable terminal hormone levels. Terminal (A) LH, (B) FSH, (C) progesterone, and (D) estradiol levels for placebo (control) and T-treated mice four cycles after T cessation (post T) (mean ± SD). 50

Figure 11. Experimental design, cyclicity, and T levels. (Top) Experimental design of the 4 study groups: mice sacrificed at 6 weeks on T (On T), parallel age-matched controls for On T (Control OT), mice sacrificed after T cessation and 4 estrous cycles after resumption of cyclicity (Post T), and parallel age-matched controls for Post T (Control PT). (Middle) All T-treated mice stopped cycling within 1 week of starting T and it took 3.5–10 weeks after T cessation at 6 weeks for mice to resume cycling. (Bottom) T levels (ng/mL, mean ± SD) were elevated during T therapy (at 6 weeks on T, $P<0.0001$), were slow to washout with mean T levels still elevated 7 weeks into the washout period (at week 13, $P<0.01$), and were not detectably different from controls when mice were sacrificed 4 estrous cycles after resumption of cyclicity. 65

Figure 12. Reduced corpora lutea on T and post T with otherwise comparable follicular distributions. Images of hematoxylin and eosin-stained ovaries from all four groups (Control OT, On T, Post T, and Control PT). Row 1 includes a representative hematoxylin and eosin-stained ovary (5X, scale 500 μm) from each group, while row 2 highlights example corpora lutea (20X, solid outline corresponding to location in 5X image, scale 100 μm), and row 3 highlights example antral follicles (20X, dashed outline corresponding to location in 5X image, scale 100 μm). Follicle counts from every 10th section for primordial (A), primary (B), and secondary (C)

follicles. Follicle counts based on 5X images of every 10th section for total antral (D) and atretic late antral (E) follicles as well as corpora lutea (F). 67

Figure 13. Ovarian stromal changes post T. Columns correspond to the four groups: Control OT, On T, Post T, and Control PT. Row 1 includes a representative hematoxylin and eosin-stained ovary (5X, scale 500 µm) from each group, with the corresponding magnified view of the ovarian stroma in row 2 (40X, scale 50 µm). Row 3 includes a representative periodic acid-Schiff-stained ovary (5X, scale 500 µm) from each group, with the corresponding magnified view of the ovarian stroma in row 4 (40X, scale 50 µm). 69

Figure 14. Notable macrophage-associated staining in the ovarian stroma post T. Columns correspond to the four groups: Control OT, On T, Post T, and Control PT. Row 1 includes representative ovarian CD68 staining (5X, scale 500 µm) from each group, with the corresponding magnified view of the ovarian stroma in row 2 (40X, scale 50 µm). Row 3 includes representative ovarian CD11b staining (5X, scale 500 µm) from each group, with the corresponding magnified view of the ovarian stroma in row 4 (40X, scale 50 µm). 70

Figure 15. Immune pathway upregulation seen post T as compared to control PT and on T. Heatmap of the top 500 variably expressed genes from whole ovary RNA-sequencing (n = 4 mice per group, 1 ovary each). The top 10 gene ontology biological process terms from LRpath for genes enriched in the following 4 comparisons: On T vs Control OT, Post T vs Control PT, Post T vs On T, and Control PT vs Control OT. In Control PT vs Control OT, the two titles too long to fully display as shown by […] are: “adaptive immune response based on somatic recombination of immune receptors built from immunoglobulin superfamily domains” and “immune response-regulating cell surface receptor signaling pathway.”..... 71

Figure 16. Components of the ovarian stroma. Central diagram of a human ovary (adapted from Gray, 1918) surrounded by boxes highlighting different ovarian stromal components including (clockwise from top center): immune cells including macrophages, dendritic cells, neutrophils, eosinophils, mast cells, B & T cells, and Natural Killer (NK) cells; incompletely characterized stromal cells (including fibroblast-like, spindle-shaped, and interstitial cells); stem cells; extracellular matrix (ECM) components; surface epithelium and tunica albuginea; rete ovarii and hilar cells; and blood vessels, lymphatic vessels, and nerves. Made using ©BioRender - biorender.com. 88

Figure 17. Ovarian stroma key areas for further research. Includes (clockwise from left): theca cell origins, hormone signaling, pathology, artificial ovary, and cell-type identification. Made using ©BioRender - biorender.com. 103

Abstract

Long-term gender-affirming testosterone (T) therapy may negatively impact reproductive capacity for transgender men transitioning from female to male. Given clinical guidelines assuming fertility loss and anecdotal evidence to the contrary, clinicians have minimal data with which to counsel transmasculine individuals interested in harvesting oocytes or carrying a pregnancy after starting T therapy. The impact of T on reproductive potential, the reversibility of this impact, and the ovarian dynamics of taking and pausing T have not been well established. The objective of my dissertation was to establish a mouse model of postpubertal gender-affirming T therapy and to utilize this model to evaluate the reversibility of T-induced changes if T is paused for reproductive purposes.

In order to establish our model, we treated postpubertal female mice with 6 weeks of T injections. The T-treated mice demonstrated acyclicity, elevated T, a reduction in serum luteinizing hormone levels, and ovarian perturbations including a lack of corpora lutea and an increased number of atretic late antral follicles. These findings are similar to changes seen with transmasculine individuals on T and support the use of mouse models of gender-affirming T therapy for reproductive inquiry.

We then investigated the reversibility of T-induced persistent diestrus in a model that allows for well-defined T cessation timing. We found that after 6 weeks of T therapy using subcutaneously implanted commercial pellets, mice promptly resumed cycling within a week of pellet removal, closely correlated with T levels returning to control levels. Four cycles after T cessation, ovarian histological analyses from T-treated mice were comparable to controls,

including the formation of corpora lutea, in support of the return of regular cyclic ovulatory function following T cessation.

Intriguingly, we found that a longer exposure to elevated T after a prolonged washout following 6 weeks of T injections resulted in an aberrant ovarian stromal phenotype and reduced number of corpora lutea four estrous cycles after T cessation. Immunohistochemical staining for macrophage-associated markers CD68 and CD11b suggests changes in ovarian stromal macrophages after resumption of cyclicity following the washout of T. Ovarian transcriptomic comparisons also support this upregulation of immune response pathways in mice after T cessation as compared to age-matched controls and mice at 6 weeks on T. Limitations of the study design prevent us from attributing these differences to the additional duration of T therapy during the washout or to changes that might be arising during the resumption of cyclicity. We postulate that this stromal macrophage response may be a temporally limited state, as related studies have described histologically similar findings, which they reported to resolve after a period of time or with superovulation.

Collectively, this dissertation characterizes a mouse model on T and interrogates changes that occur if T is paused for reproductive purposes, laying the groundwork for further functional assessments to provide insights into reproductive options after prolonged T therapy.

Chapter 1 Introduction

Similar content previously published in review article (Moravek *et al.*, 2020):

Moravek MB, **Kinnear HM**, George J, Batchelor J, Shikanov A, Padmanabhan V, Randolph JF. Impact of Exogenous Testosterone on Reproduction in Transgender Men. *Endocrinology.* 2020;161(3):1-13. doi:10.1210/endocr/bqaa014.

The gender identity of transgender and nonbinary individuals is typically not aligned with their sex assigned at birth. The size of these populations may be underestimated due to limitations in data collection, underreporting, and stigma. Estimates suggest populations in the United States of 1.4 million transgender adults, 1.2 million nonbinary adults (42% of whom identified as transgender), and 150,000 transgender adolescents (Flores *et al.*, 2016; Herman *et al.*, 2017; Wilson and Meyer, 2021).

Many transgender people pursue gender-affirming hormone therapy and/or surgeries to develop physical characteristics of their affirmed gender. In general, transgender men or transmasculine individuals were assigned female at birth and identify as men or as male. Testosterone (T) therapy is typically prescribed for postpubertal transmasculine gender-affirming hormone therapy. T is administered via intramuscular or subcutaneous injections or via a transdermal gel or patch and is continued indefinitely. Clinicians monitor T levels to ensure they are within the normal range for cisgender (non-transgender) men (Hembree *et al.*, 2017). Masculinizing effects of T often include voice deepening, cessation of menses, clitoral

enlargement, body fat redistribution, and growth of body hair (Coleman *et al.*, 2011).

Transgender men are prescribed T without a concrete understanding of the impact of this long-term therapy on their reproductive health. National and international medical organizations recommend counseling about fertility preservation prior to starting T therapy (Coleman *et al.*, 2011; Ethics Committee of the American Society for Reproductive Medicine, 2015; Hembree *et al.*, 2017). These recommendations reflect an assumption of T-induced fertility loss based on conflicting and limited data. Transmasculine fertility preservation can be challenging, as oocyte or embryo cryopreservation is expensive, invasive, and time-consuming. Due to these hurdles, many transgender men do not undergo fertility preservation prior to starting T, but later may be interested in using their gametes for reproduction or being a gestational parent (Auer *et al.*, 2018; Baram *et al.*, 2019). Although there is limited data on fertility following T therapy, there has been a recent increase in research attention in this area. Encouragingly, studies suggest that reproductive potential may remain after T therapy for at least some individuals (Light *et al.*, 2014, 2018; Adeleye *et al.*, 2019; Leung *et al.*, 2019; Yaish *et al.*, 2021). Hopefully additional research will lead to future clinical guidelines that offer more nuanced perspectives regarding reproductive options after prolonged T therapy.

In this introduction, I review what is currently known regarding the impact of masculinizing T therapy on the reproductive tract (ovaries, uterus, fallopian tubes) and describe emerging data regarding pregnancy and assisted reproductive technologies (ART). I then discuss relevant animal models, highlight key questions, and contextualize the work of this dissertation.

1.1 Impact of T on the ovaries

Although ovaries from individuals treated with masculinizing T therapy appear to share multiple characteristics with polycystic ovary morphology, these similarities do not necessarily imply broad associations between T therapy and the multifactorial and complex polycystic ovary syndrome (PCOS). Multiple studies have noted increased tunica albuginea or outer cortex collagenization, stromal hyperplasia, and stromal luteinization in T-treated ovaries (Table 1). These characteristics are also frequently observed in PCOS (Hughesdon, 1982). Ovarian follicular changes with T therapy have also been observed, although studies differ with regards to their definitions and terminology. Studies of T-treated ovaries from transgender men have reported multifollicular ovaries, multiple cystic follicles, antral follicle counts of greater than 12 follicles in an ovary, or similar follicle counts with increased atretic follicles (Table 1). Variable terminology and classifications have led to apparent conflict, with some studies saying T leads to polycystic ovary morphology (Futterweit and Deligdisch, 1986; Spinder *et al.*, 1989; Pache *et al.*, 1991; Grynberg *et al.*, 2010) and others disagreeing (Ikeda *et al.*, 2013; Caanen *et al.*, 2017). Most studies of ovarian histopathology with T therapy report some differences as compared to ovaries without T therapy, although it is difficult to ascertain if these characteristics have functional impacts beyond their roles as likely biomarkers of increased ovarian T exposure.

Limited studies report follicular reserve after T therapy as evaluated by antimüllerian hormone (AMH) levels. In a prospective study of transgender patients starting T, a significant decrease in AMH of 0.71 ng/mL from baseline (median 4.99 ng/mL) was noted after 12 months on T. However, this decrease was accounted for by the 27 transgender patients with prior PCOS and not seen for the 27 without prior PCOS (Yaish *et al.*, 2021). In two studies in which

participants were on medications in addition to T that may alter their AMH levels, one found no differences in AMH from baseline (with a progestin, Tack *et al.*, 2016) while another found that AMH decreased (with an aromatase inhibitor and a gonadotropin-releasing hormone agonist, Caanen *et al.*, 2015). Promisingly, primordial follicles have been found in ovarian cortical histology for trans men on T and oocytes collected during oophorectomies have developed normal metaphase II spindles when matured in vitro (De Roo *et al.*, 2017; Lierman *et al.*, 2017).

Most but not all individuals taking masculinizing T therapy experience menstrual suppression. The observation of the occasional corpora lutea or corpora albicantia in ovaries during T therapy suggests that some individuals may still occasionally ovulate (Futterweit and Deligdisch, 1986; Miller *et al.*, 1986; Spinder *et al.*, 1989; Ikeda *et al.*, 2013; Loverro *et al.*, 2016; Khalifa *et al.*, 2019; Lin *et al.*, 2021). A 12-week study with 22 transmasculine individuals on T utilized 3 days of elevated urinary pregnanediol-3-glucoronide as a proxy for ovulation. They found one individual with well-defined ovulation and 7 individuals with transient rises suggestive of dysfunctional ovulatory cycles. Most of these were observed in the month after T initiation, but 2 transient rises were noted after 7+ and 13+ months of T therapy (Taub *et al.*, 2020). This pattern of menstrual suppression with occasional breakthrough events is further supported by reports of pregnancies conceived while individuals were amenorrheic from T (Light *et al.*, 2014) and highlights that T is not considered sufficient contraception.

Data gathered from these observational studies has been limited by variations in T administration regimens and serum levels achieved as well as a wide range of T exposure durations. Although rarely documented in the literature, it is also worth considering that some

surgeons may have had their patients stop T for a short period of time before surgeries and histopathological comparisons may not account for these pauses (Chadha *et al.*, 1994). Further confounders include high rates of PCOS observed in transmasculine individuals prior to starting T therapy (Baba *et al.*, 2007; Mueller *et al.*, 2008; Becerra-Fernández *et al.*, 2014). Questions remain regarding the reversibility and functional implications of T-induced ovarian changes.

Table 1. Comparison of histological ovarian changes with masculinizing T.

Author, Year	**Polycystic Ovary Morphology (PCOM)?**	**Follicular Phenotype**	**Tunica Albuginea or Outer Cortex Collagenization**	**Stromal Hyperplasia**	**Stromal Luteinization**	**CL or CA**
Amirikia *et al.*, 1986		Thickened basal membrane atretic follicles	✓			No recent
Futterweit *et al.*, 1986	PCOM (13/19)	Multiple cystic follicles (17/19)	✓ (13/19)	✓ (16/19)	(5/19)	CL (3/19) CA (5/19)
Miller *et al.*, 1986		Follicular cysts (32/32)				CL (4/32) CA (32/32)
Spinder *et al.*, 1989	PCOM (18/26)	Multiple Cystic Follicles (18/26)	✓ (25/26)	✓ (21/26)	(7/26)	CL (4/26) CA (26/26)
Pache *et al.*, 1991	PCOM	2x Cystic Follicles, 3.5x atretic follicles	✓ (16/17)	✓ (17/17)	✓ (12/17)	
Chadha *et al.*, 1994		Increased cystic/atretic follicles	✓	✓	✓	
Grynberg *et al.*, 2010	PCOM (89/112)	>12 antral follicles/ovary (89/112)		✓ (112/112)		
Ikeda *et al.*, 2013	No PCOM	Similar preantral/antral follicles, more atretic transmen	✓ (10/11)	✓ (8/11)	✓ (10/11)	CL (0/11) CA (3/11)
Loverro *et al.*, 2016		Multifollicular (10/12)				CL (2/10)
Khalifa *et al.*, 2018		Bilateral cystic follicles (23/23)				CL (1/23)
Lin *et al.*, 2021		Multiple bilateral cystic follicles (20/35)		(5/35)		CL (5/35)

1.2 Impact of T on the uterus

Conflicting uterine findings have been reported with T therapy. Differences between and within studies suggest that uterine findings between individuals may vary. One study of 112 individuals reported roughly half proliferative endometria (54/112) and half atrophic endometria (50/112) (Grynberg *et al.*, 2010). Another found a similar mix of active (proliferative 33/81, secretory 3/81) and atrophic/inactive (41/81) endometria (Hawkins *et al.*, 2021). Others found a majority of active endometria (proliferative in 61/94 and secretory in 4/94), although about a quarter had atrophic endometria (23/94) (Grimstad *et al.*, 2019). Similarly, another study reported active or secretory endometria in all 12 individuals studied (Loverro *et al.*, 2016). In contrast, a study of 27 individuals found all inactive endometria (Perrone *et al.*, 2009), and a study of 40 individuals had a majority of inactive endometria (30/40) and a quarter with active endometria (7/40 proliferative, 3/40 secretory) (Lin *et al.*, 2021). Other notable uterine findings included cervical atrophy (Miller *et al.*, 1986), endometrial stromal fibrosis and tubal metaplasia (Lin *et al.*, 2021), and reduced proliferation marker expression (Perrone *et al.*, 2009). Similar to ovarian studies, uterine comparisons are also limited by T regimen, durational variability, and possible brief hormonal pauses before surgery. Persistent bleeding on T has been noted for a small fraction of individuals (12/52) as well as intermittent pelvic pain or cramping on T (30/52) (Grimstad *et al.*, 2019). Encouragingly, studies where individuals have paused T for reproductive purposes suggest that all or most individuals resumed menses with T cessation, although the time course for this resumption has not been well characterized (Light *et al.*, 2014; Armuand *et al.*, 2017; Broughton and Omurtag, 2017; Adeleye *et al.*, 2019; Leung *et al.*, 2019).

1.3 Impact of T on the fallopian tubes

Studies on fallopian tube changes with T therapy are very limited. Androgen receptor expression has been observed in human tubal epithelium, suggesting T can act directly on this tissue (Dulohery *et al.*, 2020). A study of 9 trans men found that tubal ampulla had viscous luminal secretions and cellular debris with an increase in ciliated cells, in comparison to 19 cycling controls patients with open ampullary lumen during the proliferative phase and watery secretions around ovulation turning more viscous during the secretory phase. Individuals treated with T (7 out of 9) showed partial to complete closure of the lumen of the isthmus, while control patients had an isthmus that was generally clear and open (Dulohery *et al.*, 2020). The authors suggest that tubal flushing could potentially be a therapeutic measure following T therapy for individuals aiming to conceive (Dulohery *et al.*, 2020). An earlier scanning electron microscope study of 3 individuals on T noted a qualitative reduction in ciliated cells in the distal fimbriae and ampulla, with similar cilia in the isthmic and intramural tube regions (Patek *et al.*, 1973). Short-term in vitro exposure of human fallopian tube epithelium to T therapy resulted in reduced cilia beating and reduced transcript levels for key cilia regulators (Jackson-Bey *et al.*, 2020). The reversibility of T-induced changes in fallopian tubes has also not been investigated. T-induced fallopian tube changes will be more relevant to individuals pausing T to try to conceive with minimal intervention and less relevant to those harvesting oocytes using assisted reproduction.

1.4 Pregnancies after T therapy

Multiple pregnancies have been reported in the literature in which the transmasculine individual was the gestational parent or the oocyte donor after prolonged T therapy (Table 2). Typically, these are case reports or smaller studies and do not discuss individuals who were

attempting pregnancy and may have been unsuccessful. Of note, T is contraindicated in pregnancy (Coleman *et al.*, 2011) and it is recommended for T to be paused prior to conception. While studies to date are encouraging, additional data from larger studies are needed to investigate pregnancy outcomes after multiple durations of T therapy and to study to offspring from T-exposed oocytes.

Table 2. Pregnancies after prior T therapy.

Author, Year	**# of Pregnancies after T Therapy**	**Additional Notes**
Ellis *et al.*, 2014	6	Qualitative study, screened for a successful birth. Of 8 male-identified or gender-variant gestational parents, 6 had used T, and 4 had experienced at least 1 miscarriage.
Light *et al.*, 2014	25	Survey of transgender men with successful birth. Of those who with prior T, 21/25 used their own oocytes.
Broughton & Omurtag, 2017	1 (partner carried)	Case report, 1 transgender man with IVF post T, ongoing pregnancy (partner).
Light *et al.*, 2018	11	Survey on family planning and contraception. Includes multiple pregnancies / individual & 5 abortions.
Adeleye *et al.*, 2019	3 (2 partner carried)	Retrospective chart review, includes 7 transgender men post T, 1 spontaneous abortion in transgender man, 1 ongoing pregnancy (partner).
Hahn *et al.*, 2019	1	Case report, only a few months of T pre-pregnancy.
Leung *et al.*, 2019	11 (8 partner carried)	Retrospective cohort study, prior T use in 6/7 who chose IVF with transfer. Numbers include multiple pregnancies / individual, 1 pregnancy that did not lead to live birth, 1 twin pregnancy, 2 ongoing pregnancies, and 1 individual without prior T.
Stroumsa *et al.*, 2019	1	Case report, 1 transgender man, presented to emergency room not aware of pregnancy and in labor leading to stillbirth.
Amir *et al.*, 2020	1 (surrogate carried)	Retrospective cohort study, includes 6 transgender men with prior T, 1 ongoing pregnancy (surrogate).
de Sousa Resende *et al.*, 2020	1 (partner carried)	Case report, 1 transgender man, ongoing pregnancy (partner).
Falck *et al.*, 2021	8	Qualitative study, transmasculine individuals who had given birth.
Greenwald *et al.*, 2021	1 (partner carried)	Case report, 1 transgender man, IVF on T, partner carried.
Moseson *et al.*, 2021	15	Survey of pregnancy intentions and outcomes in transgender, nonbinary, and gender-expansive people, 15 pregnancies in 12 individuals after starting T. Of these, 4 pregnancies occurred while on T (2 ended in miscarriage, 1 abortion, and 1 unknown).
Yaish *et al.*, 2021	7 (1 surrogate carried)	Prospective and cross-sectional study of ovarian reserve with T. Includes 3 transgender men with prior T that carried 6 children (one carried 4), and 1 who used a surrogate.

1.5 Assisted reproductive technology outcomes after T therapy

Over the last few years, there has been a notable increase in publications discussing assisted reproductive technology (ART) outcomes for transgender men (Table 3). Similar ART outcomes have been demonstrated in transgender men with prior T therapy as compared to transgender men without prior T therapy and cisgender women (Adeleye *et al.*, 2019; Leung *et al.*, 2019; Amir *et al.*, 2020). These 3 comparison studies in combination with multiple case reports (Broughton and Omurtag, 2017; de Sousa Resende *et al.*, 2020; Insogna *et al.*, 2020) collectively support the use of ART after pausing T therapy. Recent case reports also demonstrate successful oocyte collection after a minimal T washout period (Cho *et al.*, 2020) as well as successful oocyte collection, fertilization, and live birth without pausing T (Greenwald *et al.*, 2021). A paradigm that does not require T cessation could remove a major hurdle to use of these assisted reproductive technologies. To support patient well-being, clinicians may also include aromatase inhibitors in parallel with gonadotropin stimulation to reduce elevations of estradiol and utilize transabdominal ultrasounds when possible (Moravek *et al.*, 2020). Ovarian tissue cryopreservation at the time of a gender-affirming oophorectomy may also be a practical option for transgender men that would remove the need for ovarian stimulation. A recent study has also investigated the approach of ovarian tissue oocyte in vitro maturation (IVM) for patients on T and found it to have low efficiency (Lierman *et al.*, 2021). More comparative studies are needed, particularly addressing the use or avoidance of prolonged T cessation prior to oocyte collection.

Table 3. Assisted reproductive outcomes after initiation of T therapy.

Author, Year	# Patients with prior T Therapy	T Washout Duration	Outcomes	Key Takeaways
Broughton & Omurtag, 2017	1	3 months	16 oocytes retrieved, 13 mature, 7 mature oocytes fertilized with ICSI. Two blastocysts transferred to partner, ongoing pregnancy. One additional blastocyst cryopreserved (others lower quality).	Highlights potential for IVF after prior T. Discusses somewhat arbitrary 3-month washout.
Adeleye *et al.*, 2019	7	Approximately 6 months	Lower peak estradiol and lower number of oocytes retrieved in transgender men with T as compared to transgender men without T and cisgender controls. Differences go away when 2 outliers with low antral follicle count < 5 were removed. No differences in oocyte maturity rates. 3 pregnancies after prior T (2 with partners carrying, one ongoing, one spontaneous abortion in transgender man).	Similar outcomes after prior T as compared to control groups (with 2 outliers removed).
Leung *et al.*, 2019	16	1–12 months	No statistically significant differences between transgender patients with prior T and matched 130 cisgender controls (in age, AMH, oocytes retrieved, oocyte maturity, peak estradiol). 6 couples with prior T achieved live birth.	Similar outcomes after prior T as compared to control groups.
Amir *et al.*, 2020	6	5–21 months	No differences in oocytes retrieved, MII oocytes, oocyte maturity rates, or peak estradiol between transgender men with prior T as compared to transgender men without prior T and fertile cisgender women. Embryo cryopreservation for 5 of 6 with prior T yielded good-quality embryos, and one ongoing surrogate pregnancy.	Similar outcomes after prior T as compared to control groups including fertile cisgender women.
Cho *et al.*, 2020	1	7 days	13 oocytes retrieved, 11 mature were vitrified.	Demonstrates feasibility of short duration of T cessation prior to oocyte cryopreservation.
Insogna *et al.*, 2020	1	3 months (for round 1)	Round 1: 11 oocytes retrieved, 10 cryopreserved (6 MII, 4 GV). Round 2: 14 oocytes retrieved, 13 cryopreserved (6 MII, 1 M1, 6 GV)	Highlights potential for oocyte cryopreservation after prior T therapy.
de Sousa Resende *et al.*, 2021	1	Possibly until return of menses	16 oocytes retrieved, 12 mature oocytes. ICSI (8 2PN, one 1PN, 3 non fertilized). One blastocyst transferred to partner, ongoing pregnancy. 5 embryos cryopreserved.	Highlights potential for IVF after prior T therapy.
Greenwald *et al.*, 2021	1	No washout: continuous T	20 oocytes retrieved, 16 mature, 13 fertilized with ICSI. 5 blastocysts, only one chromosomally normally, transferred to partner, leading to developmentally normal 2-year-old.	Report of live birth with continuous use of T. Indications for further study given high aneuploidy rate.
Lierman *et al.*, 2021	83	No washout: ovarian tissue oocyte IVM on T	Mean of 23±15.8 COCs per participant were collected. In vitro maturation rate 23.8%, vitrification rate 21.5%, survival after warming 72.6%. ICSI in 139 oocytes, 34.5% fertilization, 52.1% reached day 3. One blastocyst on day 5. Aberrant cleavage in 45.8% and early embryo arrest in 91.7%. Normal genetic pattern in 42%.	Low efficiency ovarian tissue oocyte IVM for patients on T.

1.6 Animal models for gender-affirming T therapy

Animal models with a specific focus on masculinizing T therapy are relatively new. In this section I will describe findings from several recent mouse studies aimed at understanding the influence of masculinizing T on reproduction. I will also discuss relevant findings from PCOS animal model research and some of the limitations of the organizational/activational dichotomy.

The first mouse model aimed at understanding gender-affirming T therapy used ovariectomized mice to study atherosclerosis and bone health and so analyses of reproductive changes could not be performed (Goetz *et al.*, 2017, 2018). To allow for reproductive analyses, we published a mouse model of masculinizing T therapy using mice with intact reproductive axes (Chapter 2, Kinnear *et al.*, 2019). Adult female C57BL/6N mice treated with T enanthate injections twice weekly for 6 weeks stopped having estrous cycles, showed clitoromegaly, no evidence of corpus lutea formation, and an increase in atretic cyst-like late antral follicles as compared to controls. Encouragingly, there were no detectable differences in the number of primordial, primary, secondary, or total antral follicles between control mice and those treated with T for 6 weeks (Chapter 2, Kinnear *et al.*, 2019). This suggests that T therapy may not have a major impact on the ovarian reserve. Recently, another group built on this work and used in vitro fertilization to compare CF-1 mice injected with T cypionate once weekly for 6 weeks (Bartels *et al.*, 2020). They noted similar acyclicity and clitoromegaly and found a reduction in corpora lutea with similar numbers of antral and atretic follicles between T-treated mice and controls (Bartels *et al.*, 2020). Encouragingly, they performed ovarian stimulation and found similar numbers of ovulated oocytes fertilizable to the two-cell stage in mice both on T and after a period of T cessation as compared to controls (Bartels *et al.*, 2020). This supports the emerging

practice of performing oocyte harvesting without having individuals pause their T (Moravek *et al.*, 2020). For those interested in pausing T to carry a pregnancy, we have also characterized the reversibility of T-induced acyclicity after 6 weeks of treatment with a T enanthate pellet, demonstrating a prompt return of cyclic ovulatory function with corpora lutea formation after well-defined T cessation (Chapter 3, Kinnear *et al.*, 2021). Future animal model work will need to address longer durations of T therapy and multiple fertility metrics.

Animal models have also been helpful in elucidating neuroendocrine mechanisms for androgen-induced cycle suppression. A 2020 study with ovariectomized young adult female mice treated for two weeks with implants of the non-aromatizable androgen, dihydrotestosterone (DHT) found reduced LH pulsatility in DHT-treated mice as compared to controls with decreased frequency, amplitude, peak, basal, and mean LH levels (Esparza *et al.*, 2020). They also found suppression of *Kiss1* and *Tac2* gene expression in the arcuate nucleus of the hypothalamus for DHT-treated mice (Esparza *et al.*, 2020). As gonadotropin-releasing hormone neurons do not express the androgen receptor, the negative feedback from androgens may be due to downregulation of these upstream positive regulators, kisspeptin and neurokinin-B. In addition to the hypothalamus, they also reported reduced LH secretion with gonadotropin-releasing hormone (GnRH) pulse treatment in DHT-treated in vitro pituitaries (Esparza *et al.*, 2020). Ultimately, these results suggest that androgens can provide negative feedback to female gonadotropin release at both the hypothalamic and pituitary levels.

Historically, animal model research aimed at understanding the consequences of androgens on reproduction has focused on PCOS. For many PCOS animal models, hormone

doses are lower than would typically be used for masculinizing T therapy and hormones are administered in the prenatal or prepubertal periods. In contrast, the majority of individuals taking masculinizing T therapy are postpubertal. Long-term research understanding the influence of sex steroids, such as T, on adults is fairly rare. Sex steroid changes have been historically understood by an organizational/activational paradigm. In this paradigm, organizational (permanent) changes can occur during development (prenatal, prepubertal periods) and only activational (transient) changes occur in adults. An over-reliance on the strict dichotomy of the organizational/activational framework has likely limited study of sex steroid changes on adults (Arnold and Breedlove, 1985). PCOS animal model studies have been extensively reviewed, with species including mice, rats, sheep and monkeys and PCOS-inducing treatments including androgens (DHT, dehydroepiandrosterone, T), estrogen, aromatase inhibitors, antiprogestins, constant light exposure, as well as transgenic models (Abbott *et al.*, 2005; Shi and Vine, 2012; Walters *et al.*, 2012; Padmanabhan and Veiga-Lopez, 2013; van Houten and Visser, 2014). Researchers have also focused on the complex roles of androgens in normal and pathological ovarian function, particularly regarding lessons learned from androgen receptor knockout models (Walters, 2015; Walters *et al.*, 2019). Of these studies, there are a few focused on PCOS that have used relevant postpubertal androgen administration.

In a relevant postpubertal model, reduced fertility and acyclicity were seen in DHT-treated mice as compared to controls, but reversibility following DHT cessation was not examined (Ma *et al.*, 2017). Another mouse study found reversibility 30 days post cessation of DHT-induced stromal changes and lack of corporal lutea, although DHT treatment began in the peripubertal period (Sun *et al.*, 2019). Notably, DHT differs from T in that it is not aromatizable

to estradiol and is not used clinically for masculinization. A recent study comparing 12 weeks of DHT and T treatments in peripubertal mice found similar PCOS-like reproductive changes in both, but markedly more metabolic changes in DHT-treated wild-type mice as compared to those treated with T (Aflatounian *et al.*, 2020). Notably, when they then compared androgen receptor knockout mice, T induced some reproductive changes while DHT did not, suggesting that both androgenic and estrogenic pathways likely mediate T-induced reproductive alterations (Aflatounian *et al.*, 2020). Despite key differences in PCOS and transmasculine T-therapy, there is meaningful research overlap due to methodological similarities in their respective animal models.

1.7 Unanswered questions

Despite increasing research attention, even since I began my Ph.D. in 2017, multiple unanswered questions remain with regards to transmasculine reproduction. Studies present contrasting findings regarding the impact of T on the reproductive tract, including the ovaries, uterus, and fallopian tubes. The functional impact of any T-induced changes and their reversibility if T is paused for reproductive purposes has not been well established. Although studies suggest the possibility of fertility for at least some after T therapy, whether this is a something individuals can expect remains to be determined. Additionally, for those choosing ovarian stimulation with oocyte collection, questions remain regarding the option of remaining on T during this process and/or the optimal duration for pausing T prior to stimulation. As more answers emerge from ongoing research efforts, clinical guidelines will hopefully provide more nuance regarding reproductive options after prolonged T therapy.

1.8 Contextualizing my dissertation

In chapter 2, I demonstrate the feasibility of utilizing a postpubertal mouse model of T therapy as a means to study transmasculine reproduction. In chapter 3, I characterize the timeline for reversibility of T-induced acyclicity if T is paused for reproductive purposes, supporting a restoration of cyclic ovulatory function. In chapter 4, I explore aberrations in the ovarian stroma after T therapy and washout. Collectively, this dissertation characterizes a mouse model on T and interrogates changes that occur if T is paused for reproductive purposes, helping to set the stage for the use of T-treated mice for future functional reproductive assessments.

Chapter 2 A Mouse Model to Investigate the Impact of Testosterone Therapy on Reproduction in Transgender Men

Chapter previously published (Kinnear *et al.*, 2019) with permission to use in dissertation (license numbers: 5082650269144 all text, 5082650404632 figures 1-5, table):

Kinnear HM, Constance ES, David A, Marsh EE, Padmanabhan V, Shikanov A, Moravek MB. A mouse model to investigate the impact of testosterone therapy on reproduction in transgender men. *Human Reproduction.* 2019;34(10):2009–2017. doi:10.1093/humrep/dez177.

2.1 Abstract

2.1.1 Study question

Can mice serve as a translational model to investigate the reproductive effects of testosterone (T) therapy commonly used by transgender men?

2.1.2 Summary answer

T enanthate subcutaneous injections at 0.45 mg twice weekly can be used in the postpubertal C57BL/6N female mouse to investigate the reproductive effects of T therapy given to transgender men.

2.1.3 What is known already

Most models of T treatment in female mice involve prenatal or prepubertal administration, which are not applicable to transgender men who often begin T therapy after

puberty. Studies that have looked at the impact of postpubertal T treatment in female mice have generally not investigated reproductive outcomes.

2.1.4 Study design, size, duration

A total of 20 C57BL/6N female mice were used for this study. Study groups (n = 5 mice per group) included sesame oil vehicle controls and three doses of T enanthate (0.225 mg, 0.45 mg, and 0.90 mg). Mice were injected subcutaneously twice weekly for 6 weeks.

2.1.5 Participants/materials, setting, methods

Daily vaginal cytology was performed prior to initiation of treatment to confirm that all mice were cycling. At 8–9 weeks of age, therapy with subcutaneous T enanthate (0.225, 0.45, or 0.90 mg) or the vehicle control was begun. T therapy continued for 6 weeks, at which point mice were sacrificed and compared to control mice sacrificed during diestrus/metestrus. Data collected included daily vaginal cytology, weekly and terminal reproductive hormone levels, terminal body/organ weights/measurements, ovarian follicular distribution/morphology, and corpora lutea counts.

2.1.6 Main results and the role of chance

Of the mice treated with 0.90 mg T enanthate, two of five mice experienced vaginal prolapse, so this group was excluded from further analysis. T enanthate administration twice weekly at 0.225 mg or 0.45 mg resulted in cessation of cyclicity and persistent diestrus. One of five mice at the 0.225-mg dose resumed cycling after 2.5 weeks of T therapy. As compared to controls, T-treated mice had sustained elevated T levels and luteinizing hormone (LH) suppression in the terminal blood sample. T-treated mice demonstrated increases in clitoral area and atretic cyst-like late antral follicles (0.45 mg only) as compared to controls. No reduction in

primordial, primary, secondary, or total antral follicle counts was detected in T-treated mice as compared to controls, and T-treated mice demonstrated an absence of corpora lutea.

2.1.7 Limitations, reasons for caution

Mouse models can provide us with relevant key findings for further exploration but may not perfectly mirror human reproductive physiology.

2.1.8 Wider implications of the findings

To our knowledge, this report describes the first mouse model mimicking T therapy given to transgender men that facilitates analysis of reproductive changes. This model allows for future studies comparing duration and reversibility of T-induced changes, on the reproductive and other systems. It supports a role for T therapy in suppressing the hypothalamic-pituitary-gonadal axis in adult female mice as evidenced by LH suppression, persistent diestrus, and absence of corpora lutea. The increase in atretic cyst-like late antral follicles aligns with the increased prevalence of polycystic ovary morphology seen in case series of transgender men treated with T therapy. The results also suggest that T therapy does not deplete the ovarian reserve.

2.1.9 Study funding/competing interest(s)

This work was supported by the American Society for Reproductive Medicine/Society of Reproductive Endocrinology and Infertility Grant and NIH R01-HD098233 to M.B.M. and University of Michigan Office of Research funding (U058227). H.M.K. was supported by the Career Training in Reproductive Biology and Medical Scientist Training Program T32 NIH Training Grants (T32-HD079342, T32-GM07863) as well as the Cellular and Molecular Biology Program. The University of Virginia Center for Research in Reproduction Ligand Assay and

Analysis Core is supported by the Eunice Kennedy Shriver NICHD/NIH (NCTRI) Grant P50-HD28934. E.E.M. consults for Allergan. No other authors have competing interests.

Key words: testosterone, gender-affirming, hormone therapy, transgender, mouse model, postpubertal, ovary, acyclicity

2.2 Introduction

The gender identity of transgender individuals does not align with their sex assigned at birth. In the United States there are an estimated 1.4 million transgender adults (0.6%) (Flores *et al.*, 2016). Transgender people may seek cross-sex hormone therapy and/or surgery to develop physical characteristics of their affirmed gender. Masculinizing hormone therapy for transgender men typically involves parenteral (intramuscular or subcutaneous) or transdermal testosterone (T). Levels of T are monitored to ensure that they are within the range of cisgender (or non-transgender) men (Hembree *et al.*, 2017). Gender-affirming T therapy typically causes cessation of menses, body fat redistribution, clitoral enlargement, voice deepening, and increased body hair in a more masculine distribution (Coleman *et al.*, 2011).

As the effect of masculinizing T therapy on reproduction is largely unknown, national and international medical organizations recommend counseling about fertility preservation prior to starting T therapy (Coleman *et al.*, 2011; Ethics Committee of the American Society for Reproductive Medicine, 2015; Hembree *et al.*, 2017). Unfortunately, oocyte or embryo cryopreservation strategies are expensive, time consuming, and physically invasive. As such, many transgender men do not preserve gametes prior to starting T but may later express interest

in carrying a pregnancy or using their gametes in a gestational carrier (Wierckx *et al.*, 2012; De Roo *et al.*, 2016). There is minimal data on fertility after T therapy. One published survey included 21 transgender men who self-reported pregnancy and live birth using their own oocytes after prior T therapy, but these results cannot be generalized as they screened for individuals with successful births (Light *et al.*, 2014).

Studies of T-exposed ovaries in transgender men at the time of gender-affirming surgery suggest that T induces an ovarian phenotype similar to polycystic ovarian morphology. This does not imply that T therapy causes the multifactorial polycystic ovary syndrome (PCOS), as PCOS by definition excludes exogenous T therapy (The Rotterdam ESHRE/ASRM-Sponsored PCOS consensus workshop group, 2004). Furthermore, the milder hyperandrogenemia and elevated pulsatile luteinizing hormone (LH) of PCOS may not parallel the hormonal milieu of transgender men. In T-treated ovaries of transgender men, multiple studies report increased tunica albuginea collagenization (Amirikia *et al.*, 1986; Futterweit and Deligdisch, 1986; Spinder *et al.*, 1989; Pache *et al.*, 1991; Chadha *et al.*, 1994; Ikeda *et al.*, 2013), stromal hyperplasia (Futterweit and Deligdisch, 1986; Spinder *et al.*, 1989; Pache *et al.*, 1991; Chadha *et al.*, 1994; Grynberg *et al.*, 2010; Ikeda *et al.*, 2013), and increased luteinization of stromal cells (Futterweit and Deligdisch, 1986; Spinder *et al.*, 1989; Pache *et al.*, 1991; Chadha *et al.*, 1994; Ikeda *et al.*, 2013). Reports of follicular changes were more heterogeneous and included multiple cystic follicles (Futterweit and Deligdisch, 1986; Miller *et al.*, 1986; Spinder *et al.*, 1989; Pache *et al.*, 1991; Chadha *et al.*, 1994), multifollicular ovaries (Loverro *et al.*, 2016) and antral follicle count > 12 follicles per ovary (Grynberg *et al.*, 2010), although other studies report similar antral follicle counts between transgender men and controls (Ikeda *et al.*, 2013; Caanen *et al.*, 2017). Limitations to these

studies include variation in clinical treatment and higher reported rates (15–58%) of PCOS in transgender men prior to T therapy (Baba *et al.*, 2007; Mueller *et al.*, 2008; Becerra-Fernández *et al.*, 2014). In sum, there is uncertainty around T-induced reproductive outcomes and almost no data on any potential reversibility if T is paused for reproductive purposes. Given the ethical limitations of conducting these studies in humans, animal models provide a potential alternative strategy that allows for control of dosage, age, timing, appropriate controls and studies around future fertility. Unfortunately, the existing animal models of androgen administration to female animals either do not adequately parallel the long-term, postpubertal administration of T given to transgender men or are not compatible with studying reproductive capacity (Walters *et al.*, 2012; Padmanabhan and Veiga-Lopez, 2013; Goetz *et al.*, 2017). The objective of this study was to establish a mouse model mimicking T therapy given to transgender men in which the reproductive effects of masculinizing T therapy can be investigated.

2.3 Materials and Methods

2.3.1 Ethical approval

Animal studies were performed in accordance with the protocol approved by the Institutional Animal Care & Use Committee (IACUC) at the University of Michigan (PRO00007618).

2.3.2 Experimental design

Twenty C57BL/6NHsd female mice (Envigo, Indianapolis, IN, USA) were used for this study. All mice were housed in ventilated cages in groups of five in a non-barrier facility (photoperiod 12 h light & 12 h dark) with free access to food and water at the University of

Michigan, Ann Arbor. Mice were 8–9 weeks old and 19 ± 1g (mean ± SD) at the time of their first injections. Mice received twice-weekly mid-back 100-μL subcutaneous injections (Monday a.m. and Thursday p.m.) of T-enanthate in sesame oil (n = 5 mice/dose) or sesame-oil-only control (n = 5 mice). T enanthate at 0.225, 0.45, or 0.90 mg per dose was diluted from the stock solution (200 mg/mL, dissolved in sesame oil, Hikma Pharmaceuticals, Portugal). Due to vaginal prolapse in two of five mice treated with 0.90 mg T enanthate, all analyses were performed on mice in the 0.225- and 0.45-mg groups. Control mice treatment and analysis was performed prior to T-treated mice to prevent incidental exposure to T. Sesame oil was sterile-filtered prior to injection (USP/NF grade, Welch, Holme & Clark Co., Inc., Newark, NJ, USA). After 6 weeks of T or vehicle injections, mice were sacrificed, and organs harvested for histology.

2.3.3 Vaginal cytology

Daily vaginal cytology was performed for at least 2–3 cycles prior to T injection to confirm that the mice were postpubertal and cycling, and subsequently was performed throughout the 6 weeks of T therapy (Nelson *et al.*, 1990). Estrous cycle staging was based on the distribution of leukocytes, cornified epithelial cells and nucleated epithelial cells (Cora *et al.*, 2015).

2.3.4 Blood collection and hormone analysis

Lateral tail vein blood was collected weekly at the midpoint between doses (Wednesday a.m.) with collection volumes up to, but not exceeding, 0.5% of body weight (~75 μL). Terminal blood was collected 2 days after the final T injection via cardiac puncture while under isoflurane anesthesia. Blood samples were kept at 4°C overnight, centrifuged for 10 min (8100*G*) and the collected serum stored at -20 °C. Peptide hormone analysis for LH, follicle stimulating hormone

(FSH), and anti-Müllerian hormone (AMH) was performed at the Ligand Assay and Analysis Core Facility, University of Virginia Center for Research in Reproduction. The reportable range for the LH Mouse & Rat in house protocol RIA was 0.04–75.0 ng/mL. The reportable range for the FSH Mouse & Rat in house protocol RIA was 1.6–56.0 ng/mL. The reportable range for the AMH Mouse & Rat ANSH ELISA was 3.36–215 ng/mL. Steroid hormone analysis (testosterone and estradiol) was performed using liquid chromatography tandem mass spectrometry (LC-MS/MS) in the Auchus Laboratory at the University of Michigan. The limit of detection was 20 pg/mL and the limit of quantification was 50 pg/mL for both testosterone and estradiol. Instrumentation included an Agilent 6495A triple quadrupole mass spectrometer coupled to an Agilent Infinity 1260 and Infinity II 1290 liquid chromatography system.

2.3.5 Body weights and measures

Mice were weighed weekly prior to blood collection. The uterus and liver were weighed prior to fixation on the day of sacrifice. Ovary collection aimed to preserve extraovarian structures (e.g. rete ovarii) and so weights were not collected. External mouse clitoral structures were imaged while the mice were supine and anesthetized, and clitoral length and width were measured in ImageJ.

2.3.6 Histological analysis

Ovaries were fixed in Bouin's fixative. Samples were processed at the Histology Core in the Microscopy & Image Analysis Laboratory at the University of Michigan. After processing, samples were embedded in paraffin and serially sectioned at 5 μm with five sections per slide, and every other slide was stained with hematoxylin and eosin.

2.3.7 Follicle distribution analysis

Every 10th section was analyzed for the presence of primordial, primary and secondary follicles at x20 magnification using a light microscope (DM1000, Leica, Germany). Counting was performed while blinded to the experimental group. Follicle distribution was recorded as follicle type per ovary and was averaged between both ovaries. Images of every 10th section were taken at x5 magnification and used for counting total numbers of corpora lutea and antral follicles. Images for an entire ovary were examined alongside each other to prevent over counting of corpora lutea and antral follicles across sections. Primordial follicles were defined as an oocyte surrounded by a single layer of squamous granulosa cells, primary follicles as an oocyte surrounded by a single layer of cuboidal granulosa cells, and secondary follicles as an oocyte surrounded by two or more layers of granulosa cells. Primordial and primary follicles were counted when their nucleus was visible, and secondary follicles were counted when their nucleolus was present to prevent over counting. Corpora lutea were identified as discrete round structures with increased pink cytoplasmic staining with hematoxylin and eosin. Antral follicles were identified by the presence of an antral cavity. Atretic cyst-like late antral follicles were defined as a fluid-filled cyst, with an oocyte lacking connection to granulosa cells, and an attenuated granulosa cell layer (adapted from Caldwell *et al.*, 2014).

2.3.8 Statistical analysis

Data were analyzed in GraphPad Prism 7 with unit of analysis of a single mouse. Parametric and non-parametric testing was based on results of the Shapiro-Wilk normality test. Non-parametric testing included Mann-Whitney and Kruskal-Wallis with Dunn's multiple comparisons test. Parametric testing included Welch's *t*-test and ordinary one-way Analysis of Variance (ANOVA) with Bonferroni's multiple comparisons test. For analysis, non-detectable

hormone levels below the limit of detection were treated as the value set for the limit of quantification. $P < 0.05$ was considered to be statistically significant.

2.4 Results

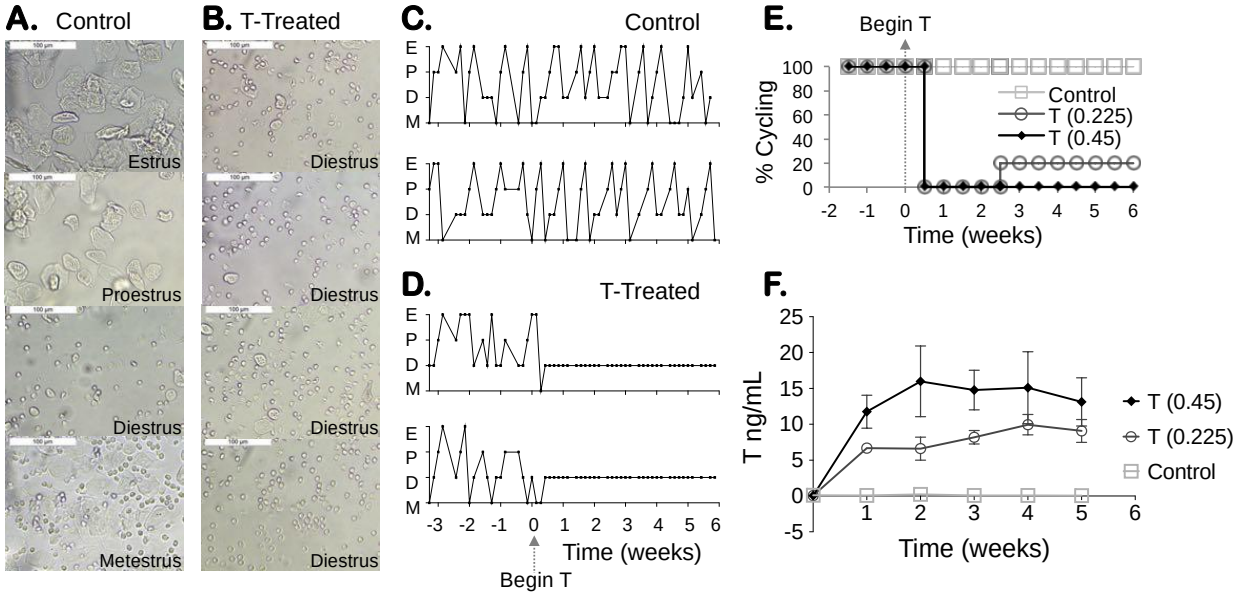

Figure 1. Longitudinal hormonal and cyclic profile. (A) Control mice injected with the sesame oil vehicle progress through the estrous cycle: metestrus (M), diestrus (D), proestrus (P), estrus (E), while mice treated with testosterone (T) show persistent diestrus as determined by the presence of round leukocytes (B) (scale 100 μm). Cyclicity of two representative control mice (C) versus two T-treated mice (D) for several cycles prior to starting injections and then during 6 weeks of T or vehicle injections. (E) Percent cyclicity for mice after starting T treatment at time 0 (control n = 5, T 0.45 mg n = 5, T 0.225 mg n = 5). (F) Longitudinal T levels for mice over 6 weeks of treatment with injections twice per week (mean ± SD).

2.4.1 T enanthate caused persistent diestrus in postpubertal adult female mice

Control mice progressed through the estrous cycle, demonstrating metestrus (M), diestrus (D), proestrus (P), and estrus (E) on vaginal cytology (Fig. 1A). In contrast, T-treated mice demonstrated persistent diestrus starting ~3–4 days after beginning T injections (Fig. 1B). Figure 1C highlights two representative control mice who continued to cycle during the pre-treatment period and 6 weeks of injections. This contrasts with two representative T-treated mice who

demonstrated cyclicity prior to starting T treatment, after which point consistent diestrus was observed (Fig. 1D). In Fig. 1E, 100% of the control mice continued to cycle throughout the 6 weeks of injections, while 100% of the T-treated mice at 0.45 mg twice weekly stopped cycling (Fig. 1E). For mice treated with 0.225 mg twice weekly, one mouse (20%) demonstrated some cyclic changes in vaginal cytology starting at 2.5 weeks of T treatment (Fig. 1E).

2.4.2 T enanthate induced elevated serum T levels

Levels of T were measured every week over the six-week period for T-treated and control mice. T levels (ng/mL, mean ± SD) in T-treated female mice (<0.05) were comparable to controls (0.1 ± 0.1) prior to starting T (Week 0). Levels were significantly different in subsequent weeks following T injections between control mice (Week 1: 0.10 ± 0.07, Week 2: 0.2 ± 0.3, Week 3: 0.08 ± 0.02, Week 4: 0.07 ± 0.05, Week 5: 0.06 ± 0.01) and T-treated mice at twice weekly T doses of 0.225 mg (Week 1: 7 ± 1, Week 2: 7 ± 4, Week 3: 8 ± 2, Week 4: 10 ± 3, Week 5: 9 ± 4) and 0.45 mg (Week 1: 12 ± 2, Week 2: 16 ± 5, Week 3: 15 ± 3, Week 4: 15 ± 5, Week 5: 13 ± 3) (Fig. 1F).

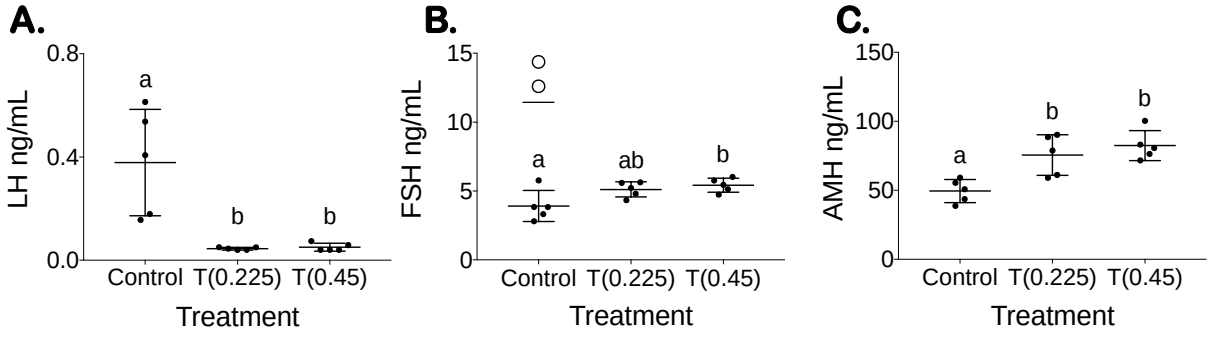

Figure 2. Terminal hormone levels. (A) LH, (B) FSH with open circles for mice in proestrus/estrus not included in calculations, and (C) anti-Müllerian hormone (AMH) levels for control and mice treated with T after 6 weeks of T enanthate at 0.225 and 0.45 mg twice per week (mean ± SD).

2.4.3 T Enanthate suppressed LH, minimally changed FSH, and increased AMH

Terminal hormones were collected 2 days following the final T injection. Terminal LH levels (ng/mL, mean ± SD) in T-treated mice were suppressed (0.225 mg at 0.045 ± 0.005, 0.45 mg at 0.05 ± 0.02) as compared to control mice (0.4 ± 0.2) in diestrus/metestrus (Fig. 2A, $P < 0.05$). Terminal FSH levels (ng/mL, mean± SD) were not significantly different for T-treated mice at the 0.225-mg dose (5.1 ± 0.6), although they were statistically significantly higher in T-treated mice at the 0.45 mg dose (5.4 ± 0.5, $P < 0.05$) when compared to the controls (4 ± 1) (Fig. 2B). Of note, these FSH levels were lower than the FSH levels observed for 2 control mice sacrificed in proestrus/estrus, which were not included in the analysis (Fig. 2B, open circles). AMH levels (ng/mL, mean ± SD) were significantly increased in T-treated mice at both doses (0.225 mg 76 ± 15, 0.45 mg 82 ± 11) versus control mice (50 ± 8) (Fig. 2C, $P < 0.05$).

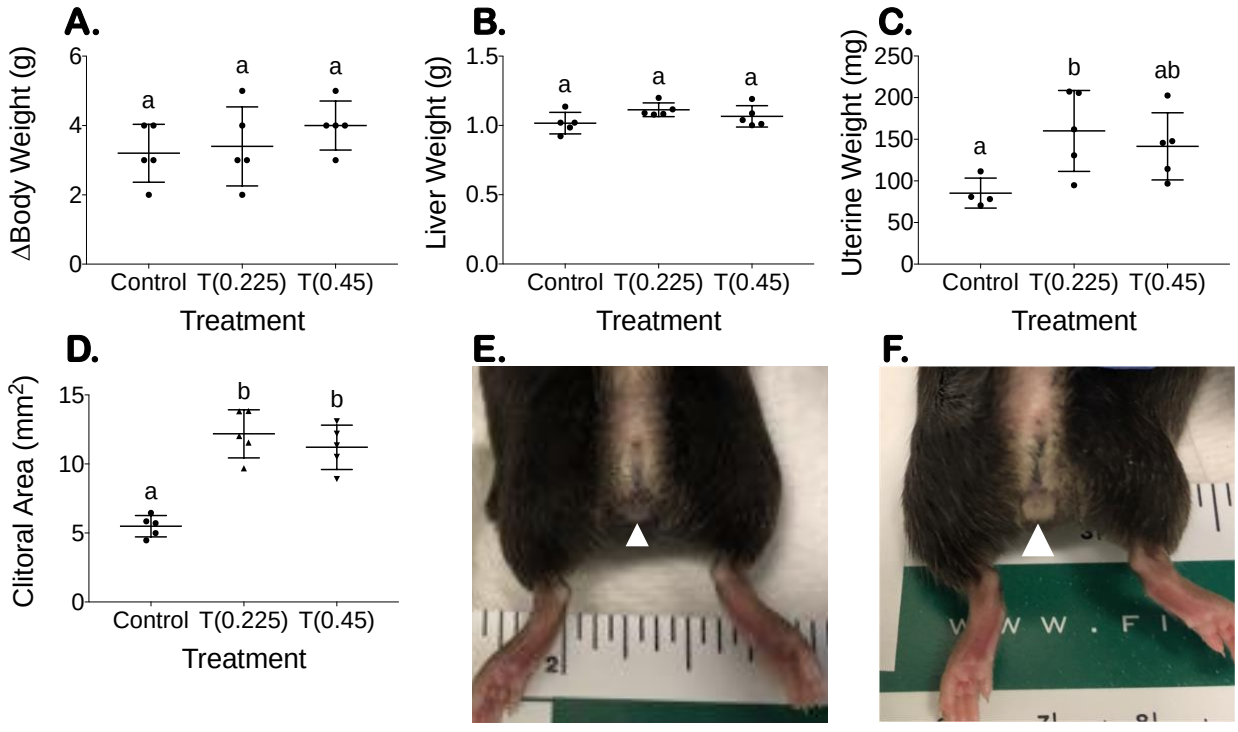

Figure 3. Terminal body measurements (mean ± SD). (A) Increase in body weight over 6 weeks, (B) terminal liver weight (normalized to terminal average of 22.5 g mouse), (C) terminal uterine weight (normalized to terminal

average of 22.5 g mouse), and (D) terminal clitoral area. Increased clitoral size between (E) controls and (F) mice treated with T, with white arrowhead pointing to clitoral structure.

2.4.4 T enanthate increased uterine weight and clitoral area

There was no significant difference between the increase in body weight (g) for T-treated mice (0.225 mg 3.4 ± 1.1 g, 0.45 mg 4.0 ± 0.7 g) versus control mice (3.2 ± 0.8 g) over the 6-week period (Fig. 3A). T enanthate also did not significantly increase terminal liver weight (g) (normalized to terminal average of 22.5 g mouse) after 6 weeks in T-treated mice (0.225 mg 1.11 ± 0.05 g, 0.45 mg 1.07 ± 0.08 g) as compared to control mice (1.02 ± 0.08 g) (Fig. 3B). Terminal uterine weight (mg) (normalized to terminal average of 22.5 g mouse) was significantly elevated in T-treated mice at 0.225 mg (160 ± 49) as compared to control mice (85±18) (Fig. 3C, $P < 0.05$). Normalized uterine weight in T-treated mice at 0.45 mg (142 ± 40) was not significantly different from 0.225-mg T-treated mice or controls (Fig. 3C). T-treated mice demonstrated a significantly enlarged clitoral area (0.225 mg 12.2 ± 1.7 mm^2, 0.45 mg 11.2 ± 1.6 mm^2) (Fig. 3D and F - white triangle) as compared to controls (5.5 ± 0.8 mm^2) (Fig. 3D and E - white triangle) ($P < 0.05$).

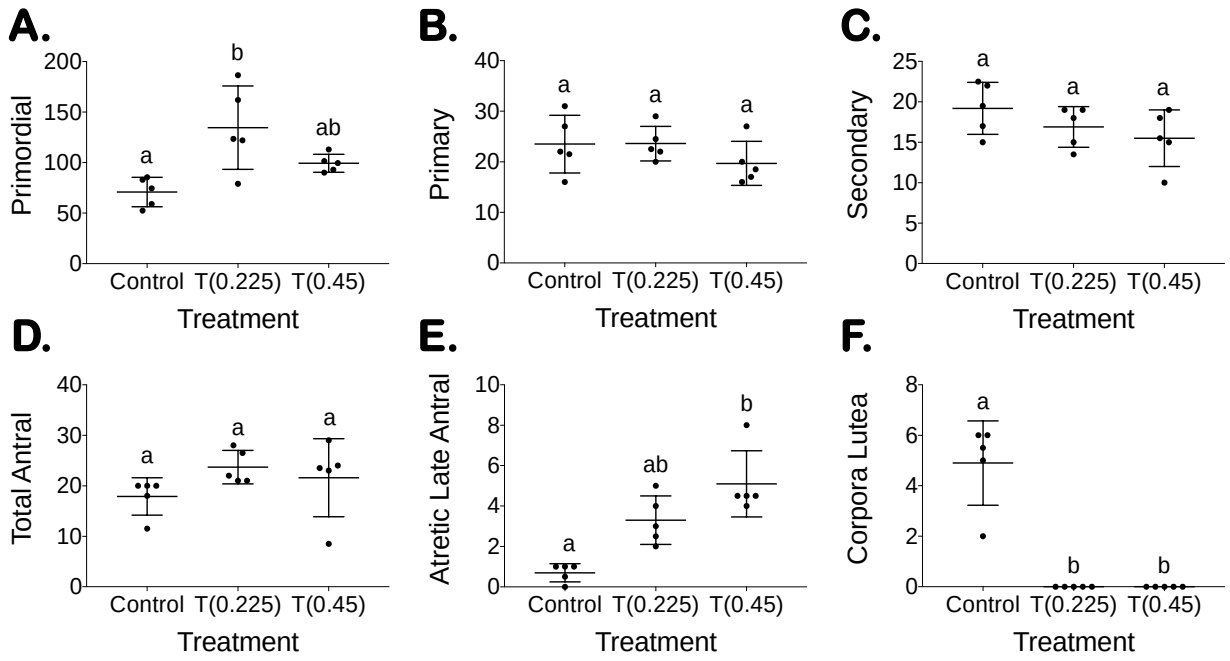

Figure 4. Follicle counts for every 10th section for primordial (A), primary (B), secondary (C), total antral (D), atretic cyst-like late antral (E) follicles as well as corpora lutea (F).

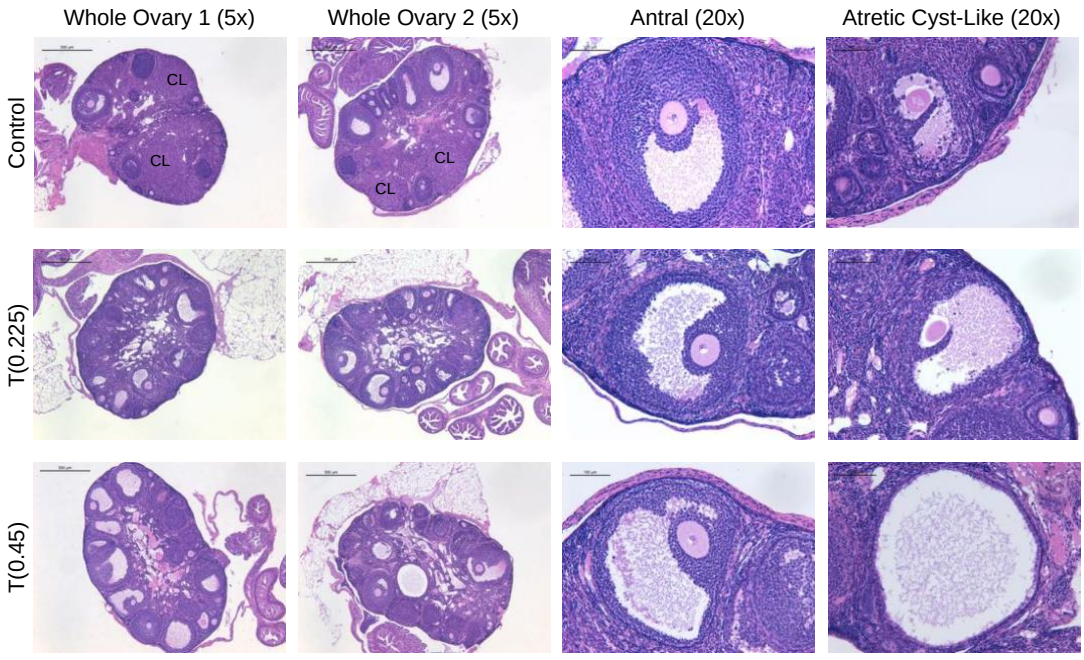

Figure 5. Perturbed histology in mice treated with T. Hematoxylin and eosin-stained control ovaries with corpora lutea (Row 1) and T-treated ovaries at 0.225 mg (Row 2) and 0.45 mg (Row 3) after 6 weeks of treatment (Columns 1 and 2, x5, scale 500 μm). Antral follicles with oocytes surrounded by several layers of cumulus granulosa cells from control (Row 1) and T-treated mice at 0.225 mg (Row 2) and 0.45 mg (Row 3) doses (Column 3, x20, scale 100 μm). Atretic cyst-like late antral follicles from control (Row 1) and T-treated mice at 0.225 mg (Row 2) and 0.45 mg (Row 3) (Column 4, x20, scale 100 μm).

2.4.5 T enanthate minimally changed the pre-antral follicle distribution

T-treated mice at 0.225 mg had a significant increase in the number of primordial follicles (0.225 mg 135 ± 41) as compared to controls (71 ± 15) (Figure 4A, $P < 0.05$), while 0.45 mg (0.45 mg 99 ± 9) did not differ significantly from controls or T-treated mice at 0.225 mg (Fig. 4A). No differences were detected in primary follicle counts (0.225 mg 24 ± 3, 0.45 mg 20 ± 4) as compared to control mice (24 ± 6) (Fig. 4B) or for secondary follicle counts (0.225 mg 17 ± 3, 0.45 mg 16 ± 4) as compared to control mice (19 ± 3) (Fig. 4C).

2.4.6 T enanthate increased atretic cyst-like late antral follicles and prevented corpora lutea formation

Representative histology for whole ovaries, antral follicles and atretic cyst-like late antral follicles is shown in Fig. 5. T-treated mice did not demonstrate differences in total antral follicle counts (0.225 mg 24 ± 3, 0.45 mg 22 ± 8) as compared to controls (18 ± 4) (Fig. 4D). T-treated mice at 0.45 mg demonstrated increased atretic cyst-like late antral follicles (5 ± 2) when compared to control mice (0.7 ± 0.4) (Fig. 4E, $P < 0.05$). T-treated mice had an absence of corpora lutea (0.225 mg 0 ± 0, 0.45 mg 0 ± 0), which was significantly different than controls (5 ± 2) (Fig. 4F, $P < 0.05$).

2.5 Discussion

Table 4. Comparison of reproductive changes seen in transgender men given T therapy and in our mouse model of postpubertal T therapy.

Reproductive Effects of Postpubertal T Therapy	Transgender Men with T Therapy	Mouse Model with T Therapy
Acyclicity	✓[a]	✓
T in male range	✓[b]	✓
LH reduction	✓[c]	✓
Ovarian phenotype similar to polycystic ovary morphology	✓[d]	✓

Citations: [a](Meyer *et al.*, 1986; Grimstad *et al.*, 2019), [b](Hembree *et al.*, 2017), [c](Spinder *et al.*, 1989; Wierckx *et al.*, 2014), [d](Futterweit and Deligdisch, 1986; Spinder *et al.*, 1989). T, testosterone.

The above-described mouse model mimics several reproductive perturbations observed in transgender men on T therapy (Table 4), and therefore can likely be used for preliminary investigation of the reproductive effects of T therapy given to transgender men. Due to vaginal prolapse observed in the 0.90-mg group, and breakthrough cyclicity observed in the 0.225-mg group, we propose that 0.45 mg T enanthate injected subcutaneously twice weekly is the ideal dose for the model. We selected subcutaneous T administration to parallel the parenteral (intramuscular and subcutaneous) administration methods commonly used for masculinizing hormone therapy in transgender men (Hembree *et al.*, 2017). Implants, such as those made from silastic tubing, are also commonly used for androgen administration in animal models (Walters *et al.*, 2012) and may warrant future study in mouse models of masculinizing hormone therapy. Additionally, histological analysis suggests similar numbers of primordial, primary, and secondary follicles between control and T-treated mice. These results suggest that T treatment may not affect overall ovarian reserve, and there is likely a pool of normal primordial follicles to recruit once the more advanced, abnormal-appearing follicles have been cleared.

Prior animal models have demonstrated changes in ovarian architecture and reproductive function in response to androgen administration, usually in the context of PCOS. In PCOS models, however, androgen treatment is typically initiated prenatally or in the prepubertal period (Walters *et al.*, 2012; Caldwell *et al.*, 2014; van Houten and Visser, 2014), which does not directly translate to postpubertal gender-affirming hormone therapy. The historical paradigm for sex-steroid-induced changes held that organizational (permanent) changes were possible during development and activational (transient) changes took place during adulthood. This framework has likely limited research around changes induced by long-term sex steroid administration in adults because of the assumption that persistent changes would not occur (Arnold and Breedlove, 1985). Of the studies that have examined postpubertal androgen administration on reproduction, one study notes that adult mice treated with dihydrotestosterone (DHT) stopped cycling and had reduced fertility compared to controls (Ma *et al.*, 2017), but DHT is not used for masculinizing therapy in transgender men. Another study treated adult female mice with T for 1 week and demonstrated reduced mature oocyte production from superovulation; however, the short treatment duration limits generalizability (Yang *et al.*, 2015). A model has been recently proposed to mimic cross-sex T therapy; however, mice were ovariectomized prior to T initiation, preventing analysis of reproductive changes (Goetz *et al.*, 2017). Several studies on malarial susceptibility have utilized adult female mice treated with 0.90 mg T twice weekly (Benten *et al.*, 1997; Delić *et al.*, 2010), but did not investigate reproductive changes. Finally, although the description of the ovarian phenotype with T therapy varies across the limited number of studies in transgender men, most studies point to a polycystic ovary morphology-like presentation, including reports of multiple cystic follicles similar to the increase in atretic cyst-like late antral follicles seen in our model (Futterweit and Deligdisch, 1986; Spinder *et al.*, 1989).

Utilizing a mouse model of T therapy in transgender men has limitations and may not perfectly mirror human physiology. In considering development of an animal model to mimic masculinizing T therapy, genealogically, non-human primates are optimal, but they are cost-prohibitive, and their long reproductive lifespan and gestational cycle limits their utility, particularly when studying effects on offspring (van Houten and Visser, 2014). Sheep models have similar limitations (Padmanabhan and Veiga-Lopez, 2013). Although polyovular, rodents have been used extensively in studies of fertility and ovarian function and are frequently used to model PCOS (Walters *et al.*, 2012), and rodent models can be capitalized upon prior to validating key findings in non-human primates for human translation. Mice are easy to handle and maintain, have a well-characterized reproductive cycle, are relatively inexpensive, and have a short generation time and accelerated lifespan (van Houten and Visser, 2014). Importantly, the follicles in the mouse ovary closely resemble those in the human ovary, and many of the genes expressed in ovarian follicles are highly conserved in mice and humans (Walters *et al.*, 2012). Although they differ from humans in that their ovarian differentiation occurs postnatally (Smith *et al.*, 2014a), this difference should not be relevant to studies of postpubertal ovarian function that are not examining *in utero* insults.

In summary, we have reported the first mouse model mimicking T therapy given to transgender men that allows for investigation of reproductive outcomes. This model is simple and inexpensive to establish, can be used in any mouse laboratory, and allows for investigation of reproductive phenotype with T cessation and comparative fertility in controlled manner that is unethical to study in humans. Furthermore, this model can provide a tool for researchers studying the effects of masculinizing T therapy on other aspects of reproduction, other organ systems and

transgenerational effects. Furthering the understanding of reproductive changes during masculinizing T therapy, and the reversibility of any observed changes, will hopefully lead to improved counseling for transgender men considering fertility preservation or family building in the future.

2.6 Acknowledgements

The authors thank Richard Auchus, MD, PhD, at the University of Michigan for performing steroid hormone analyses and the University of Virginia Center for Research in Reproduction Ligand Assay and Analysis Core for performing peptide hormone analyses.

2.7 Authors' Roles

H.M.K. designed the study, acquired and interpreted the data and drafted the article. E.S.C. contributed to study design, data acquisition and article review. A.D. contributed to study design, data acquisition and article review. E.E.M. contributed to study design and article review. V.P. designed the study and contributed to data interpretation and article review. A.S. designed the study and contributed to data interpretation and article review. M.B.M. conceived and designed the study and contributed to data interpretation and article review.

2.8 Funding

American Society for Reproductive Medicine/Society of Reproductive Endocrinology and Infertility Grant; National Institutes of Health (R01-HD098233 to M.B.M.); University of Michigan Office of Research funding (U058227). Career Training in Reproductive Biology and

Medical Scientist Training Program T32 NIH Training Grants (T32-HD079342, T32-GM07863 to H.M.K.); Cellular and Molecular Biology Program (to H.M.K.). The University of Virginia Center for Research in Reproduction Ligand Assay and Analysis Core is supported by the Eunice Kennedy Shriver National Institute of Child Health and Human Development/National Institutes of Health (National Centers for Translational Research in Reproduction and Infertility) Grant (P50-HD28934).

2.9 Conflict of Interest:

E.E.M. consults for Allergan. No other authors have competing interests.

Chapter 3 Reversibility of Testosterone-Induced Acyclicity After Testosterone Cessation in a Transgender Mouse Model

Chapter previously published (Kinnear *et al.*, 2021) with permission to use in dissertation:

Kinnear HM[†]**,** Hashim PH[†], Dela Cruz C, Rubenstein G, Chang FL, Nimmagadda L, Brunette MA, Padmanabhan V, Shikanov A, Moravek MB. Reversibility of Testosterone-Induced Acyclicity after Testosterone Cessation in a Transgender Mouse Model. *F&S Science.* 2021;2(2):116-123. doi:10.1016/j.xfss.2021.01.008.[†]*joint first author*

3.1 Abstract

3.1.1 Objective

To establish if cessation of testosterone (T) therapy reverses T-induced acyclicity in a transgender mouse model that allows for well-defined T cessation timing.

3.1.2 Design

Experimental laboratory study using a mouse model.

3.1.3 Setting

University-based basic science research laboratory.

3.1.4 Animals

A total of 10 C57BL/6NHsd female mice were used in this study.

3.1.5 Intervention(s)

Postpubertal C57BL/6NHsd female mice were subcutaneously implanted with T enanthate (n = 5 mice) or placebo (n = 5 mice) pellets. Pellets were surgically removed after 6 weeks to ensure T cessation, after which the mice were followed for four estrous cycles after the resumption of cyclicity.

3.1.6 Main outcome measure(s)

Primary outcomes included daily vaginal cytology and weekly T levels before, during, and after T enanthate or placebo pellet implantation and removal. Secondary outcomes included ovarian follicle distribution and corpora lutea numbers, body metrics, and terminal diestrus hormone levels.

3.1.7 Result(s)

T-treated mice (100%) resumed cycling within one week of T pellet removal after six weeks of T therapy. T levels were significantly elevated during T therapy and decreased to control levels after surgical pellet removal. No detectable differences were observed in the follicle count, corpora lutea formation, diestrus hormone levels, or body metrics after four estrous cycles, with the exception of persistent increased clitoral area between T-treated mice and controls. One T-treated mouse was sacrificed early due to vaginal prolapse and not included in subsequent analyses.

3.1.8 Conclusion(s)

Our results demonstrated a close temporal relationship between estrous cycle return and T levels dropping to control levels following T pellet removal. The return of regular cyclic ovulatory function is also supported by the formation of corpora lutea and the lack of detectable

differences in key reproductive parameters as compared to controls four cycles after T cessation. These results may be relevant to understanding the reversibility of T-induced amenorrhea and possible anovulation in transgender men interested in pausing T to pursue pregnancy or oocyte donation. Results may be limited by duration of T treatment, lack of functional testing, and physiological differences between mice and humans.

Key words: testosterone, transgender, mouse model, ovary, reversibility

3.2 Introduction

Individuals whose gender identity does not align with their sex assigned at birth may identify as transgender. An estimated 1.4 million adults in the United States self-identify as transgender, comprising about 0.6% of the population (Flores *et al.*, 2016); however, the actual number may be higher because of the surrounding stigma and limited data collection. Transgender individuals may seek medical treatment to affirm their gender identity through gender-affirming hormone treatment and/or surgery (Hembree *et al.*, 2017). For transgender men, testosterone (T) is typically used for masculinizing hormone therapy and is administered intramuscularly, subcutaneously, or transdermally. T therapy causes the development of male physical contours, deepening of the voice, increased facial and body hair, and clitoral growth along with changes in body composition, such as the redistribution of fat and changes in muscle mass (T'Sjoen *et al.*, 2019).

Physicians have limited data to draw from while counseling patients about fertility after starting T therapy. Studies conducted to date regarding gender-affirming T therapy and

reproduction may leave “more questions than answers” (Moravek *et al.*, 2020). As such, counseling about fertility preservation is currently recommended before starting gender-affirming T therapy (Coleman *et al.*, 2011; Ethics Committee of the American Society for Reproductive Medicine, 2015; Hembree *et al.*, 2017). T therapy typically leads to cessation of menses and the induction of ovarian characteristics of polycystic ovary morphology including collagenization of the tunica albuginea, stromal hyperplasia, and luteinization of stroma cells (Moravek *et al.*, 2020). Previous studies have suggested that many transgender men do not preserve their gametes before beginning T therapy, potentially because of the expensive, invasive, and time-consuming nature of ovarian fertility preservation methods (Auer *et al.*, 2018; Baram *et al.*, 2019); however, some of these individuals may later be interested in using their gametes for reproduction.

For individuals interested in fertility after beginning T therapy, only a limited amount of research has been conducted regarding the reversibility of menstrual suppression and possible anovulation if T therapy is paused for reproductive purposes. There are anecdotal reports of clinics pausing T therapy for 1 to 6 months prior to ovarian stimulation for oocyte harvesting, although others have not paused T therapy at all (Moravek *et al.*, 2020). Given the health risks to the fetus posed by in utero T exposure, pausing T therapy is essential before attempting to carry a pregnancy (Wolf *et al.*, 2002). Light et al. (Light *et al.*, 2014) surveyed 41 transgender men with successful birth outcomes, of which 25 had previously been on T therapy. Of these 25 transgender men with previous T exposure, 80% resumed menses within 6 months after stopping T and 20% conceived while amenorrhoeic (Light *et al.*, 2014). Others have also reported anecdotal resumption of menses in some transgender men following T cessation for reproductive

purposes, although the timing and menstrual cycle architecture has not been well-characterized. In qualitative interviews of 15 transgender men pursuing fertility preservation, Armuand et al. noted that T therapy was discontinued in 7 of the men who had already begun T therapy until menstruation resumed, which took approximately 3–6 months (Armuand *et al.*, 2017). A case series on transgender and gender-nonconforming patients undergoing in vitro fertilization included a transgender man who had previously started receiving T and resumed menses one month after discontinuation of this therapy (Broughton and Omurtag, 2017). In a comparison of ovarian stimulation for fertility preservation, including seven transgender men with prior T therapy, the time off T before stimulation was 1–13 months and all of them were reported as not experiencing amenorrhea at the start of the treatment cycle (Adeleye *et al.*, 2019). A comparison of assisted reproductive technology outcomes in a cohort of transgender men, of whom 16 had previously been on T therapy, noted that menses resumed in 13 (81.2%) of these men after stopping T therapy for 1–12 months before their assisted reproductive technology cycle (Leung *et al.*, 2019).

We developed a mouse model to evaluate the impact of gender-affirming T therapy on reproductive function (Kinnear *et al.*, 2019). For postpubertal female mice treated for six weeks with male range T therapy, we noted that T induced the cessation of cyclicity with persistent diestrus, a decrease in terminal luteinizing hormone (LH) levels, and an increase in atretic cyst-like late antral follicles with a lack of corpora lutea (Kinnear *et al.*, 2019). The continued persistence or reversibility of these T-induced reproductive alterations is yet to be fully established. This study aimed to investigate the reversibility of T-induced changes on estrous

cyclicity in a mouse model mimicking the T therapy used by transgender men, which also allows for well-defined timing of T cessation.

3.3 Materials and Methods

3.3.1 Ethical approval

Animal studies were completed in compliance with the protocol approved at the University of Michigan (PRO00007618) by the Institutional Care & Use Committee.

3.3.2 Experimental design

This study used 10 C57BL/6NHsd female mice (Envigo, Indianapolis, IN, USA). Mice were housed in groups of five in ventilated cages within a non-barrier facility with 12-hour light/dark cycles and free access to food and water at the University of Michigan, Ann Arbor. Mice were administered T therapy via a subcutaneously implanted T enanthate pellet (5 mg/pellet, 60-day release, n = 5 mice) or a placebo pellet (n = 5 mice) (Innovative Research of America, Sarasota, FL, USA). At the time of pellet administration, mice were 9–10 weeks old with a body mass of 18.6 ± 0.7 g (mean ± SD). After 6 weeks of T therapy, pellets were surgically removed with the mice under isoflurane anesthesia to ensure well-defined timing of T cessation. Daily vaginal cytology and weekly blood collection were performed. After the resumption of cyclicity and four estrous cycles, mice were sacrificed during diestrus and their ovaries were harvested for histological analysis. We estimated that we would need at least three mice per group to detect the expected differences in T levels and percent cyclicity between T-treated mice and control mice at 90% power.

3.3.3 Vaginal cytology

Vaginal cytology was performed daily throughout the study, for at least two cycles before T therapy, throughout the 6-week T therapy period, and subsequently following T cessation to track the four estrous cycles. The stages of the estrous cycle were based on the distribution of cornified epithelial cells, nucleated epithelial cells, and leukocytes (Cora *et al.*, 2015).

3.3.4 Weekly blood collection and serum hormone analysis

Blood was collected weekly from the lateral tail vein. Collections did not exceed 0.5% of body weight. Cardiac puncture under isoflurane anesthesia was performed to collect terminal blood. Blood samples were stored overnight at 4°C. The next day, blood samples were centrifuged for 10 min (8100 g) and serum was collected and stored at -20°C. Peptide hormone analysis for LH and follicle-stimulating hormone (FSH) and steroid hormone analysis (testosterone, estradiol, progesterone) were performed at the Ligand Assay and Analysis Core Facility, University of Virginia Center for Research in Reproduction. The reportable ranges that can be detected with a coefficient of variation of <20% for the different hormonal measures were as follows: Testosterone Mouse and Rat enzyme-linked immunosorbent assay (Immuno-Biological Laboratories, Inc.; Minneapolis, MN, USA), 0.10–16 ng/mL (or 0.20–32 ng/mL with a 2x dilution); LH Mouse and Rat in house protocol radioimmunoassay, 0.04–75.0 ng/mL; FSH Mouse and Rat in house protocol radioimmunoassay, 2.1–45 ng/mL; Progesterone Mouse and Rat enzyme-linked immunosorbent assay (Immuno-Biological Laboratories, Inc.; Minneapolis, MN, USA), 0.15–40 ng/mL; and Estradiol Mouse and Rat enzyme-linked immunosorbent assay (Calbiotech, Inc.; El Cajon, CA, USA), 3–300 pg/mL.

3.3.5 Body weights and measures

All mice were weighed weekly before blood collection. On the day of sacrifice, the uterus and liver were weighed before fixation. Weights of the collected ovaries were not taken due to a desire to preserve extra ovarian structures (e.g. rete ovarii, oviducts). The images of external clitoral structures were taken while mice were under anesthesia and in the supine position. ImageJ was used to measure clitoral length and width.

3.3.6 Histological analysis

Bouin's solution was used to fix the ovaries and extraovarian structures. All samples were sent to the Histology Core in the School of Dentistry at the University of Michigan for processing. The samples embedded in paraffin were sectioned serially with a thickness of 5 μm. Hematoxylin and eosin were used to stain every other slide.

3.3.7 Ovarian morphometry

Follicle counts were performed for every 10^{th} section throughout one entire ovary per mouse at a magnification of x20–40 to identify primordial, primary, and secondary follicles using a light microscope (DM1000, Leica, Germany, 22 ± 3 (mean ± SD) slides examined per ovary). Experimental groups were blinded before analysis. The follicle distribution in an ovary was recorded by follicle type. An oocyte surrounded by a single layer of squamous granulosa cells was identified as a primordial follicle. An oocyte surrounded by a single layer of cuboidal granulosa cells was identified as a primary follicle, while secondary follicles had multiple layers (two or more) of cuboidal granulosa cells. Primordial and primary follicles were counted when a nucleus was present, while secondary follicles were counted when the nucleolus was present, to prevent overcounting. Every 10^{th} section throughout one entire ovary per mouse was imaged

using a light microscope (DM1000, Lecia, Germany) at a magnification of x5 for counting corpora lutea and antral follicles and images were examined alongside each other to prevent overcounting. Antral follicles were identified on the basis of the presence of an antral cavity. Late cyst-like antral follicles that did not have an oocyte connected to granulosa cells and had an attenuated granulosa cell layer (adapted from (Caldwell 2014)) were labelled as atretic. The corpora lutea were identified by their increased eosinophilic cytoplasmic staining in discrete rounded structures.

3.3.8 Statistical analysis

GraphPad Prism 8 was used to analyze the data with a single mouse being the unit of analysis. Results of the Shapiro-Wilk normality test were used to determine the need for parametric or non-parametric testing. Parametric testing included ordinary one-way analysis of variance with Bonferroni's multiple comparisons test and Welch's t-test. The Mann-Whitney test was used for non-parametric testing. $P<.05$ was considered the threshold for statistical significance. For analysis purposes, hormone levels below the level of detection were treated as the value set for the lower limit of quantification.

3.4 Results

3.4.1 T-induced persistent diestrus promptly reverses after the T levels drop

All T-treated mice stopped cycling and were in persistent diestrus within one week of T pellet implantation (Fig. 6B, representative examples Fig. 6C). Notably, within one week of T cessation (defined as removal of pellets), 100% of T-treated mice resumed cycling (Fig. 6B, representative examples Fig. 6C). All control mice implanted with a placebo pellet cycled

throughout the pre-treatment, post-implantation, and post-removal periods (Fig. 6B, representative examples Fig. 6C). Longitudinal serum T levels (ng/mL, mean ± SD) were comparable at week 0 in the control (0.37 ± 0.08) and T-treated (0.32 ± 0.09) mice before pellet implantation. Mice implanted with T pellets exhibited elevated T levels six weeks after pellet release (week 1: 20 ± 3, week 2: 12 ± 2, week 3: 9 ± 2, week 4: 7 ± 1, week 5: 6.4 ± 0.6, week 6: 5 ± 1), which were significantly higher (P<.0001) than those of control mice (week 1: 0.35 ± 0.10, week 2: 0.34 ± 0.12, week 3: 0.29 ± 0.10, week 4: 0.36 ± 0.07, week 5: 0.38 ± 0.12, week 6: 0.26 ± 0.06). Following pellet removal at six weeks, the T levels of T-treated mice (week 7: 0.51 ± 0.03, week 8: 0.53 ± 0.06, and week 9: 0.45 ± 0.17) were comparable those of control mice (week 7: 0.47 ± 0.11, week 8: 0.50 ± 0.16, week 9: 0.61 ± 0.18) (Fig. 6A). Subcutaneously implanted T pellets were relatively intact upon surgical removal (Fig. 6A).

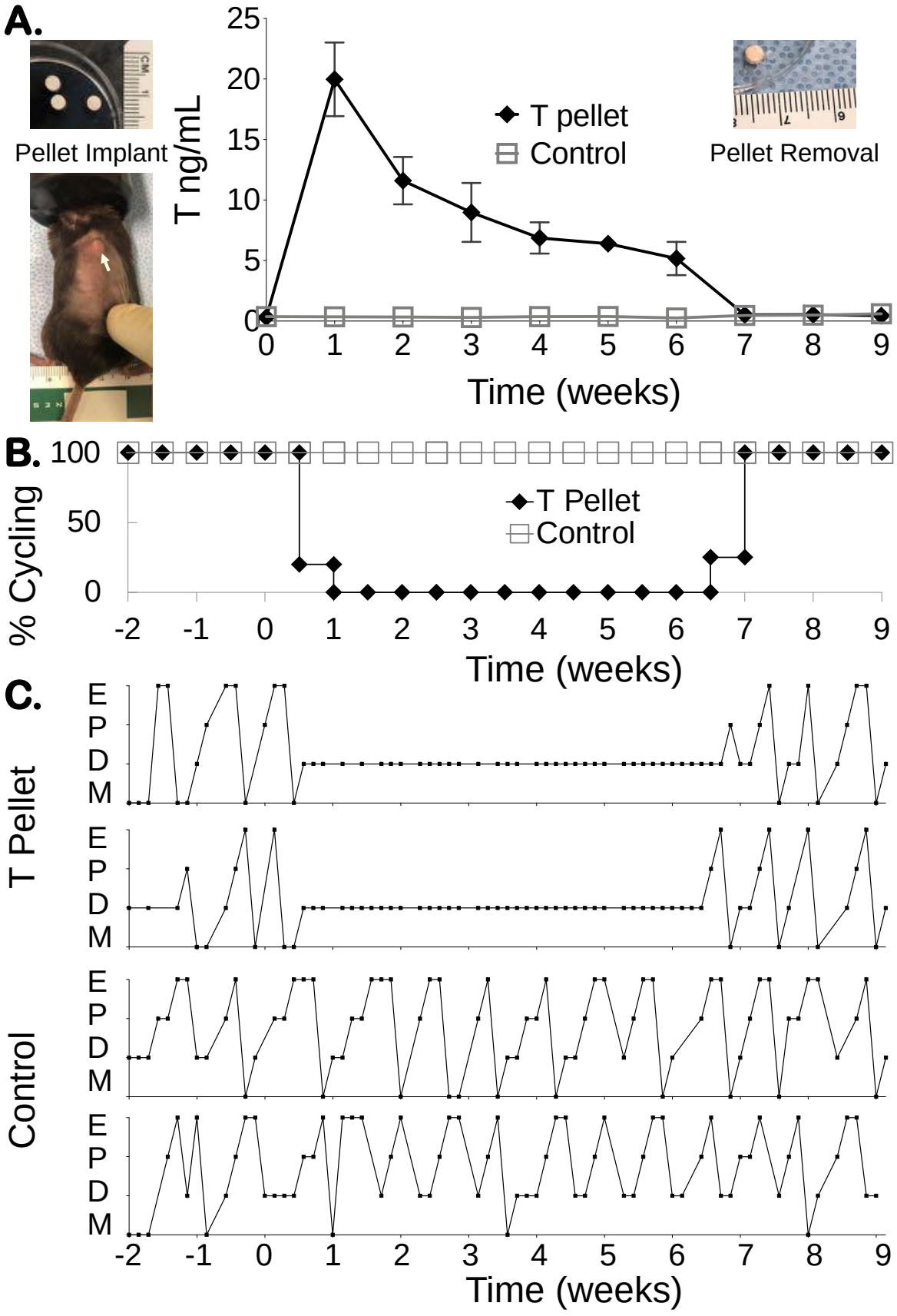
A.
Pellet Implant
Pellet Removal
T ng/mL
25
20
15
10
5
0
T pellet
Control
0 1 2 3 4 5 6 7 8 9
Time (weeks)
B.
% Cycling
100
50
0
T Pellet
Control
-2 -1 0 1 2 3 4 5 6 7 8 9
Time (weeks)
C.
T Pellet
Control
E
P
D
M
-2 -1 0 1 2 3 4 5 6 7 8 9
Time (weeks)

Figure 6. Reversibility of T-induced estrous cycle changes after T cessation. (A) Mice were subcutaneously implanted with a placebo (control) or T enanthate pellet at week 0, which was then removed after 6 weeks. Longitudinal weekly T levels were measured before pellet implantation (week 0), during T therapy (weeks 1–6) and following pellet removal (weeks 7–9) (mean ± SD, error bars shorter than symbol not shown, arrow points to subcutaneously implanted pellet). (B) All mice treated with T pellets at week 0 stopped cycling and demonstrated persistent diestrus until pellet removal at week 6, at which point estrous cyclicity resumed. (C) Two representative mice implanted with T pellets showed persistent diestrus during T therapy and prompt resumption of cyclicity following pellet removal, while two representative control mice continued cycling throughout the study (E = estrus, M = metestrus, D = diestrus, P = proestrus). The green-shaded rectangle indicates the 6-week T therapy, while the purple-shaded rectangle highlights 3 weeks following T cessation.

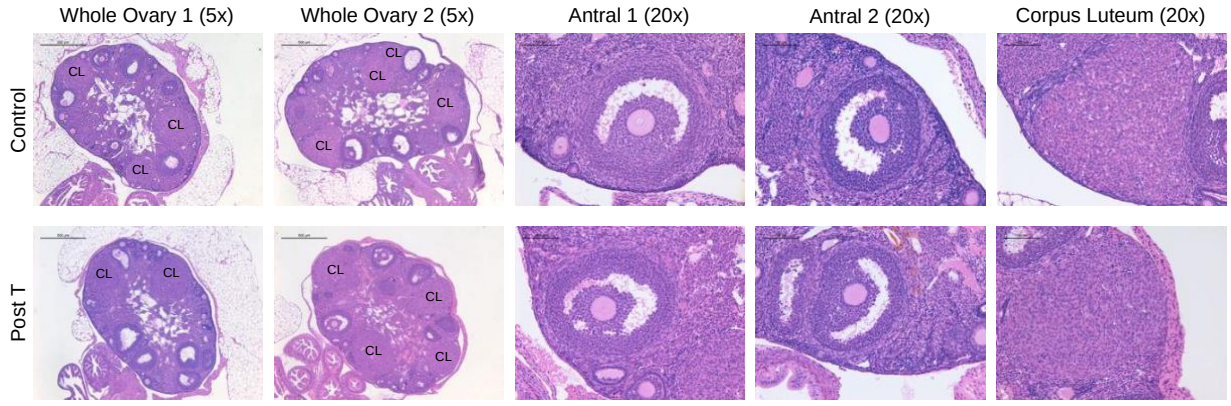

Figure 7. Comparable ovarian histology. Corpora lutea were noted in the ovaries of control mice (row 1) and post T mice (row 2) (columns 1 and 2; magnification, x5; hematoxylin and eosin stain; scale, 500 µm). Post T mice were sacrificed after T cessation and four estrous cycles. Examples of higher magnification of antral follicles (columns 3 and 4; magnification, x20; scale, 100 µm) and corpora lutea (column 5; magnification, x20; scale, 100 µm) in the ovaries of control mice (row 1) and post T mice (row 2).

3.4.2 Corpora lutea noted with comparable follicle distribution following T cessation

Representative hematoxylin and eosin-stained control and post T ovaries, antral follicles, and corpora lutea are displayed in Figure 7. After resumption of cyclicity, previously T-treated mice demonstrated corpora lutea formation and did not significantly differ from controls in terms of follicular distribution counts. No significant difference was detected in primordial follicles in mice post T (171 ± 15) compared with those in control mice (160 ± 44) (Fig. 8A), in primary follicles in mice post T (44 ± 21) compared with those in control mice (41 ± 5) (Fig. 8B), or in

secondary follicles in mice post T (26 ± 7) compared with those in control mice (25 ± 8) (Fig. 8C). No significant difference was detected in the total number of antral follicles (33 ± 6) or in atretic late antral follicles in mice post T (0.5 ± 1) compared with those in the respective controls (30 ± 10 and 0.8 ± 0.4, respectively) (Fig. 8D, 8E). No significant difference was detected in the corpora lutea counts between mice post T (5 ± 2) and control mice (8 ± 4) (Fig. 8F).

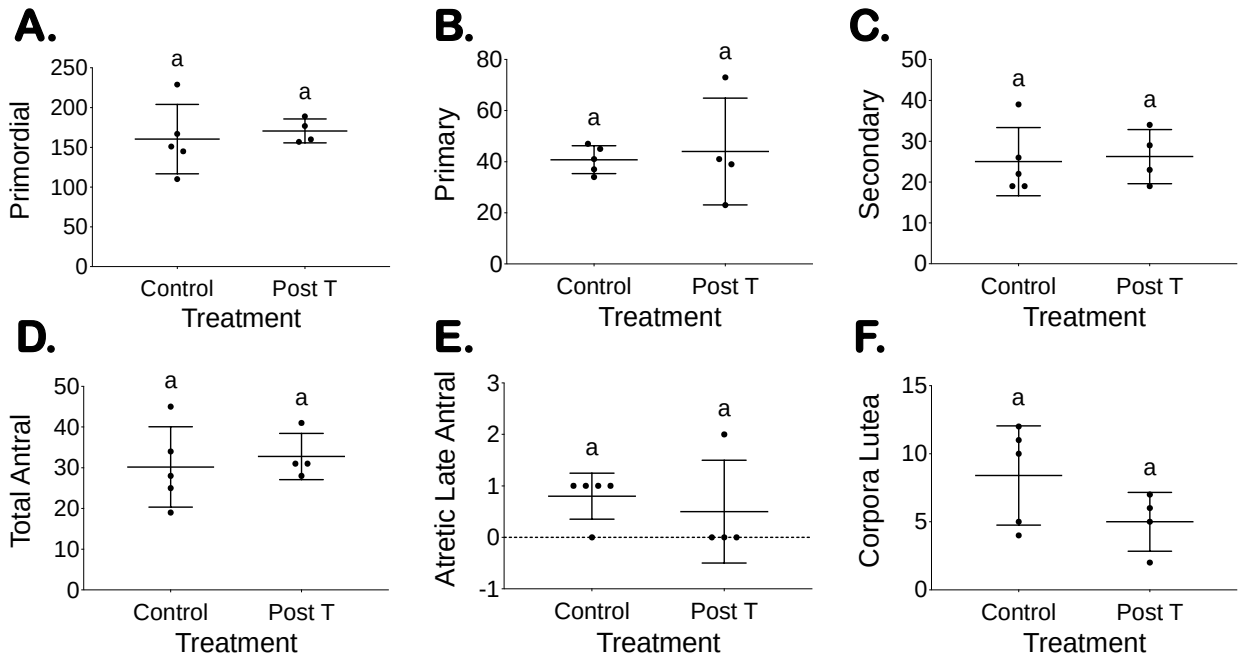

Figure 8. Comparable follicle counts in every 10th section between placebo (control) and T-treated mice sacrificed four cycles after T cessation (post T) for (A) primordial, (B) primary, (C) secondary, (D) total antral, and (E) atretic late antral follicles in addition to (F) corpora lutea.

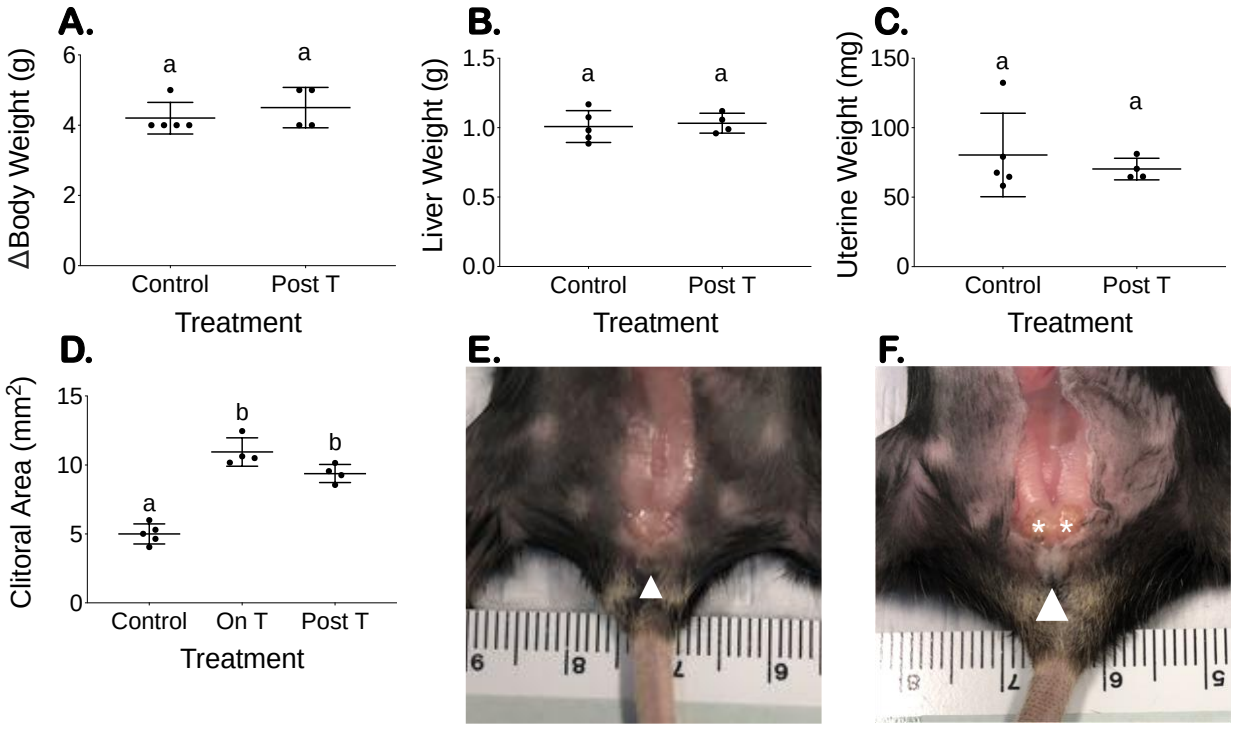

Figure 9. Terminal body measurements comparable except for persistent clitoromegaly. (A) Body weight increase over approximately 9 weeks, (B) terminal liver weight (normalized to terminal average of 22.9 g mouse), and (C) terminal uterine weight (normalized to terminal average of 22.9 g mouse) (mean ± SD). Increased clitoral area measured at 6 weeks on T remains persistently elevated four estrous cycles following T cessation (D) (mean ± SD). Clitoral size remains enlarged in mice post T (F) compared with that in control mice (E); white arrowheads indicate clitoral structure, while asterisks indicate glands enlarged by T therapy that are not readily visible in the control.

3.4.3 Body metrics comparable except for persistent T-induced clitoromegaly

The overall change in body weight (g) over approximately 9 weeks did not significantly differ between the control (4.2 ± 0.4) and T-treated mice (4.5 ± 0.6) (Fig. 9A). Normalized terminal liver and uterine weights were also comparable between control mice (liver: 1.01 ± 0.11 g, uterus: 80 ± 30 mg) and mice post T therapy (liver: 1.03 ± 0.07 g, uterus: 70 ± 8 mg) (Fig. 9B and C). T-treated mice demonstrated significantly increased clitoral areas at 6 weeks on T therapy, which persisted four cycles after T cessation (On T 10.9 ± 1.0 mm^2; Post T 9.4 ± 0.7 mm^2) as compared with the clitoral areas of control mice (5.0 ± 0.7 mm^2) (Fig. 9D, $P<.0001$). The T-induced external clitoral size differences (white arrowheads) and internal gland

enlargement (asterisks) are shown for an example mouse post T (Fig. 9F) as compared to a control mouse (Fig. 9E).

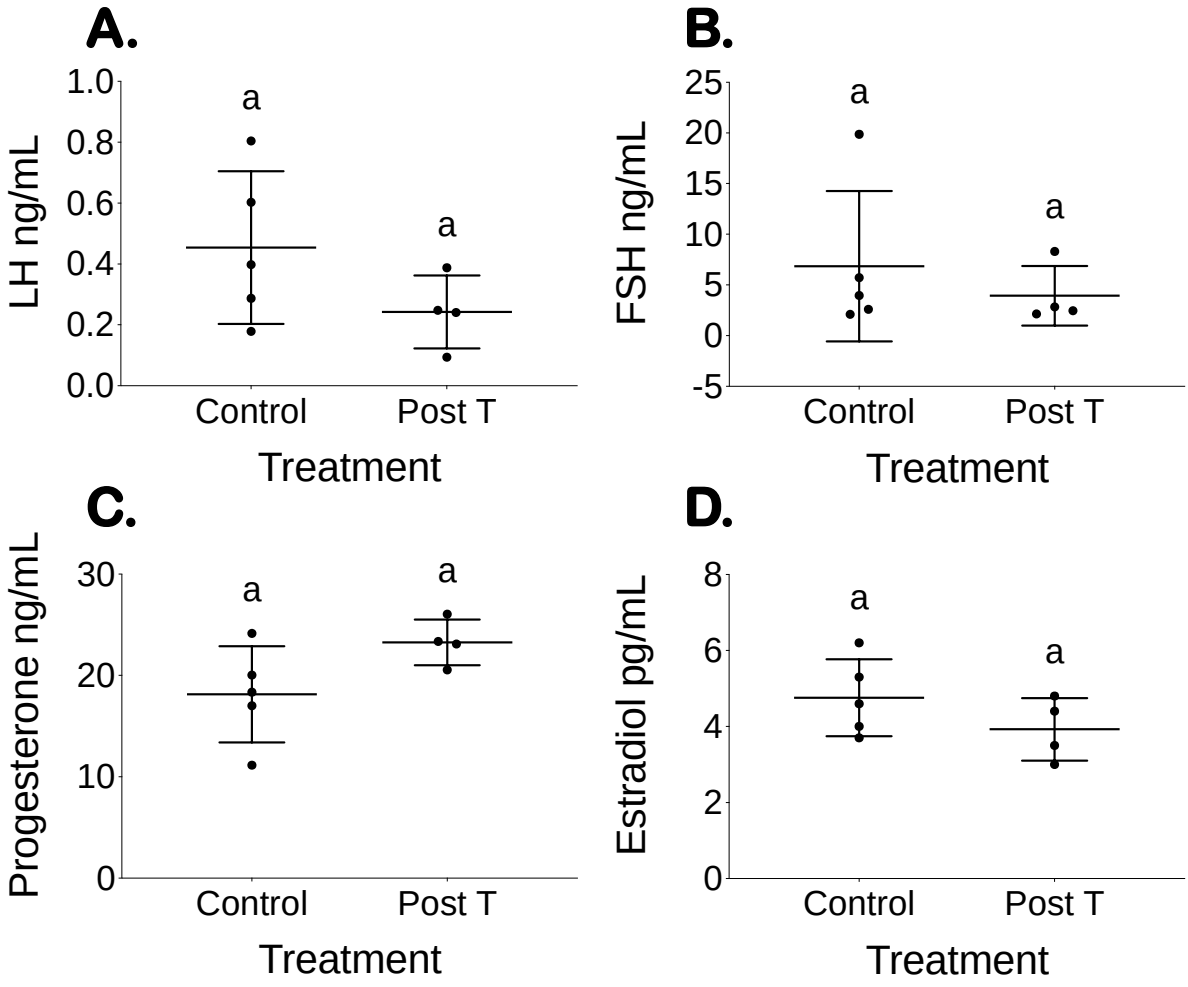

Figure 10. Comparable terminal hormone levels. Terminal (A) LH, (B) FSH, (C) progesterone, and (D) estradiol levels for placebo (control) and T-treated mice four cycles after T cessation (post T) (mean ± SD).

3.4.4 Terminal hormone levels comparable following T cessation

Blood for terminal hormones analyses was collected during diestrus four estrous cycles after T pellet removal or from parallel diestrus controls. After the cessation of T therapy, no detectable differences were observed in the levels (mean ± SD) of LH, FSH, progesterone, or

estradiol in mice post T (LH, 0.2 ± 0.1 ng/mL; FSH, 4 ± 3 ng/mL; progesterone, 23 ± 2 ng/mL; and estradiol, 3.9 ± 0.8 pg/mL) compared with control mice (LH, 0.5 ± 0.3 ng/mL; FSH, 7 ± 7 ng/mL; progesterone, 18 ± 5 ng/mL; and estradiol, 4.8 ± 1.0 pg/mL) (Fig. 10).

3.5 Discussion

In this study, after pellet removal, T-treated mice in persistent diestrus all resumed cycling within a week. Pellet removal allows for a more precise assessment of estrous cycle reversibility timing than has previously been examined.

Our previous study, investigating the effects of injectable T enanthate on postpubertal female mice, demonstrated T-induced persistent diestrus with a lack of corpora lutea (Kinnear *et al.*, 2019). Other studies also noted T-induced persistent diestrus with a lack of corpora lutea in peripubertal mice treated with silastic T implants for 12 weeks (Aflatounian *et al.,* 2020). One recent study found that female mice injected weekly with T cypionate experienced persistent diestrus with a significant reduction in corpora lutea (Bartels *et al.*, 2020). In this study, some mice were followed after T cessation and resumption of cyclicity was reported; however, given that they only measured T levels once in the washout period (6 weeks after their last T injection), they were unable to tightly couple the estrous cycle return timing to the current hormonal milieu. A limitation to models using injectable T, including our previous study, is that subcutaneously injected hormones suspended in oil may take multiple weeks to fully washout (Deanesly and Parkes, 1933). This makes precise determination of T cessation timing difficult to ascertain.

Given the lack of corpora lutea previously noted during T therapy in T-treated female mice (Kinnear *et al.*, 2019), the formation of corpora lutea four cycles after the resumption of cyclicity following T cessation is a promising result. Coupled with prompt estrous cycle return and no detectable differences in terminal diestrus hormone levels, these results suggest possible resumption of regular ovulatory cyclic function. We further assessed the ovarian follicular distribution and did not detect any significant differences between mice after T cessation and their parallel controls. Terminal body parameters, including overall body weight increase, diestrus uterine weight, and liver weight, were comparable between mice after T cessation compared with controls, with the exception of a slight, but not significant reduction in T-induced clitoromegaly. In contrast to our study, Bartels et al. (2020) reported that T-induced clitoromegaly was no longer visually apparent 6–7 weeks after their last T injection, although they did not report the measurements or note if they observed any T-induced internal clitoral gland changes.

The limitations of our study include the 6-week duration of T administration, which may not be reflective of more long-term gender-affirming T therapy in humans. In addition, one T-treated mouse had to be sacrificed early due to vaginal prolapse that began during T therapy. Further investigations of T-induced structural changes to the vaginal epithelium and pelvic floor as well as longer-term assessments of T-induced reproductive changes are needed to completely understand the reproductive consequences of T therapy in transgender men. Although mouse models of gender-affirming T therapy may not fully reflect human physiology, many similarities exist in the reproductive function regulation and ovarian follicle development between mice and

humans (Walters *et al.*, 2012), such that findings from mouse models can be used to guide future clinical research directions.

3.6 Conclusion

In summary, we have shown prompt reversibility of acyclicity in female mice treated with T enanthate pellets for 6 weeks after well-defined pellet removal. After four cycles following T pellet removal, no significant differences were detected in key reproductive parameters between T-treated mice and control mice. Although further work is needed to understand the reversibility of T-induced amenorrhea and possible anovulation in transgender men interested in pausing T therapy to pursue pregnancy or egg donation, our results suggest that cycle return may be tightly coupled to T levels dropping.

3.7 Authors' Roles

H.M.K. and P.H.H. designed the study, obtained and analyzed the data, and drafted the manuscript. C.D.C., G.R., F.L.C., L.N, and M.A.B. contributed to the data acquisition, analysis, and manuscript drafting/review. V.P. and A.S. designed the study and contributed to the data interpretation and manuscript review. M.B.M. conceived and designed the study and contributed to the data interpretation and manuscript review.

3.8 Acknowledgement

The authors thank the University of Virginia Center for Research in Reproduction Ligand Assay and Analysis Core for performing hormone analyses.

3.9 Funding

Supported by National Institutes of Health (R01-HD098233 to M.B.M., F30-HD100163 and T32-HD079342 to H.M.K.), American Society for Reproductive Medicine/Society for Reproductive Endocrinology and Infertility Grant to M.B.M., University of Michigan Office of Research funding (U058227) to A.S. The University of Virginia Center for Research in Reproduction Ligand Assay and Analysis Core is supported by the Eunice Kennedy Shriver National Institute of Child Health and Human Development/National Institutes of Health (National Centers for Translational Research in Reproduction and Infertility) grant (P50-HD28934).

3.10 Conflict of Interest

No authors report competing interests.

Chapter 4 Ovarian Stromal Aberrations Are Present After Testosterone Cessation in a Transgender Mouse Model

Authors: Hadrian M. Kinnear,[1,2] Prianka H. Hashim,[3] Cynthia Dela Cruz,[3] Faith L. Chang,[4] Gillian Rubenstein,[5] Likitha Nimmagadda,[4] Venkateswaran R. Elangovan,[6] Andrea Jones,[4] Margaret A. Brunette,[4] D. Ford Hannum,[7] Jun Z. Li,[7] Vasantha Padmanabhan,[3,6] Molly B. Moravek,[3,8,9] and Ariella Shikanov[1,3,4*]

[1]Program in Cellular and Molecular Biology, [2]Medical Scientist Training Program, [3]Department of Obstetrics and Gynecology, [4]Department of Biomedical Engineering, [5]Women's and Gender Studies Department, [6]Department of Pediatrics and Communicable Diseases, [7]Department of Computational Medicine and Bioinformatics, [8]Division of Reproductive Endocrinology and Infertility, [9]Department of Urology, University of Michigan, Ann Arbor, MI 48109, USA.

4.1 Abstract

Some transmasculine individuals may be interested in pausing gender-affirming testosterone (T) therapy and carrying a pregnancy. The ovarian impact of taking and pausing T is not completely understood. The objective of this study was to utilize a mouse model mimicking transmasculine T therapy to characterize the ovarian dynamics following cessation of T for reproductive purposes. We injected postpubertal 9–10-week-old female C57BL/6N mice once weekly with 0.9 mg of T enanthate in sesame oil or with a sesame oil vehicle control for six

weeks. All T-treated mice stopped cycling and demonstrated persistent diestrus within one week of starting T therapy, while control mice cycled regularly. After 6 weeks of T therapy, one group of T-treated mice and age-matched vehicle-treated diestrus controls were sacrificed. Another group of T-treated mice were maintained after stopping T therapy and sacrificed in diestrus four estrous cycles after the resumption of cyclicity along with age-matched vehicle-treated controls. Ovarian histological analysis revealed marked stromal changes with clusters of large round cells in the post T group as compared to both age-matched controls and mice at six weeks on T. These clusters exhibited strong periodic acid-Schiff staining for polysaccharides, suggesting potential phagocytic function. Notably, many of these cells also demonstrated intense positive staining for macrophage markers CD68 and Cd11b. Ovarian RNA sequencing also found upregulation of immune pathways post T as compared to age-matched controls and ovaries at six weeks on T. Cessation of T therapy for a longer duration may be required for normalizing the ovarian phenotype.

4.2 Introduction

Transmasculine individuals may utilize gender-affirming testosterone (T) therapy, typically via intramuscular or subcutaneous injections or via transdermal applications (Hembree *et al.*, 2017). Although current clinical guidelines encourage discussion of fertility preservation prior to starting T therapy (Coleman *et al.*, 2011; Ethics Committee of the American Society for Reproductive Medicine, 2015; Hembree *et al.*, 2017), emerging literature suggests that individuals may be able to use their gametes for reproduction after being on T (Light *et al.*, 2014, 2018; Ellis *et al.*, 2015; Broughton and Omurtag, 2017; Adeleye *et al.*, 2019; Leung *et al.*, 2019; Amir *et al.*, 2020; Falck *et al.*, 2020; Greenwald *et al.*, 2021; Moseson *et al.*, 2021). In particular,

some transmasculine individuals may be interested in pausing T to carry a pregnancy. Although several studies have documented transmasculine pregnancies after varied durations of T therapy, these studies often selected for individuals with successful pregnancies and so do not provide information about individuals who may have had difficulty conceiving or carrying to term (Light *et al.*, 2014; Ellis *et al.*, 2015; Falck *et al.*, 2020). In particular, the impact on the ovary of taking and pausing T is not well understood. As ovaries can provide both the oocyte and early hormonal support for a pregnancy, a better understanding of ovarian dynamics offers relevant reproductive information to transmasculine individuals considering pausing T to pursue pregnancy.

Several T-induced changes to ovarian follicles and corpora lutea have been reported, generally based on histology collected during gender-affirming oophorectomies. T has been shown to suppresses menstrual cycles, potentially due to androgen-induced negative feedback at neural and pituitary levels (Esparza *et al.*, 2020). Given this menstrual suppression, human ovaries often display increased cystic or atretic follicles and sparse or absent corpora lutea (Moravek *et al.*, 2020). Encouragingly, a relatively normal cortical distribution of primordial to primary follicles has been reported from analyses of human ovaries on T (De Roo *et al.*, 2017). We have developed a mouse model mimicking transmasculine T therapy and found an increase in atretic large antral follicles in C57BL/6N mice at six weeks on T, with no detectable loss in primordial follicles (Kinnear *et al.*, 2019). In these mice, we also reported no corpora lutea in mice on T (Kinnear *et al.*, 2019). Bartels *et al.* subsequently performed 6 weeks of T injections in CF-1 mice and reported a reduction in corpora lutea in T-treated mice and no detectable differences in antral or atretic antral follicles (Bartels *et al.*, 2020). Encouragingly, these mice produced fertilizable eggs with superovulation on T (Bartels *et al.*, 2020). Bartels *et al.* noted

that their approach matches a clinical situation where the transmasculine individual does not plan to carry the pregnancy themselves at that time and they do not report a thorough ovarian histological comparison after washout (Bartels *et al.*, 2020). For transmasculine individuals interested in carrying a pregnancy, T should be paused and it is important to consider both follicular development and corpora lutea formation after T cessation and washout. In a previous study focused on resumption of cyclicity, we have noted that after T implants were removed at six weeks, C57BL/6N mice promptly started to cycle and ovaries formed corpora lutea after four estrous cycles (Kinnear *et al.*, 2021). Beyond our previous study, there is limited literature looking at ovarian histology if T is paused for reproductive purposes.

Notable T-induced changes to the ovarian stroma have also been reported for transmasculine individuals. Studies have reported increased collagenization of the tunica albuginea or outer cortex (Futterweit and Deligdisch, 1986; Spinder *et al.*, 1989; Chadha *et al.*, 1994; Ikeda *et al.*, 2013), stromal hyperplasia (Futterweit and Deligdisch, 1986; Spinder *et al.*, 1989; Pache *et al.*, 1991; Grynberg *et al.*, 2010; Ikeda *et al.*, 2013), and luteinization of stromal cells for individuals on T (Futterweit and Deligdisch, 1986; Spinder *et al.*, 1989; Pache *et al.*, 1991; Ikeda *et al.*, 2013), which are characteristics also frequently observed in polycystic ovary syndrome (Hughesdon, 1982). There has been minimal investigation of this stromal hyperplasia or luteinization beyond descriptive observations. Recent reports have demonstrated similar stromal changes in polycystic ovary mouse models using mice treated with dihydrotestosterone (DHT) (Candelaria *et al.*, 2019; Sun *et al.*, 2019). Mice showed clusters in the ovarian stroma of hyperplastic and lipid-filled cells after two months of DHT treatment starting at postnatal day 25 (Candelaria *et al.*, 2019). Similarly, Sun et al., 2019 observed a DHT-induced hypertrophic lipid-

filled stroma after 60 days of DHT treatment starting at postnatal day 25 (Sun *et al.*, 2019). Cellular characterization of prolonged T- or DHT-induced changes to the ovarian stroma has been challenging, in part due to the fact that many of the cell types of the ovarian stroma are not well understood (Kinnear *et al.*, 2020).

Investigating ovarian histological changes if T is paused for reproductive purposes is logistically difficulty in human patients. Mouse models of gender-affirming T therapy can help to fill this gap. We previously removed T implants after six weeks and compared mice four cycles after resumption of cyclicity (Kinnear *et al.*, 2021). As gender-affirming T therapy is frequently injection-based, the objective of this study was to utilize an injection-based mouse model mimicking transmasculine T therapy to characterize the ovarian dynamics if T is paused for reproductive purposes. Unexpectedly, this study design allowed us to capture ovaries after T cessation in the midst of notable stromal changes and to subsequently probe more deeply into this unusual stromal state.

4.3 Materials and Methods

4.3.1 Ethical approval

All animal work was conducted in compliance with a protocol approved by the University of Michigan Institutional Animal Care & Use Committee (PRO00007618, PRO00009635).

4.3.2 Experimental design

This study used forty C57BL/6NHsd female mice (Envigo, Indiana, IN, USA). Mice were housed in groups of five in ventilated cages and had free access to food and water and a 12-hour light/dark cycle within a non-barrier facility at the University of Michigan. Mice started T therapy at 9–10 weeks old (body mass 18.7 ± 0.7, mean ± SD). Controls received a sesame oil only injection. T therapy was administered via a weekly (Thurs PM) subcutaneous mid-back injection (100 μL). Each dose included 0.9 mg T enanthate, diluted with sesame oil from a 200 mg/mL stock (Hikma Pharmaceuticals, Portugal). Sesame oil was sterile filtered before use (USP/NF grade, Welch, Holme & Clark Co., Inc., Newark, NJ, USA). All T-treated mice (n = 20) were treated with T for six weeks. At six weeks on T, one cohort was sacrificed ("On T," n = 10) and compared to parallel age-matched controls ("Control for On T or Control OT," n = 10). In a separate cohort, T was stopped after 6 weeks and allowed to washout. These mice were followed until resumption of estrous cyclicity and sacrificed after 4 estrous cycles ("Post T," n = 10), with parallel age-matched controls ("Control for Post T or Control PT," n = 10). All mice were sacrificed in diestrus and ovaries were collected for further analysis.

4.3.3 Vaginal cytology

Vaginal cytology was collected daily starting 2–3 weeks prior to the first T injection and continuing until sacrifice. The distribution of leukocytes, cornified epithelial cells, and nucleated epithelial cells was evaluated to determine estrous cycle stage.

4.3.4 Blood collection and hormone analysis

Blood for T analysis was collected from the lateral tail vein at volumes not exceeding 0.5% of the bodyweight at the midpoint between doses (Mon AM). Terminal blood collection

was performed via cardiac puncture under isoflurane anesthesia. After overnight storage at 4°C, blood samples were centrifuged for 10 min (≤8100G) and serum was collected and stored until analysis at -20°C. Hormone analyses were performed by the Ligand Assay and Analysis Core Facility at the University of Virginia Center for Research in Reproduction. The reportable range for a coefficient of variance <20% for the Testosterone Mouse and Rat enzyme-linked immunosorbent assay was 0.10–16 ng/mL or 0.20–32 ng/mL with a 2x dilution (Immuno-Biological Laboratories, Inc.; Minneapolis, MN, USA).

4.3.5 Ovarian histological and follicular distribution analysis

Mouse ovaries within perigonadal fat (one per mouse) were fixed overnight at 4°C in Bouin's fixative (n = 5/group) or 4% paraformaldehyde (n= 5/group), paraffin-embedded at the University of Michigan School of Dentistry Histology Core, serially sectioned (5μm) with 5 sections per slide, and stained with hematoxylin and eosin (every other slide). All imaging was conducted using a light microscope (DM1000, Leica, Germany). Bouin's fixed ovaries were used for follicular distribution analyses, corpora lutea counts, and periodic acid-Schiff staining. Paraformaldehyde fixed ovaries were used for immunohistochemical analyses and corpora lutea counts. Counters were blinded to experimental group. Primordial, primary, and secondary follicles were counted in every 10^{th} section throughout one entire ovary per mouse at 20-40x magnification. For corpora lutea and antral follicle counts, images at 5x magnification were taken of every 10^{th} section and analyzed alongside each other to prevent overcounting. Primordial follicles were identified by an oocyte with a single squamous granulosa cell layer, primary follicles by an oocyte with a single cuboidal granulosa cell layer, and secondary follicles by an oocyte with two or more granulosa cell layers. To prevent overcounting, we counted primordial and primary follicles with a visible nucleus and secondary follicles with a visible

nucleolus. Discrete round structures with eosinophilic cytoplasm were identified as corpora lutea. Antral follicles were determined by the presence of antral fluid. Atretic late antral follicles were defined as an oocyte lacking connection to granulosa cells and an attenuated granulosa cell layer in a follicle with a well-defined antrum.

4.3.6 Ovarian immunohistochemical analysis & periodic acid-Schiff staining

Ovarian samples fixed in 4% paraformaldehyde, paraffin-embedded and serially sectioned (5μm sections, 5 sections/slide) were used for immunohistochemical analyses. Samples were deparaffinized with xylenes (2 x 10 min), re-hydrated in an ethanol series (100/90/70/50/30/0%, 5 min each), treated for 30 minutes at room temperature with a peroxide block, rinsed in deionized water and followed with 20 minutes of heat-mediated antigen retrieval in 0.1 M sodium citrate buffer pH 6 using a steamer, permeabilized using tris-buffered saline (TBS) with 0.1% Triton X 100 (TBS-T, 2 x 3 min), blocked for 1 hour at room temperature in TBS with 10% normal goat serum (NGS), and incubated overnight at 4°C with primary antibody in TBS with 1% NGS. On the following day, samples were washed with TBS-T/TBS (2 x 3 min each), and biotinylated goat anti-rabbit secondary was added for 10 minutes at room temperature (Abcam rabbit specific HRP/DAB detection IHC kit ab64261, Abcam, Cambridge, UK). After a TBS-T/TBS wash (2 x 3 min each), strepdavidin peroxidase was added for 10 minutes at room temperature (ab64261 kit). After another TBS-T/TBS wash (2 x 3 min each), 3,3'-diaminobenzidine was added for 10 minutes at room temp (ab64261 kit). Samples were then washed with DI water (1 min), counterstained with hematoxylin (2 min with tap water rinse), followed by an ethanol series (30/50/70/90/100%, 5 min each) and xylenes (2 x 10 min) after which samples were mounted with Permount. Additional positive control tissues and secondary only controls for non-specific staining were utilized. Primary antibodies were used at dilutions in

alignment with manufacturer recommendations: Anti-CD68 (rabbit polyclonal, ab125212, Abcam, dilution 1:500), Anti-CD11b (rabbit monoclonal, ab133357, Abcam, dilution 1:4000). A periodic acid-Schiff staining kit (Sigma-Aldrich Inc., St Louis, MO, 395B) was utilizing to stain Bouin's fixed ovaries that were paraffin-embedded and serially sectioned (5μm sections, 5 sections/slide). Slides were deparaffinized in xylenes (2 x 10 min), rehydrated in an ethanol series (100/90/70/50/30/0%, 5 min each), immersed in periodic acid solution for 5 minutes at room temperature, washed with DI water (3 x 3 min), immersed in Schiff's reagent for 15 minutes at room temperature, washed in running tap water for 5 minutes, and counterstained with hematoxylin (90 seconds with tap water rinse), followed by an ethanol series (30/50/70/90/100%, 5 min each) and xylenes (2 x 10 min) after which samples were mounted with Permount. All samples (n= 3–5 mice/group) were imaged with a light microscope (DM1000, Leica, Germany).

4.3.7 Ovarian RNA-sequencing analysis

Mouse ovaries were micro dissected from perigonadal fat at the time of sacrifice and stored frozen in RNAlater at -20°C. Tissue disruption and homogenization were performed using the Kimble Biomasher II and QIA shredder homogenizer. RNA was extracted following manufacturer instructions using the Qiagen RNeasy Mini Kit with Qiagen RNase-Free DNase set and subsequently stored at -80°C. Paired-end RNA sequencing with poly-A selection was performed by the University of Michigan Advanced Genomics Core on the Illumina NovaSeq PE150 using 7.5% of a 300 cycle S4 shared flow cell with 30–40 million reads per sample. Read mapping and counts were performed by the Advanced Genomics Core. Reads were trimmed using Cutadapt v2.3 (Martin, 2011), FastQC v0.11.8 (Andrews, 2010) was used to ensure data quality and Fastq screen v0.13.0 (Wingett and Andrews, 2018) was used to screen for various types of contamination. Reads were mapped to the reference genome GRCm38 (ENSEMBL)

using STAR v2.7.8a (Dobin *et al.*, 2013) and count estimates assigned to genes with RSEM v1.3.3 (Li and Dewey, 2011). Differential expression was analyzed using DESeq2 (Love *et al.*, 2014). Gene enrichment was assessed via LRpath using GO biological process with 50–500 genes, a p-value cutoff of 0.05 and directional analysis for mouse samples identified with Entrez gene IDs (Kim *et al.*, 2012).

4.3.8 Statistical analysis

GraphPad Prism 9 was used for data analysis. One mouse was the unit of analysis. The Shapiro-Wilk normality test was used to determine parametric and non-parametric testing. Welch's t-test and Brown-Forsythe and Welch's one-way analysis of variance with Dunnett's T3 multiple comparisons test were used for parametric testing. Mann-Whitney and Kruskal-Wallis with Dunn's multiple comparisons test were used for non-parametric testing. P-values less than 0.05 were considered statistically significant.

4.4 Results

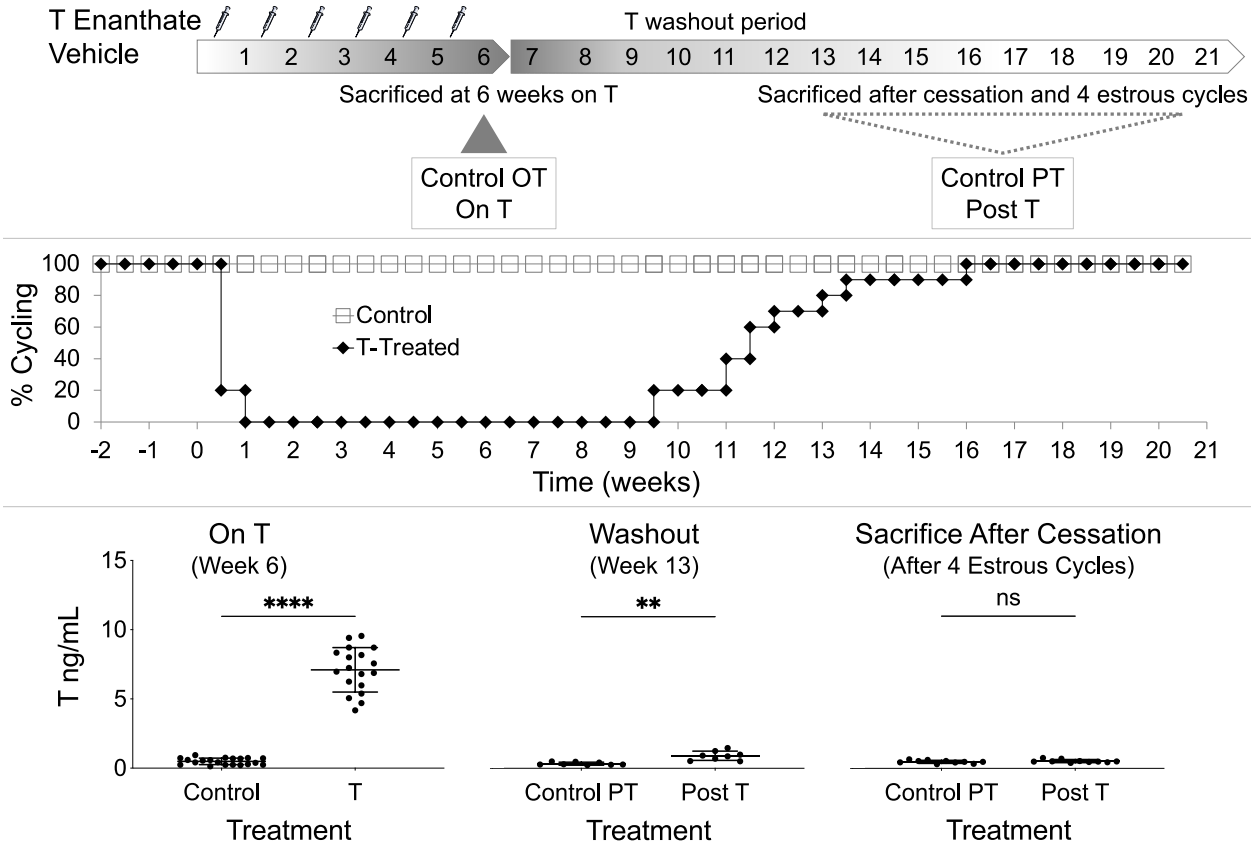

Figure 11. Experimental design, cyclicity, and T levels. (Top) Experimental design of the 4 study groups: mice sacrificed at 6 weeks on T (On T), parallel age-matched controls for On T (Control OT), mice sacrificed after T cessation and 4 estrous cycles after resumption of cyclicity (Post T), and parallel age-matched controls for Post T (Control PT). (Middle) All T-treated mice stopped cycling within 1 week of starting T and it took 3.5–10 weeks after T cessation at 6 weeks for mice to resume cycling. (Bottom) T levels (ng/mL, mean ± SD) were elevated during T therapy (at 6 weeks on T, $P<0.0001$), were slow to washout with mean T levels still elevated 7 weeks into the washout period (at week 13, $P<0.01$), and were not detectably different from controls when mice were sacrificed 4 estrous cycles after resumption of cyclicity.

4.4.1 Mice stop cycling during T therapy and resume cycling as T slowly washes out

Within one week of starting T-injections, all T-treated mice stopped cycling and demonstrated persistent diestrus on vaginal cytology (Fig. 11, middle). After cessation of T injections at 6 weeks, mice subsequently took 3.5–10 weeks to resume cycling (Fig. 11, middle). All control mice cycled throughout the study (Fig. 11, middle). T levels (ng/mL, mean ± SD)

were significantly elevated (P<0.0001) in T-treated mice (7.1 ± 1.6) as compared to controls (0.5 ± 0.2) when measured at 6 weeks on T (Fig. 11, bottom). T injections were slow to washout and average T levels were still significantly elevated (0.9 ± 0.3) as compared to controls (0.3 ± 0.1) 7 weeks into the washout period (at week 13) (P< 0.01, Fig. 11, bottom). Mice were sacrificed 4 estrous cycles after resumption of cyclicity, at which point T levels (0.53 ± 0.11) were not significantly different from controls (0.48 ± 0.11, Fig. 11, bottom).

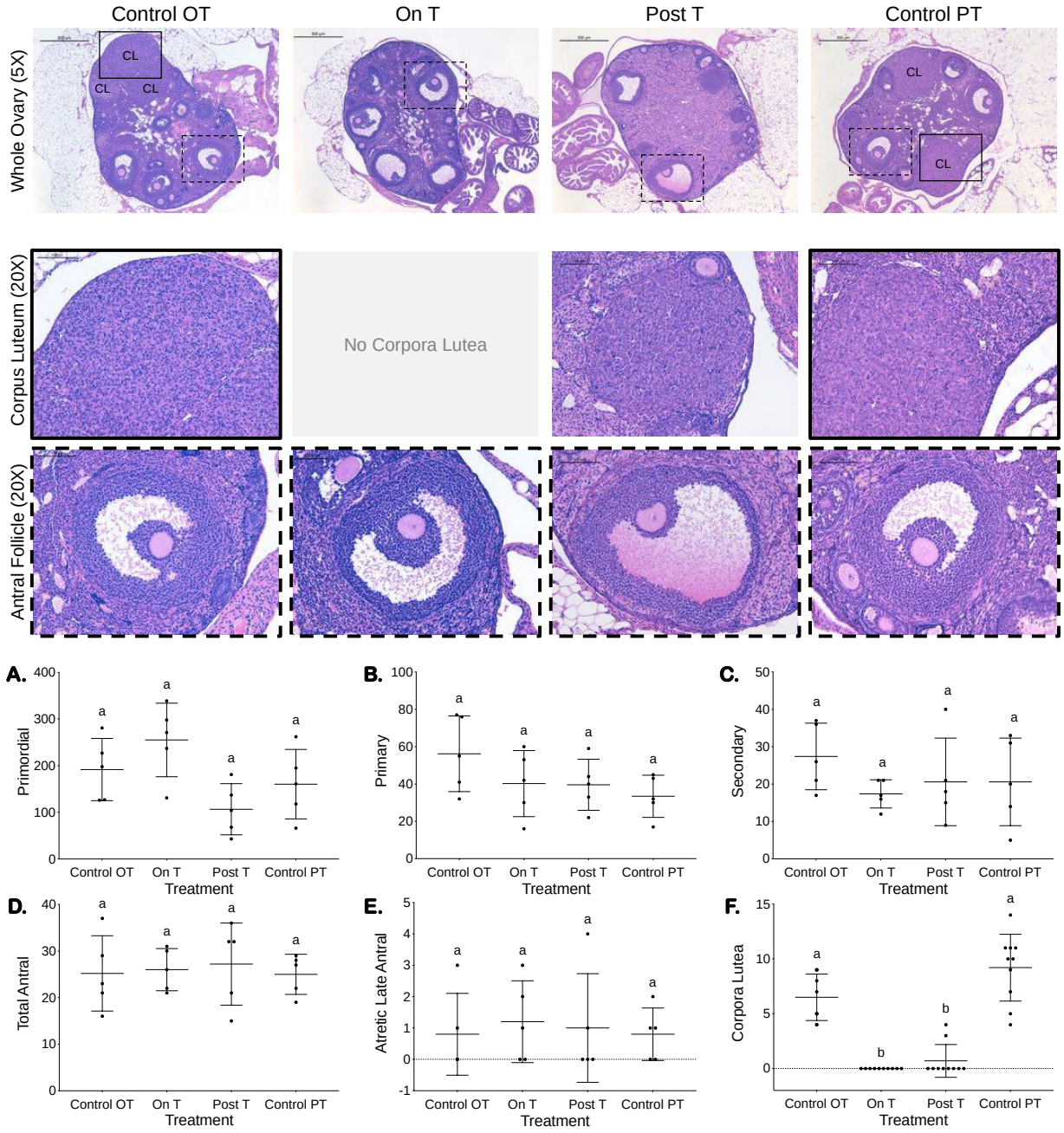

Figure 12. Reduced corpora lutea on T and post T with otherwise comparable follicular distributions. Images of hematoxylin and eosin-stained ovaries from all four groups (Control OT, On T, Post T, and Control PT). Row 1 includes a representative hematoxylin and eosin-stained ovary (5X, scale 500 µm) from each group, while row 2 highlights example corpora lutea (20X, solid outline corresponding to location in 5X image, scale 100 µm), and row 3 highlights example antral follicles (20X, dashed outline corresponding to location in 5X image, scale 100 µm). Follicle counts from every 10th section for primordial (A), primary (B), and secondary (C) follicles. Follicle counts based on 5X images of every 10th section for total antral (D) and atretic late antral (E) follicles as well as corpora lutea (F).

4.4.2 Reduced corpora lutea On T and Post T with otherwise comparable follicular distributions

Figure 12 displays a representative hematoxylin and eosin-stained ovary (5X) with magnified views of corpora lutea and antral follicles (20X) from each group. Corpora lutea were not observed in ovaries from any mice on T and were only seen for 2 of 10 mice post T, with counts (mean ± SD) significantly lower than for control ovaries (Control OT 6.5 ± 2.1, On T 0 ± 0, Post T 0.7 ± 1.5, Control PT 9.2 ± 3.0, Fig. 12F). No other significant differences were detected in follicle counts (mean ± SD) for primordial follicles (Control OT 192 ± 67, On T 255 ± 79, Post T 107 ± 55, Control PT 160 ± 75, Fig. 12A), primary follicles (Control OT 56 ± 20, On T 40 ± 18, Post T 40 ± 14, Control PT 33 ± 11, Fig. 12B), secondary follicles (Control OT 27 ± 9, On T 17 ± 4, Post T 21 ± 12, Control PT 21 ± 12, Fig. 12C), total antral follicles (Control OT 25 ± 8, On T 26 ± 5, Post T 27 ± 9, Control PT 25 ± 4, Fig. 12D), or atretic late antral follicles (Control OT 0.8 ± 1.3, On T 1.2 ± 1.3, Post T 1.0 ± 1.7, Control PT 0.8 ± 0.8, Fig. 12E).

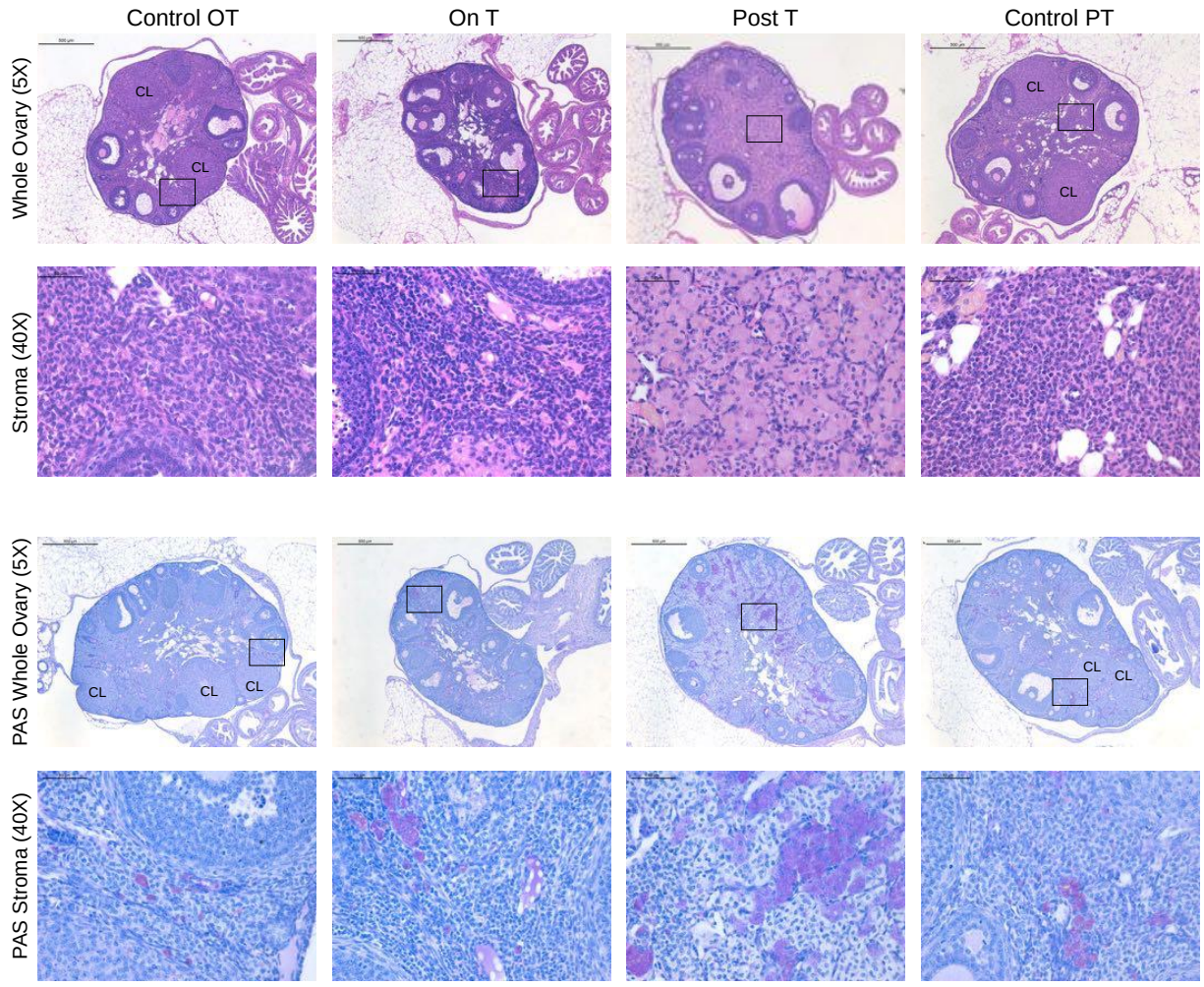

Figure 13. Ovarian stromal changes post T. Columns correspond to the four groups: Control OT, On T, Post T, and Control PT. Row 1 includes a representative hematoxylin and eosin-stained ovary (5X, scale 500 µm) from each group, with the corresponding magnified view of the ovarian stroma in row 2 (40X, scale 50 µm). Row 3 includes a representative periodic acid-Schiff-stained ovary (5X, scale 500 µm) from each group, with the corresponding magnified view of the ovarian stroma in row 4 (40X, scale 50 µm).

4.4.3 Stromal changes in ovaries Post T

While examining the follicular distributions in hematoxylin and eosin-stained ovaries, we unexpectedly found marked ovarian stromal changes in Post T ovaries, including the presence of large round eosinophilic cells, some of which were in clusters (Fig. 13, rows 1 and 2). These changes occurred throughout the stroma of most of the Post T ovaries. A few similar cells were seen in ovaries from other groups, including Control PT and On T (Fig. 13, rows 1 and 2). The

stroma in Post T ovaries also displayed increased clusters of cells that stained intensely with periodic acid-Schiff (Fig. 13, rows 3 and 4), which stains polysaccharides, and has been seen in phagocytic cells including ovarian multi-nucleated macrophage giant cells (Briley *et al.*, 2016).

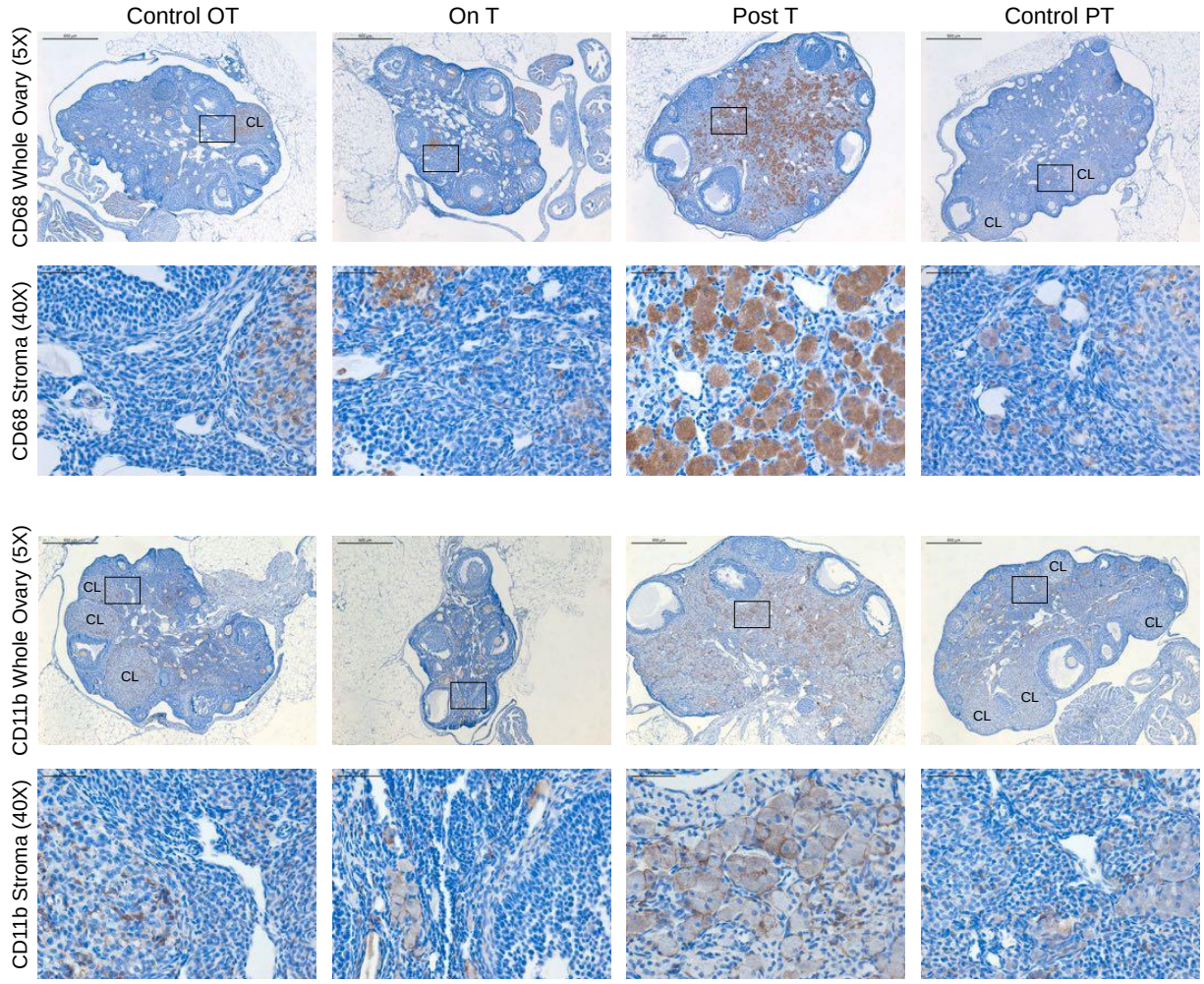

Figure 14. Notable macrophage-associated staining in the ovarian stroma post T. Columns correspond to the four groups: Control OT, On T, Post T, and Control PT. Row 1 includes representative ovarian CD68 staining (5X, scale 500 µm) from each group, with the corresponding magnified view of the ovarian stroma in row 2 (40X, scale 50 µm). Row 3 includes representative ovarian CD11b staining (5X, scale 500 µm) from each group, with the corresponding magnified view of the ovarian stroma in row 4 (40X, scale 50 µm).

4.4.4 Notable macrophage-associated staining in the ovarian stroma Post T

Given this increase in periodic acid-Schiff staining, we conducted immunohistochemical staining for two macrophage-associated markers, CD68 and Cd11b. Although these stains

revealed the presence of macrophages in all ovaries, both CD68 (Fig. 14, rows 1 and 2) and CD11b (Fig. 14, rows 3 and 4) demonstrated uniquely prominent expression in the large and rounded cells of ovarian stroma Post T.

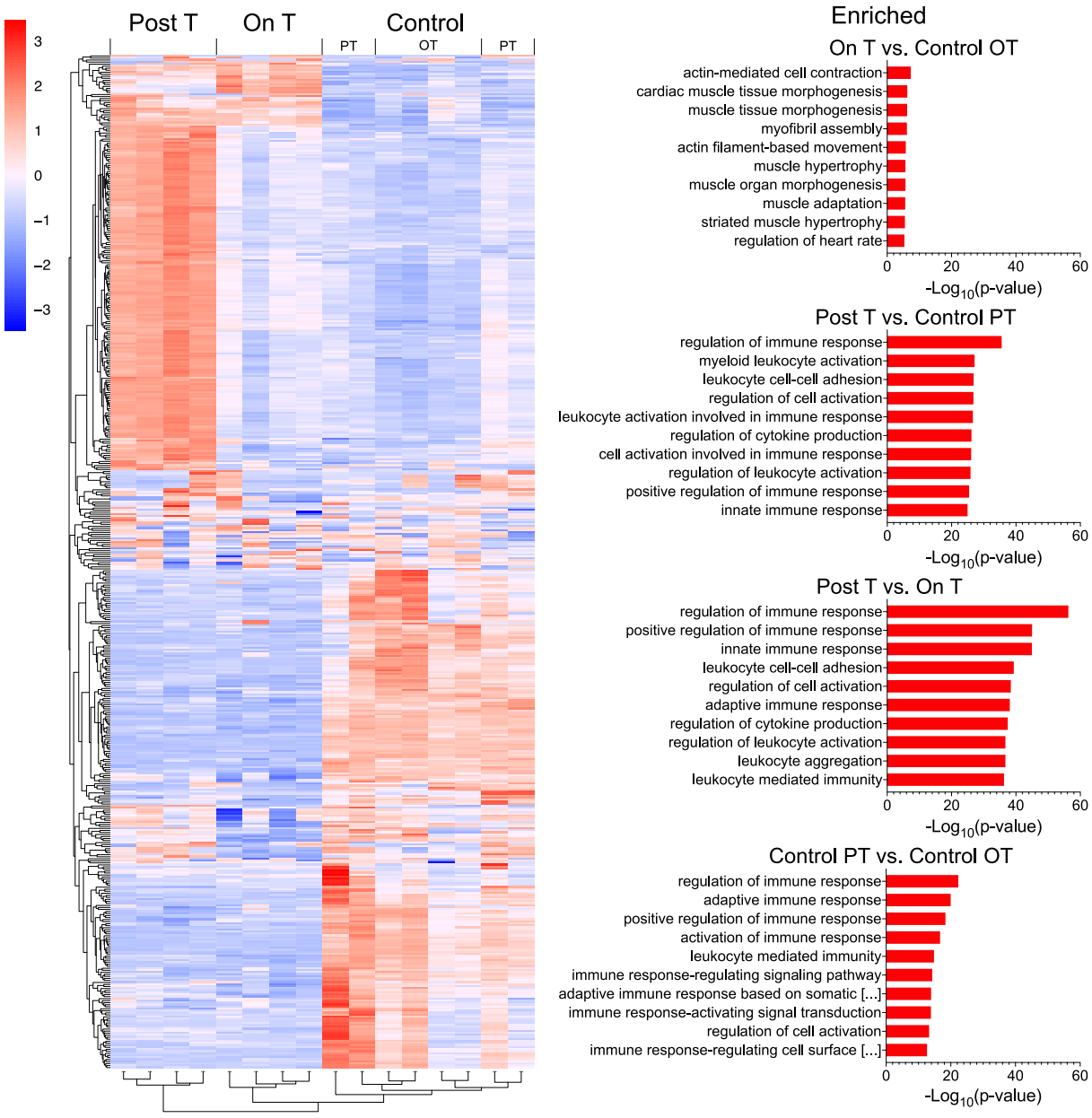

Figure 15. Immune pathway upregulation seen post T as compared to control PT and on T. Heatmap of the top 500 variably expressed genes from whole ovary RNA-sequencing (n = 4 mice per group, 1 ovary each). The top 10 gene ontology biological process terms from LRpath for genes enriched in the following 4 comparisons: On T vs Control OT, Post T vs Control PT, Post T vs On T, and Control PT vs Control OT. In Control PT vs Control OT, the two titles too long to fully display as shown by […] are: "adaptive immune response based on somatic recombination of immune receptors built from immunoglobulin superfamily domains" and "immune response-regulating cell surface receptor signaling pathway."

4.4.5 Immune pathway upregulation seen Post T as compared to Control PT and On T

Whole ovary bulk RNA-sequencing (n = 4 mice per group, 1 ovary each) demonstrated differences in ovarian gene expression between groups. A heatmap of the top 500 variably expressed genes shows a set of highly upregulated (red) genes for mice Post T that are not observed for mice on T or for any of the controls (Fig. 15, heatmap top left). Analysis in *LRpath* suggests immune pathway upregulation Post T when compared to Control PT or On T groups, with the majority of the top 10 gene ontology biological process terms for these comparisons relating to immune system function (Fig. 15, right).

4.5 Discussion

Transmasculine individuals may be interested in pausing gender-affirming T to carry a pregnancy, but there are gaps in knowledge regarding the ovarian impact of taking and pausing T. In this study, we utilized an injection-based mouse model mimicking transmasculine T therapy to characterize ovarian dynamics on T and after T cessation. Unexpectedly, we were able to capture ovaries after T cessation (Post T) in the midst of notable stromal changes with abundant large round cell clusters (Fig. 13). Comparable changes were not observed in parallel age-matched controls (Control PT) or in mice on T for 6 weeks (On T) (Fig. 13). We subsequently pursued additional analyses aimed at characterizing these ovarian stromal changes in our mice Post T. Due to the technical limitations of our injection-based study design, we cannot separate out whether it is the additional duration of T present during the washout or the removal of T and resumption of cycling (or both) that led to these stromal changes.

For further characterization of the ovarian stroma, we performed periodic acid-Schiff staining. Periodic acid-Schiff stains polysaccharides and strong periodic acid-Schiff staining has been previously reported in multinucleated macrophage giant cells present in the ovaries of aging mice (Briley *et al.*, 2016). As we observed intense periodic acid-Schiff staining in the ovarian stroma Post T (Fig. 13), we then conducted immunohistochemical staining for macrophage markers. An abundance of these enlarged ovarian stromal cells stained positive for CD68 in mice Post T in contrast to age-matched controls (Control PT) and to mice on T for 6 weeks (On T) (Fig. 14). CD68 is a common macrophage marker, as macrophages highly express CD68 in cell surface, lysosomal, and endosomal membranes (Chistiakov *et al.*, 2017). CD68 is also expressed in other cell types, including other mononuclear phagocytes (such as microglia, osteoclasts, and myeloid dendritic cells), with lower levels found in other cell types (Chistiakov *et al.*, 2017). We further stained for Cd11b, a marker of macrophages and other myeloid cells (Carlock *et al.*, 2013), and noted a similar pattern of increased expression in the stroma Post T (Fig. 14). In alignment with these observed histologic changes representing a stromal immune response with an abundance of macrophages, we found significant upregulation of immune response pathways in a whole ovary RNA sequencing analysis for Post T mice as compared to age-matched controls (Control PT) and mice on T for six weeks (On T) (Fig. 15).

Macrophages are a predominant immune cell type in the ovary and appear to play critical physiologic roles through both phagocytic and secretory functions (reviewed in Wu *et al.*, 2004). They typically are present at low levels in immature or resting ovaries, increase around ovulation near the theca vasculature, and migrate into developing corpora lutea (Norman and Brannstrom, 1994). Ablation of macrophages and other myeloid cells using Cd11b-DTR mice led to infertility

and hemorrhagic ovaries with impaired corpora lutea (Turner *et al.*, 2011; Care *et al.*, 2013). There appear to be multiple subsets of ovarian macrophages and macrophage changes in the mouse ovary are likely dynamic over the course of the estrous cycle (Carlock *et al.*, 2013; Pepe *et al.*, 2018). Macrophages changes also occur with ovarian aging, with a unique population of multinucleated macrophage giant cells noted in aging mouse ovaries that were not seen in younger mice (Briley *et al.*, 2016). Inflammaging refers to aging-related chronic inflammation, which has been demonstrated in mouse ovaries with corresponding increases in immune-related genes and immune cell populations (Zhang *et al.*, 2020; Lliberos *et al.*, 2021). We noted an increase in immune response pathways in older (Control PT) versus younger (Control OT) control mice (Fig. 15). Importantly, enrichment for immune response pathways held for Post T mice when compared to their corresponding age-matched controls (Control PT) and there was a categorical difference in staining for macrophage markers, with intense staining observed for the majority of the stroma Post T and only for few cells in the Control PT stroma (Fig. 14).

Some similar ovarian stromal changes have been previously noted in DHT-treated mice (Candelaria *et al.*, 2019; Sun *et al.*, 2019). Stromal cells from DHT-treated mice have been shown to stain positive for adipocyte differentiation-related protein (Sun *et al.*, 2019), a marker of lipid droplets, and potentially consistent with a lipid-laden macrophage phenotype. Importantly, both studies in DHT-treated mice mentioned resolution of these stromal changes, suggesting that this may be a transient state. Candelaria et al., reported resolution of stromal changes with superovulation and Sun et al., reported resolution 30 days after DHT capsule removal (Candelaria *et al.*, 2019; Sun *et al.*, 2019). At present, the functional impact of these stromal changes has not been determined. If these stromal changes do indeed represent a

transient state, waiting for more time or potentially using gonadotropin stimulation could be recommended for individuals coming off of T to try to conceive.

Although our study design does not provide a means of testing these hypotheses, we speculate that this stromal expansion represents a transient state after prolonged T-induced anovulation. Residual cells from follicular atresia may have built up in the stroma and some may respond to luteinizing stimuli and possibly trigger immune infiltration. Perhaps the cyclic immune regulation of the corpora lutea formation and regression process has lost some boundaries and spread throughout the stroma. If superovulation including a luteinizing dose of human chorionic gonadotropin could help resolve a similar stromal phenotype (Candelaria *et al.*, 2019), perhaps LH surge levels are not yet sufficient for ovulation with regular corpora lutea formation. As time has also helped resolve a similar stromal phenotype (Sun *et al.*, 2019), perhaps time allows LH surge levels to fully return and immune cells to finish clearing atretic residual luteinizing cells in the stroma.

Outside of the scope of this paper, our RNA-sequencing data suggests additional pathways for future study. We noted an enrichment of muscle-related pathways for ovaries on T when compared to age-matched controls, suggestive of potential myofibroblast or smooth muscle changes (Fig. 15). We found a depletion in ovaries on T as compared to age-matched controls for pathways related to transforming growth factor beta stimulus and lipid biosynthetic processes, encouraging additional exploration of T-induced ovarian hormonal and metabolic changes.

4.6 Acknowledgements

The authors thank the University of Michigan Advanced Genomics Core and University of Michigan Bioinformatics Core for their support with RNA sequencing and initial data processing and the University of Virginia Center for Research in Reproduction Ligand Assay and Analysis Core for their support with hormone analyses.

4.7 Authors' Roles

H.M.K. designed the study, acquired and analyzed the data, and drafted the article. P.H.H. contributed to the study design, data acquisition, and article review. C.D.C. assisted with histological analyses and article review. F.L.C. assisted with RNA sequencing and article review. G.R. and L.N. assisted with histological analyses and article review. V.R.E. and A.J. assisted with RNA sequencing study design and article review. M.A.B. assisted with murine sample collection and article review. D.F.H. and J.Z.L. assisted with RNA sequencing data analysis and article review. V.P. and M.B.M. contributed to overall study design, data interpretation, and article review. A.S. directed the study and contributed to data interpretation and article review.

4.8 Financial Support

This work was supported by National Institutes of Health grants (R01-HD098233 to M.B.M., F30-HD100163 and T32-HD079342 to H.M.K.), American Society for Reproductive Medicine / Society for Reproductive Endocrinology and Infertility Grant to M.B.M., Michigan Institute for Clinical and Health Research grants (KL2 TR 002241 and UL1 TR 002240) to C.D.C., University of Michigan Office of Research funding (U058227) to A.S. The University of

Virginia Center for Research in Reproduction Ligand Assay and Analysis Core was supported by the Eunice Kennedy Shriver NICHD/NIH Grants P50-HD028934 and R24-HD102061.

Chapter 5 Discussion, Reflections, and Future Directions

5.1 Discussion of Findings

Long-term gender-affirming testosterone (T) therapy may negatively impact reproductive capacity for transgender men transitioning from female to male. Given clinical guidelines assuming fertility loss (Hembree *et al.*, 2017) and anecdotal evidence to the contrary (Light *et al.*, 2014), clinicians have minimal data with which to counsel transmasculine individuals interested in harvesting oocytes or carrying a pregnancy after starting T therapy. The impact of T on reproductive potential, the reversibility of this impact, and the ovarian dynamics of taking and pausing T have not been well established (Moravek *et al.*, 2020). The objective of my dissertation was to establish a mouse model of postpubertal gender-affirming T therapy and to utilize this model to evaluate the reversibility of T-induced changes if T is paused for reproductive purposes.

In chapter 2, I demonstrated that after 6 weeks of T injections, T-treated mice presented with acyclicity, elevated T, a reduction in serum luteinizing hormone levels, and ovarian perturbations including a lack of corpora lutea and an increased number of atretic late antral follicles. These findings are similar to changes seen with transmasculine individuals on T and support the use of mouse models of gender-affirming T therapy for reproductive inquiry (Kinnear *et al.*, 2019).

In chapter 3, I investigated the reversibility of T-induced persistent diestrus in a model that allows for well-defined T cessation timing. I found that after 6 weeks of T therapy using subcutaneously implanted commercial pellets, mice promptly resumed cycling within a week of pellet removal. I tracked weekly T levels during the 6-week administration period and for 3

weeks after cessation, demonstrating a close temporal relationship between the return of estrous cyclicity and T levels dropping to control levels after pellet removal. Four cycles after T cessation, ovarian histological analyses from T-treated mice were comparable to controls, including the formation of corpora lutea. This tight coupling of cycle return and T cessation had not been previously established, and supports a return of regular cyclic ovulatory function following T cessation. These findings may be relevant to understanding the reversibility of T-induced amenorrhea and possible anovulation in transgender men interested in pausing T to pursue pregnancy or oocyte donation (Kinnear *et al.*, 2021).

In chapter 4, I found that a longer exposure to elevated T after a prolonged washout following 6 weeks of T injections resulted in an aberrant ovarian stromal phenotype and reduced number of corpora lutea four estrous cycles after T cessation. Immunohistochemical staining for macrophage-associated markers CD68 and CD11b suggests changes in ovarian stromal macrophages after resumption of cyclicity following the washout of T. Ovarian transcriptomic comparisons also support this upregulation of immune response pathways in mice after T cessation as compared to age-matched controls and mice at 6 weeks on T. Limitations of the study design prevent us from attributing these differences to the additional duration of T therapy during the washout or to changes that might be arising during the resumption of cyclicity. I postulate that this stromal macrophage response may be a temporally limited state, as related studies have described histologically similar findings which they reported to resolve after a period of time or with superovulation (Candelaria *et al.*, 2019; Sun *et al.*, 2019).

Collectively, this dissertation characterizes a mouse model on T and interrogates changes that occur if T is paused for reproductive purposes. Studies building on this work that assess the reproductive impact of multiple durations of T therapy through natural breeding and in vitro

fertilization are ongoing in the Shikanov laboratory, with plans to follow the offspring of these mice. Ongoing work is also focused on the development of a mouse model mimicking the transmasculine adolescent treatment paradigm of GnRH agonist puberty blockers followed by gender-affirming T therapy.

5.2 Reflections on Experimental Design Choices

While I feel that these studies reasonably approximate the T therapy utilized by transmasculine individuals, I believe that there may be related reasonable approaches that yield slightly different findings. I would encourage the field to avoid the presumption of developing a perfect model and embrace the slight technical differences between studies. In moments where multiple slightly different studies converge on similar findings, this increases the validity of these findings, and in moments where studies diverge, it allows us to better interrogate the potential impact of these experimental design choices. In particular, I want to draw attention to the experimental design choices of species and mouse strain, T administration method, and study duration.

Rigorous controlled studies on the reproductive effects and reversibility of gender-affirming T therapy cannot be ethically performed in humans. Using animal models, T can be paused to evaluate reversibility and studies comparing fertility outcomes can be conducted. Animal models can also allow for more uniformity of dosage, age, duration, and appropriate controls. While non-human primates would be an optimal model, they offer logistical challenges due to cost and long developmental timelines. My goal in this dissertation was to capitalize on the affordability and logistical ease of working with a mouse model, as mice have been extensively utilized for reproductive and fertility studies. My work predominately utilized

C57BL/6 mice, a common inbred mouse strain of intermediate fecundity (Chapin *et al.*, 1993). A related study utilized a similar approach in CF-1 mice, which is an albino outbred strain. In their study, they noted similar estrous cycle suppression and reduced, but not absent corpora lutea on T (Bartels *et al.*, 2020). This contrasts with our studies in C57BL/6 mice, where we have not observed any corpora lutea in mice actively undergoing T therapy at any of the doses tested. Preliminary work from the Shikanov laboratory in CD-1 mice, a similar outbred strain, has also shown reduced, but not absent corpora lutea on T. CD-1 mice are vigorous breeders, with large litters and greater numbers of corpora lutea and follicles. Although they are frequently used for reproductive studies due their vigorous breeding, they have been shown to be less sensitive to reproductive toxicants when compared to average or poorer breeding strains (Morrissey *et al.*, 1989; Chapin *et al.*, 1993). I would encourage further interrogation to better understand the mechanisms behind any species or strain differences.

T administration method and dosing presents an additional experimental design characteristic that may have an impact on findings. While similar average T levels can be approximated using subcutaneous injections at weekly or twice weekly doses, pellets, or silastic implants, the overall pharmacokinetic profiles of these administration methods vary quite a bit. Implantable T pellets may produce a 1–2-week period of particularly elevated T at the start of a study, falling into steadier levels as the weeks progress (Kinnear *et al.*, 2021). In contrast, injectable T levels may appear to be steadier when measured at a weekly midpoint between doses, but likely have short peaks after and troughs before injections that are difficult to measure in rodents due to limitations of blood collection with regards to volume and frequency (Kinnear *et al.*, 2019). We have also noted differences in washout timing due to the ease of surgical removal of T implants and the formation of lingering oil depots with injections. There may be

further differences in hypothalamic-pituitary-gonadal (HPG) axis regulation and GnRH or LH pulsatility or suppression based on T administration method. As T can be aromatized to estradiol, differences in the pharmacologic T profile could also lead to estradiol fluctuations at the systemic or local levels. If functional differences are found in studies that differ only in T administration method, I would encourage temporal hormonal comparisons across the HPG axis at a more granular level.

Study duration also represents a critical area of experimental design decision making. Our team has selected 6 weeks as a shorter timepoint and 12–15 weeks as a longer timepoint for comparison. Mouse lifespan is much shorter than human lifespan and mouse cycles are typically 4–6 days in length, in comparison to an average 28-day human menstrual cycle. As we wanted to study postpubertal mice and assess reproductive function before they reached middle or older age, we selected timepoints that would allow for a 13-week natural breeding study while mice were still under 10 months old (Flurkey *et al.*, 2007). As in any study design that includes a treatment duration, one can always ask what might happen if we treated mice for a longer period of time. Similarly, when looking at reversibility, changes that may be present for a short period of time after T cessation could potentially resolve if given more time. Logistically, I found that the timeline for investigating mice for 6 weeks on T typically also required an additional month prior for shipping, acclimatization, and confirmation of cyclicity prior to T. For studies that then investigate reversibility, such as the study in chapter 4, some mice were monitored for more than 20 weeks from arrival to sacrifice. As such, there are natural limitations on how many durations are possible to test.

5.3 Future Directions

5.3.1 Emergence of trans science

Following in the footsteps of Oncofertility, Trans Science has the potential to develop into a broader phenomenon, complete with interdisciplinary conferences and networks of scholars. To date, much of this work has been situated under the umbrellas of Transgender Medicine, Transgender Health, Gender Studies, Reproduction, and Endocrinology. While Transgender Medicine or Transgender Health ideally centers the needs of trans people and their access to gender-affirming care, Trans Science would probe more deeply into the mechanisms underlying these gender-affirming therapies. At its best, Trans Science would not question the importance of gender-affirming care nor threaten access to such care. It would instead look to more deeply understand the influence of gender-affirming hormones and surgeries on physiology so as to improve upon current treatment options and provide decisional context to trans people and their providers.

When looking at the physiological list of effects of gender-affirming therapies, a Trans Science approach might ask: "and what else"? One example of the "and what else" approach would be studying the impact of T on vestigial structures, such as the rete ovarii (remnants of the mesonephric/Wolffian ducts) or in prostate-like glands. Our mouse studies support the influence of T on structural changes to the extraovarian rete ovarii and emerging pathology literature from transmasculine individuals on T has noted epididymis-like hypertrophy observed in the rete ovarii (Singh *et al.*, 2017; Lin *et al.*, 2021) as well as prostatic-like glands in vaginal and cervical tissue (Anderson *et al.*, 2020; Lin *et al.*, 2021). Other potential "and what else" areas for investigation include the impact of gender-affirming T therapy on the pelvic floor, the oviduct, and the gut and vaginal microbiomes.

For trans people holding complex medical histories distinct from their trans status, Trans Science would also allow for interrogation of how gender-affirming hormone therapies might interact with prior diagnoses such as polycystic ovary syndrome or endometriosis or other hormonal treatments such as birth control. Trans Science scholars might study if lower T doses sometimes used by non-binary individuals leads to different outcomes than the more frequently prescribed male-level T. Other individuals may take T for interrupted periods of time, by choice or necessity. Trans Science could probe more deeply into these nuances to ascertain the possible impact of these interruptions. Ideally, Trans Science centers the lived experiences of trans people in co-creation of scientific knowledge. For this emerging field I would propose the development of Trans Science community research frameworks and Trans Science animal model frameworks. Such frameworks could help guide collaborations and encourage the pursuit of affirming questions, while avoiding the pursuit of questions with a high likelihood of causing harm. These collaborations could help with validation of findings across hormone delivery modalities and model systems. Ultimately this research could help trans people and their clinicians to make more informed clinical decisions and could influence clinical treatment and screening guidelines.

5.3.2 Ovarian stromal physiology

As part of my dissertation, I conducted a thorough review of the literature published on the ovarian stroma, an often-overlooked aspect of the ovary (Kinnear *et al.*, 2020). The ovarian follicle represents the functional unit of the ovary known as the ovarian parenchyma, whereas the ovarian stroma thus refers to the components of the ovary that are not ovarian follicles. In this review (Appendix), I encourage future study using more granular transcriptomic and spatial approaches to characterize the multiple cell types of the ovarian stroma and to better understand their steroidogenic potential, physiologic changes, and alterations in pathologic conditions.

Ultimately, it will be important to assess the functional impact of any ovarian stromal changes. My work probing more deeply into stromal macrophage changes after T cessation (chapter 4) contributes in a small way both to Trans Science and to the emerging ovarian stromal field of inquiry. Exciting ongoing research in the Shikanov lab is focused on investigating single-cell and spatial transcriptomics of healthy human ovarian stroma.

Appendix: The Ovarian Stroma as a New Frontier

Appendix previously published as review article (Kinnear *et al.*, 2020) with permission to use in dissertation (license number 1124067-1):

Kinnear HM, Tomaszewski CE, Chang FL, Moravek MB, Xu M, Padmanabhan V, Shikanov A. The Ovarian Stroma as a New Frontier. *Reproduction.* 2020;160(3):R25-R39. doi:10.1530/REP-19-0501.

Abstract

Historically, research in ovarian biology has focused on folliculogenesis, but recently the ovarian stroma has become an exciting new frontier for research, holding critical keys to understanding complex ovarian dynamics. Ovarian follicles, which are the functional units of the ovary, comprise the ovarian parenchyma, while the ovarian stroma thus refers to the inverse or the components of the ovary that are *not ovarian follicles*. The ovarian stroma includes more general components such as immune cells, blood vessels, nerves, and lymphatic vessels, as well as ovary-specific components including ovarian surface epithelium, tunica albuginea, intraovarian rete ovarii, hilar cells, stem cells, and a majority of incompletely characterized stromal cells including the fibroblast-like, spindle-shaped, and interstitial cells. The stroma also includes ovarian extracellular matrix components. This review combines foundational and emerging scholarship regarding the structures and roles of the different components of the ovarian stroma in normal physiology. This is followed by a discussion of key areas for further research regarding the ovarian stroma, including elucidating theca cell origins, understanding

stromal cell hormone production and responsiveness, investigating pathological conditions such as polycystic ovary syndrome (PCOS), developing artificial ovary technology, and using technological advances to further delineate the multiple stromal cell types.

What is the ovarian stroma and what does it do?

Organs are comprised of two components: (1) the parenchyma, or the specialized tissue that performs the function of the organ, and (2) the stroma, which is typically the supporting tissue (Young *et al.*, 2014; Mescher, 2018). Ovarian follicles, which are the functional units of the ovary, comprise the ovarian parenchyma. Conceptualizing the stroma as the inverse of the parenchyma, the ovarian stroma thus refers to the components of the ovary that are *not ovarian follicles*. The ovarian stroma is comprised of general components such as immune cells (Wu *et al.*, 2004), blood vessels (Reeves, 1971), nerves (Neilson *et al.*, 1970), and lymphatic vessels (Brown *et al.*, 2010), as well as ovary-specific components. These ovary-specific components include ovarian surface epithelium (Auersperg *et al.*, 2001), tunica albuginea (Reeves, 1971), intraovarian rete ovarii (Wenzel and Odend'hal, 1985), hilar cells (Neilson *et al.*, 1970), ovarian stem cells (Hummitzsch *et al.*, 2015), a majority of incompletely characterized stromal cells that includes the fibroblast-like, spindle-shaped, and interstitial cells (Reeves, 1971), and possibly other cell types not included in this list. In addition to these cell types, ovarian extracellular matrix (ECM) provides structural and biochemical support to surrounding cells and is a key component of the stroma (Berkholtz *et al.*, 2006) (Fig. 16 and Table 5). Some studies have used the broad terms 'ovarian interstitial stroma' or 'theca interstitial cells' (TICs) to refer to the heterogeneous stromal compartment (e.g. Tingen *et al.*, 2011; Hummitzsch *et al.*, 2019). For the purpose of this review, we will interpret the ovarian stroma as the broadly inclusive non-

follicular components of the ovary. We also want to highlight that the term ‘stromal cells’ does not refer to a single homogenous cell population. Instead, when feasible, we recommend more specific descriptions like ‘stromal macrophages’ to refer to individual components of the stromal compartment. What is known about the multiple cell types and components of the stroma is detailed subsequently.

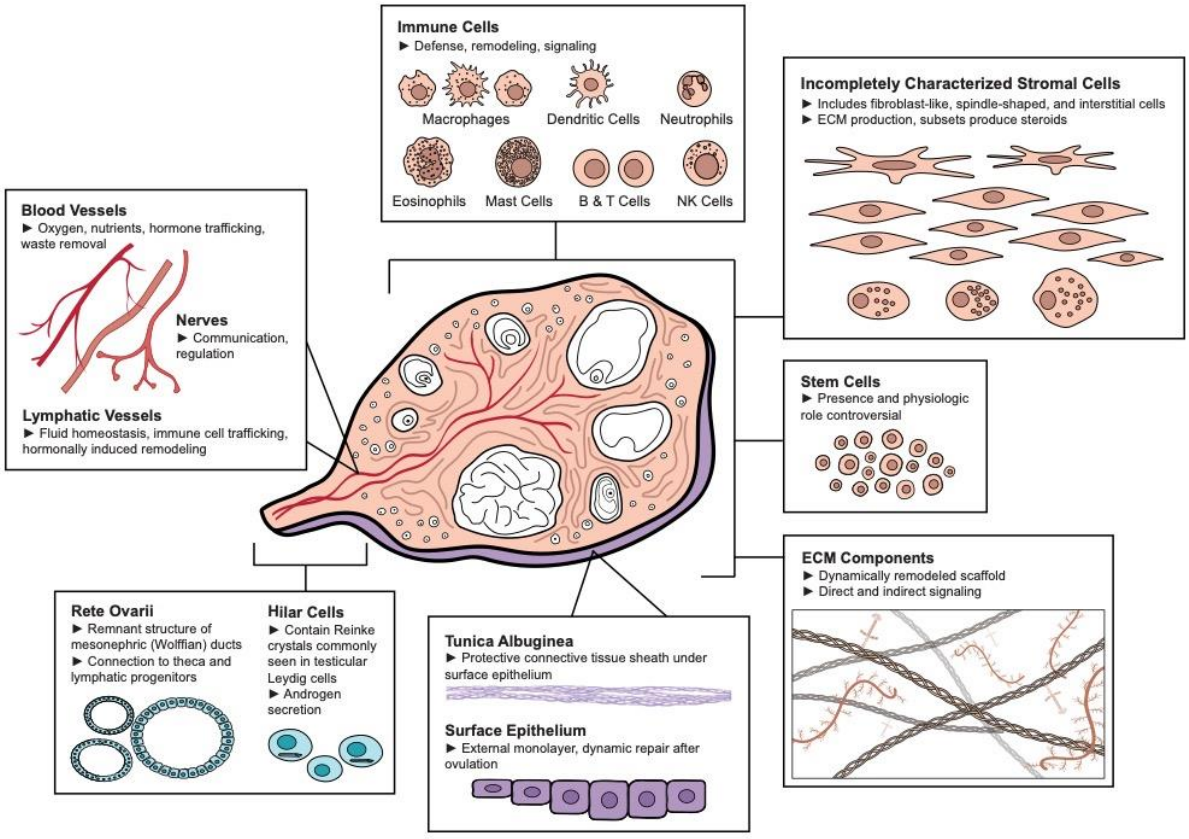

Figure 16. Components of the ovarian stroma. Central diagram of a human ovary (adapted from Gray, 1918) surrounded by boxes highlighting different ovarian stromal components including (clockwise from top center): immune cells including macrophages, dendritic cells, neutrophils, eosinophils, mast cells, B & T cells, and Natural Killer (NK) cells; incompletely characterized stromal cells (including fibroblast-like, spindle-shaped, and interstitial cells); stem cells; extracellular matrix (ECM) components; surface epithelium and tunica albuginea; rete ovarii and hilar cells; and blood vessels, lymphatic vessels, and nerves. Made using ©BioRender - biorender.com.

Table 5. General and ovary-specific components of the ovarian stroma.

General Components	**Subsets**	**Regionality**	**Function**	**Example Cellular Markers**	**Further Research Required**
Immune cells	Macrophages, dendritic cells, neutrophils, eosinophils, mast cells, B Lymphocytes, T Lymphocytes, Natural Killer cells	Throughout stroma, around theca vasculature	Defense, remodeling, signaling	Leukocyte: CD45 Myeloid: CD11b Macrophages: CD68 Dendritic Cells: CD11c Neutrophils: CD16 Eosinophils: CD193 Mast Cells: CD117 Lymphoid: B Lymphocytes: CD19 T Lymphocytes: CD3 Natural Killer: CD56[1]	Cyclic, hormonal, temporal dynamics, pathologic relevance
Blood vessels	Endothelial cells, pericytes, smooth muscle cells	Branching medullary spirals to cortical arcades	Oxygen, nutrients, hormone trafficking	Endothelial cells: VE-Cadherin Pericytes: PDGFRB Smooth muscle cells: α-SMA[2]	Dynamic role of oxygen tension, pathologic role and management in PCOS
Nerves	Neurons, glial cells	Branching medulla to cortex	Communication, can regulate hormone secretion and vasoconstriction[3]	Neurons: MAP2 Glia: SOX10[4]	Neuronal regulation of stromal cell types, pathologic relevance
Lymphatic vessels	Endothelial cells, smooth muscle cells	Branching medulla to cortex, vasculature association	Fluid homeostasis, immune cell trafficking, hormonally induced remodeling[5]	Endothelial cells: LYVE1[6] Smooth muscle cells: α-SMA	Dynamic regulation, pathologic relevance
Ovary-Specific Components	**Subsets**	**Regionality**	**Function**	**Possible Cellular Markers**	**Gaps in Knowledge**
Surface epithelium		External monolayer of ovary	Supports repair after ovulation, dynamic	CK7, CK8, CK18, CK19, Plakophilin-2, Desmoglein-2[7]	Heterogeneity, pathologic contributions
Tunica albuginea		Outer layer under surface epithelium	Protection	Minimal cellularity	Physiologic and pathologic contributions
Intraovarian rete ovarii		Hilar region, medulla	Connection to progenitor populations, including theca and lymphatics[8]	CK19, Vimentin[9]	Physiologic role in adults, pathologic relevance
Hilar cells		Hilar region, nerve trunk association	Contain Reinke crystals commonly seen in testicular Leydig cells, androgen secretion[10]	Not established	Physiologic role, pathologic relevance
Stem cells			Physiologic role in adults not established	Oogonial: DDX4 or IFITM3 (controversial)[11]	Presence & potential physiologic role in adults
Incompletely characterized stromal cells	Up to 5 different types of fibroblast-like/spindle-shaped/ interstitial cells identified[12]	Subsets mainly in cortex, subsets mainly in medulla	Subsets associated with production of collagens I or III, subsets are steroid producing with cytoplasmic lipids and vacuoles[12]	COUP-TFII[13]; COUP-TFII and/or ARX[14]; DCN, LUM for theca/stroma[15]; some express PDGFRA, DCN, COL1A1, COL6A1, STAR, and/or CYP17A1[16]; some TCF21, COL1A2, STAR[17]	Cellular identification and ontology, regionality, steroid production, common and differentiating markers
Extracellular matrix components	Collagens, glycoproteins, proteoglycans, ECM-affiliated proteins, ECM regulators, secreted factors	Stiff cortex with radially aligned collagen fibers and less dense medulla	Scaffold, direct and indirect signaling, dynamically remodeled, stiffness involved in follicular dormancy[18]	Extracellular	ECM composition and structure not adjacent to follicles

[1]*http://docs.abcam.com/pdf/immunology/immune-cell-markers-poster.pdf, https://media.cellsignal.com/www/pdfs/science/pathways/Immune-Cell-Markers-Human.pdf, accessed March 2020;* [2]*https://www.rndsystems.com/research-area/endothelial-progenitor-and-endothelial-cell-markers, accessed March 2020;* Rensen *et al.*, 2007*;* Kizuka-Shibuya *et al.*, 2014*;* [3]Uchida, 2015*;* [4]*https://docs.abcam.com/pdf/neuroscience/neural-markers-guide-web.pdf, accessed March 2020;* [5]Brown *et al.*, 2010*;* [6]Kong *et al.*, 2017*;* [7]Hummitzsch *et al.*, 2013; Hartanti *et al.*, 2020*;* [8]Svingen *et al.*, 2012; Liu *et al.*, 2015*;* [9]Russo *et al.*, 2000*;* [10]Neilson *et al.*, 1970; Erickson *et al.*, 1985*;* [11]Hummitzsch *et al.*, 2015*;* [12]Reeves, 1971*;* [13]Hummitzsch *et al.*, 2013*;* [14]Rotgers *et al.*, 2018*;* [15]Fan *et al.*, 2019*;* [16]Wagner *et al.*, 2020*;* [17]Wang *et al.*, 2020*;* [18]Irving-Rodgers and Rodgers, 2006; Kawamura *et al.*, 2013.

General Cell Types of the Ovarian Stroma

Immune Cells

Cells of the immune system appear to play critical roles in supporting ovarian physiologic processes. Immune cells, including macrophages, mast cells, and eosinophils, are present in immature or resting ovaries at low levels throughout the stroma. These levels tend to increase around ovulation, particularly near the theca vasculature, with subsequent migration into developing corpora lutea (Norman and Brannstrom, 1994). Ovarian immune cells serve multiple functions, including phagocytosis and antigen presentation, tissue remodeling via proteolytic enzymes, and secretion of soluble signals including cytokines, chemokines, and growth factors (Norman and Brannstrom, 1994; Wu *et al.*, 2004). Macrophages are a predominant ovarian immune cell type, with other immune cells present including B and T lymphocytes, Natural Killer cells, dendritic cells, neutrophils, eosinophils, and mast cells (Norman and Brannstrom, 1994; Suzuki *et al.*, 1998; Carlock *et al.*, 2013; Kenngott *et al.*, 2016; Fan *et al.*, 2019; Zhang *et al.*, 2020) (Fig. 16 and Table 5). Ovarian macrophages have received ongoing attention with regard to their role in reproductive homeostasis and their regulation by estrogen (reviewed in Wu *et al.*, 2004; Pepe *et al.*, 2018). Ovaries may contain multiple macrophage subsets, and phenotypes can range from classical inflammatory (M1) to alternative tissue remodeling (M2) during different parts of the ovarian cycle (Carlock *et al.*, 2013; Pepe *et al.*, 2018). Increased proportions of M2 macrophages, monocyte-derived macrophages, and multinucleated macrophages have been seen with murine ovarian aging (Briley *et al.*, 2016; Zhang *et al.*, 2020). Macrophage and other myeloid cell depletion using the CD11b-DTR mouse model has resulted in infertility, with hemorrhagic ovaries, ovarian endothelial cell depletion, impaired corpora lutea formation, and diminished progesterone production (Turner *et al.*, 2011; Care *et al.*, 2013).

Although ovarian immune cells, particularly macrophages, have been the subjects of ongoing research, gaps in knowledge remain regarding cyclic, hormonal, and temporal dynamics as well as contributions to ovarian pathologic conditions (Table 5).

Blood Vessels

The vasculature of the ovary supports critical ovarian functions and includes blood vessel endothelial cells, pericytes, and smooth muscle cells (Fig. 16 and Table 5). Ovarian blood vessels travel through connective tissue to provide tissue oxygenation, hormone trafficking, and nutrients, in addition to supporting waste removal. The medulla of the human ovary typically contains the larger blood vessels and at the cortico-medullary junction, small medullary arteries branch to cortical arterioles (Reeves, 1971). These cortical arterioles form vascular arcades of interconnected short straight vessels of fixed length running along the connective tissue fascicles. With pressure, the cortical arterioles could be compressed to form avascular regions as part of the formation of stigma for ovulation (Reeves, 1971). Medullary vessels include spiraling arteries and arterioles, which may allow expansion with growth (Reeves, 1971). The microvasculature of the ovary contributes to folliculogenesis and corpora lutea formation. Follicles contain a basal lamina between their granulosa and theca cell compartments, allowing for a blood-follicle barrier (Siu and Cheng, 2012). With the formation of the theca cell layer, follicles develop microvasculature between the theca cells that supports the increased growth and development of the follicle, yet never passes beyond the basal lamina before ovulation. The formation of the corpus luteum, a highly vascular structure, occurs after theca microvasculature invades into the granulosa layer following ovulation (Rolaki *et al.*, 2005). Gaps in knowledge remain around the role of oxygen tension, as regulated by ovarian vasculature. Oxygen tension

may have regulatory effects in the ovary, with *in vitro* studies demonstrating that oxygen levels can impact bovine granulosa cell luteinization and rat corpora lutea progesterone production (Gafvels *et al.*, 1987; Baddela *et al.*, 2018). Dysfunction of ovarian vasculature has been implicated in the pathophysiology of PCOS (Di Pietro *et al.*, 2018), and additional studies are needed to address the pathologic role and therapeutic management of altered ovarian angiogenesis (Table 5).

Nerves

Neilson *et al.*'s (1970) review describes widespread innervation present in the ovarian stromal compartment, noting that some nerves follow blood vessels in the medulla while others branch among the cells in the stroma (Fig. 16 and Table 5). In mouse gonadal development, neural crest neurons colonize the ovary, differentiate into neurons and glia, and form dense neural networks in the medulla that extend towards cortical regions (McKey *et al.*, 2019). Functionally, both sympathetic and parasympathetic innervation of the ovary has been demonstrated, and regulation by the sympathetic nervous system has been shown to inhibit estradiol secretion and cause vasoconstriction (reviewed in Uchida, 2015). In a PCOS model, estradiol-treated rats demonstrated increased ovarian sympathetic activity and cystic anovulatory ovaries, with improvement noted in cyclicity and corpora lutea formation following superior ovarian nerve transection (Barria *et al.*, 1993). Further study is warranted regarding the neuronal regulation of different cell types in the stroma, physiologic consequences of denervation, and neuronal contributions to pathology (Table 5).

Lymphatic Vessels

Lymphatic vasculature includes small capillaries comprised of endothelial cells without a basement membrane that have large gaps between cells to allow fluid, cellular, and macromolecular transport. These capillaries feed into larger collecting vessels with basement membranes, valves, and smooth muscle (Fig. 16 and Table 5). The ovary has a rich lymphatic network, closely associating with blood vasculature, extending from the medulla into the cortex adjacent to developing follicles, with some species variability in regard to presence in the corpus luteum (Brown and Russell, 2014). The lymphatic system typically helps to maintain fluid homeostasis by returning extravascular fluid and proteins back to the bloodstream and participating in immune cell trafficking. In the developing mouse ovary, lymphatic vessels only appeared postnatally, potentially arising from the extraovarian rete ovarii, as seen in a *Prox1*-EGFP mouse model, where *Prox1* expression marks the commitment of endothelial cells to the lymphatic lineage (Svingen *et al.*, 2012). Lymphatic vasculature has been shown to remodel in response to hormonal regulation in mouse ovaries (Brown *et al.*, 2010). Although lymphatic vasculature plays essential physiologic roles in the ovary, the dynamic regulation and pathologic relevance of the ovarian lymphatics remains to be fully elucidated (Table 5).

Ovary-Specific Cell Types of the Ovarian Stroma

Ovarian Surface Epithelium

The surface epithelium of the ovary is a heterogenous flat to cuboidal epithelial layer derived from the mesoderm, also called the “germinal epithelium” because of the false past belief that it contributed to germ cell formation (Auersperg *et al.*, 2001) (Fig. 16 and Table 5). The keratin-rich ovarian surface epithelial cell layer helps to facilitate repair after ovulation and

dynamically expands and contracts with cyclic ovarian changes (Xu *et al.*, 2018; Hartanti *et al.*, 2020). Scanning electron microscopy and immunofluorescence of the surface epithelium of developing fetal bovine ovaries demonstrated expansion from the hilar region to surround the entire ovary, with changes corresponding to underlying stromal rearrangement (Hartanti *et al.*, 2020). Although fetal ovarian surface epithelial cells had been previously thought to be a developmental source for granulosa cells, more recent studies suggest that ovarian surface epithelial cells instead share a common progenitor with granulosa cells, known as the Gonadal Ridge Epithelial-Like (GREL) cell (Auersperg *et al.*, 2001; Hummitzsch *et al.*, 2013). Although definitive markers have not been identified, surface epithelial cells have increased expression of the cytokeratins 7, 8, 18, and 19 as well as plakophillin-2 and desmoglein-2 (Hummitzsch *et al.*, 2013; Hartanti *et al.*, 2020) (Table 5). Further work remains regarding identifying definitive markers, understanding heterogeneity, and clarifying the pathologic contributions of the ovarian surface epithelium.

Tunica Albuginea

The ovarian tunica albuginea, positioned beneath the surface epithelium, is a thin and hypocellular connective tissue sheath, which serves as a protective layer for the ovary (Reeves, 1971). The tunica albuginea is collagen-rich and undergoes remodeling prior to ovulation. Using electron microscopy, Okamura *et al*, (1980) observed a decrease in presence of collagen bundles at the human follicular apex as follicles reached the preovulatory stage. This degradation was paralleled by an increase in apical fibroblasts with developed cytoplasm and lysosome-like granules, which were suspected to contain collagenases for degradation of the tunica albuginea

(Okamura *et al.*, 1980). There has been limited study of the ovarian tunica albuginea and further work can help to clarify physiologic and pathologic roles and regulation (Fig. 16 and Table 5).

Intraovarian Rete Ovarii

The rete ovarii are remnants of the mesonephric (Wolffian) ducts that typically form part of the male reproductive tract and regress in the female reproductive tract. They are often found as groups of tubules lined by cuboidal or columnar epithelium in the hilus of the ovary or extending through the medulla, as well as in the extraovarian space (reviewed in Wenzel and Odend'hal, 1985) (Fig. 16 and Table 5). There has been limited investigation into the function of the rete ovarii, particularly after development, where they may play relevant roles. In a study of murine theca cell lineages, one of the two identified progenitor populations of theca cells migrated from the adjacent mesonephros and was potentially related to the rete ovarii (Liu *et al.*, 2015; Rotgers *et al.*, 2018). Ovarian lymphatic vasculature origins have also been connected to the rete ovarii (Svingen *et al.*, 2012). Although they are not necessarily specific markers, increased levels of cytokeratin 19 and vimentin have been noted in human rete ovarii (Russo *et al.*, 2000). Further study is needed to elucidate the physiologic role of the rete ovarii in adults as well as the pathologic relevance (Table 5).

Hilar Cells

There are reports of distinct cells located in the ovarian hilus with Reinke crystals, which are commonly found in testicular Leydig cells (Neilson *et al.*, 1970) (Fig. 16 and Table 5). These cells are frequently located in clusters associated with a nerve trunk (Neilson *et al.*, 1970). They appear to synthesize and secrete androgens in response to LH stimulation, although their

physiologic role has not been well-established (Erickson *et al.*, 1985). Hyperplasia of these hilar cells has been implicated in virilization in postmenopausal women (Delibasi *et al.*, 2007). Cellular markers have not been established and the physiologic role and pathologic relevance of these cells remains generally uncharacterized.

Ovarian Stem Cells

The ovary may contain stem cells for a variety of different cell types, including somatic (e.g., granulosa, surface epithelial, thecal, stromal) and germline stem cells (reviewed in Hummitzsch *et al.*, 2015) (Fig. 16 and Table 5). The presence and importance of ovarian germline (oogonial) stem cells has been a controversial topic, although the ovarian follicular reserve is generally lost with age without substantive renewal. Putative ovarian oogonial stem cells were first isolated through DEAD (Asp-Glu-Ala-Asp) box polypeptide 4 (DDX4, also known as VASA) tagging and cell sorting and have been shown to develop into oocytes, although isolation of DDX4 positive cells has been questioned, particularly related to assumptions about cytoplasmic vs surface expression and antibody cross-reactivity (Johnson *et al.*, 2004; Zarate-Garcia *et al.*, 2016). Others have disputed the presence of oogonial stem cells, noting that oogonial stem cells were not detectable using sensitive single-cell lineage-tracing in adult female mice (Lei and Spradling, 2013). Additionally, postnatal DDX4-expressing cells generated using a *Rosa26*$^{rbw/+}$*; Ddx4-Cre* fluorescent reporter mouse were not seen to be mitotically active nor participating in follicular renewal (Zhang *et al.*, 2012). A recent single-cell sequencing study isolated human Abcam DDX4-positive cells and concluded these cells were perivascular cells rather than oogonial stem cells (Wagner *et al.*, 2020). In contrast, cell line establishment of female germline stem cells has been described using cells from human ovarian

cortical tissue fragments present in follicular aspirates, which differentiated into oocyte-like cells (Ding *et al.*, 2016). Isolated, purified, and cultured female germline stem cells from an EGFP-transgenic mouse were shown to differentiate into oocytes, capable of restoring function and generating offspring in a mouse model of premature ovarian failure (Wu *et al.*, 2017). The presence of ovarian germline stem cells continues to be a highly contested topic, generally eclipsing the discussion of somatic stem cells. The addition of human mesenchymal stem cells originating from amniotic fluid has also been used to help restore ovarian function in mouse models of premature ovarian failure, suggesting a role for somatic stem cells in improving altered paracrine signaling and the stroma microenvironment (Liu *et al.*, 2019).

Incompletely Characterized Stromal Cells

The majority of the ovarian stroma is comprised of a mixed population of incompletely characterized cells commonly referred to as stromal cells (Reeves, 1971). This includes the populations of cells also described as fibroblast-like, spindle-shaped cells, or interstitial cells (Fig. 16 and Table 5). In general, fibroblasts secrete ECM proteins, such as collagen, for cellular support, scaffolding, and repair. A retrospective study of histologic sections from non-pathologic human ovaries from 167 women between the ages of 17 and 79 carried out with the goal of describing the morphology of various types of stromal cells identified five types of fibroblast-like/interstitial stromal cells (Reeves, 1971). While recent human single-cell RNA-sequencing studies (e.g., Fan *et al.*, 2019) confirm the presence of multiple stromal cell clusters, a comprehensive and complete characterization of stromal cell types throughout the ovary is lacking. The distribution and subtypes of stromal cells will likely differ with their location in the ovary (e.g. cortex vs. medulla). The stromal cell distribution is also likely to be affected by cyclic

structural changes, as follicles grow and ovulate, and corpora lutea develop. Changes are also evident over the reproductive lifespan, including increases in fibrotic collagen as demonstrated in aging murine and primate ovaries (Briley *et al.*, 2016; Wang *et al.*, 2020). Some possible cellular markers that have been identified include COUP-TFII and/or ARX (Hummitzsch *et al.*, 2013; Rotgers *et al.*, 2018). Other studies have used *DCN* and *LUM* to identify populations of human theca/stroma cells (Fan *et al.*, 2019). Higher expression in some of the human cells considered to be stroma was demonstrated for markers *PDGFRA*, *DCN*, *COL1A1*, *COL6A1*, *STAR*, and/or *CYP17A1* (Wagner *et al.*, 2020). A different study delineated nonhuman primate ovarian stroma by expression of *TCF21*, *COL1A2*, and/or *STAR* (Wang *et al.*, 2020). For these incompletely characterized stromal cell types, careful ontology, further marker identification, and attention to nuances of regionality and steroid production are critical next steps (Table 5).

Extracellular Matrix (ECM) Components

Structure & Definition

The ECM is composed of fibril- and network-forming proteins, proteoglycans, and glycosaminoglycans, the composition of which is unique to each tissue (Fig. 16 and Table 5). Cells secrete soluble ECM components to the extracellular compartments where cell-secreted enzymes such as lysyl oxidase (LOX) crosslink the ECM precursors into large networks (Theocharis *et al.*, 2016). These matrices regulate cellular functions including adhesion, migration, and proliferation through cell receptor interactions, mechanotransduction, and cell interaction with ECM-sequestered growth factors (Taipale and Keski-Oja, 1997).

Several reviews have covered the extensive list of ECM components that exist broadly in tissues and specifically in the ovary; most notably, collagen types I, III, IV, and VI, fibronectin, and laminin (Berkholtz *et al.*, 2006; Irving-Rodgers and Rodgers, 2006). Collagens I and III have been shown to be distributed in concentric layers connected by bundles in human cortical stroma (Lind *et al.*, 2006). A recent proteomic study examining the ECM of the human ovarian cortex revealed that collagens comprise nearly half of the ECM proteins and associated factors, the most dominant of which was collagen VI, a basement membrane-anchoring ECM protein (Ouni *et al.*, 2019). Another recent proteomic study examined ECM compositional differences between porcine cortex and medulla, showing increased expression of collagen I, agrin, elastin microfibril interfacer 1, and fibronectin in the cortex compared to the medulla (Henning *et al.*, 2019). These proteomic studies both identified over 80 ECM and ECM-associated proteins, in categories of collagens, glycoproteins, proteoglycans, ECM-affiliated proteins, ECM regulators, and secreted factors (Henning *et al.*, 2019; Ouni *et al.*, 2019).

Many studies of ECM have focused on matrix within follicles during development. Follicles have a unique pericellular matrix called the basal lamina, composed primarily of laminin and type IV collagen stabilized by nidogen and perlecan which separates the granulosa and theca cell compartments (Irving-Rodgers and Rodgers, 2006). As follicles grow, they continuously remodel the basal lamina to allow for expansion of the follicle as granulosa cells proliferate. Granulosa cells have been shown to produce the major components of the basal lamina, although theca and other cells in the ovarian stroma may contribute to basal lamina deposition in later stages (Rodgers *et al.*, 1999). The basal lamina also plays a role in mediating granulosa cell growth and antrum formation through growth factor sequestration and signaling.

Perlecan in the basal lamina is able to bind growth factors and is charge and size selective, serving as a barrier to diffusion of growth factors between the granulosa and theca cell compartments, allowing the follicular fluid and basal lamina to become reservoirs of factors to promote healthy folliculogenesis (McArthur *et al.*, 2000).

Mechanics

The ovary has two major compartments which differ in their ECM composition and structure – a stiff cortex where primordial follicles reside in dormancy, and a less dense medulla where antral follicles vigorously remodel the ECM through proteolytic degradation as they reach preovulatory stages. Decellularized human and bovine ovarian tissue reveals radially aligned collagen fibers in the cortex, lending to its increased stiffness, whereas the medulla is composed of a network of pores with anisotropic collagen fibers, suggesting differences between cortical and medullary ECM-producing stromal cells (Laronda *et al.*, 2015; Chiti *et al.*, 2018). The prominence of ovarian cortical and medullary regionalization can differ across species and is notably reduced in rodent ovaries when compared to human ovaries (Jiménez, 2009). The mechanical properties of these regions have important roles in mechanotransduction for the follicles as they activate and develop. Primordial follicle dormancy has been shown to be regulated by the Hippo signaling pathway, where rigidity of the ovarian cortex inactivates yes-associated protein (YAP) and transcriptional coactivator with PDZ-binding motif (TAZ) to inhibit growth (Kawamura *et al.*, 2013). Follicle activation can be initiated with disruption of the Hippo signaling pathway, for example, when follicles are isolated from the cortex, further illustrating the importance of ECM mechanical properties in maintenance of the follicular reserve (Kawamura *et al.*, 2013). After activation, early stage follicle growth and survival is still

dependent on a stiff matrix, as has been shown *in vitro* (Hornick *et al.*, 2012). As follicles grow, they require a softer matrix for expansion as provided by the medullar region of the ovary, and *in vitro* studies have shown improved growth, survival, and steroidogenesis of later stage follicles in permissive matrices (West *et al.*, 2007; West-Farrell *et al.*, 2009).

Function: Signaling and Remodeling

ECM components play a large role in regulating cell functions through both direct and indirect signaling. Fibronectin and laminin contain integrin-binding sequences (most notably Arg-Gly-Asp, or RGD) which allow cells to directly interact with the ECM and initiate signaling cascades for proliferation and differentiation as follicles develop (Monniaux *et al.*, 2006). ECM also has an indirect role in signaling as it acts as a reservoir of growth factors and cytokines and mediates their presentation to cells both when they are bound and when they are released upon ECM degradation. ECM is a dynamic structure in tissues, continuously being remodeled by the cells which reside in it through matrix metalloproteinases (MMPs), tissue inhibitors of matrix metalloproteinases (TIMPs), and plasminogen activators (McIntush and Smith, 1998). Follicles and other ovarian stromal cells secrete these enzymes to soften the surrounding ECM and allow for follicular expansion, and in this process cytokines and growth factors bound to the ECM are released. Several growth factors known to be key regulatory molecules in folliculogenesis including fibroblast growth factor, transforming growth factor beta, platelet derived growth factor, hepatocyte growth factor, and insulin-like growth factor have ECM-binding motifs or can be sequestered within the ECM through binding factors such as follistatin (Logan and Hill, 1992). In this way, ECM remodeling is a mechanism by which growth factor bioavailability can be mediated or disrupted in some pathological conditions (McIntush and Smith, 1998). If

dysregulated, ECM degradation may also trigger pathogen-free inflammation. For example, hyaluronan is a glycosaminoglycan that forms low molecular weight fragments during turnover, which have been shown in cultured murine stromal cells to increase the secretion of type 2 inflammatory cytokines and activate genes involved in eosinophil recruitment, while also leading to adverse effects on cultured follicles (Rowley *et al.*, 2020).

At the final stages of follicular maturation the ECM again plays an important role in ovulation. Follicles are stimulated by the LH surge to produce large amounts of MMPs and plasminogen activator to degrade the ECM at the apical region of the follicle (Curry and Smith, 2006). This process is further amplified by the release of tumor necrosis factor-alpha (TNF-a) from the degraded ECM to promote collagenase production and apoptosis of ovarian epithelial cells (Curry and Smith, 2006). The weakened cellular and ECM components at the apical region, along with pressure from the follicular fluid and increased vascular pressure, facilitate follicular rupture and expulsion of the oocyte into the periovarian space (Matousek *et al.*, 2001).

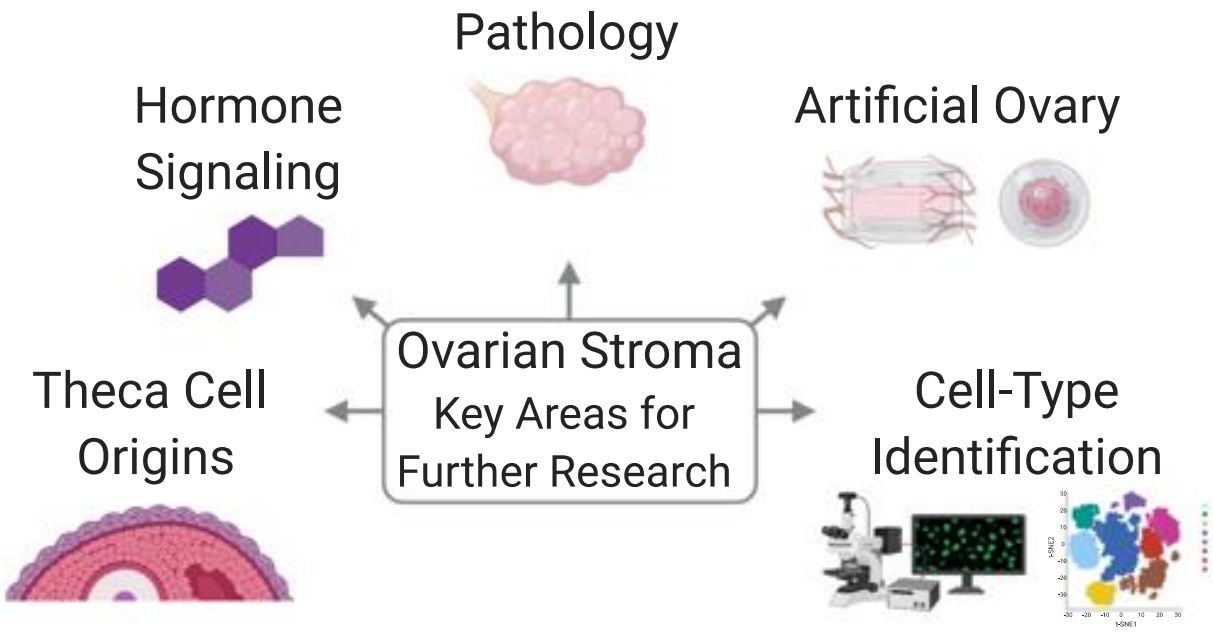

Figure 17. Ovarian stroma key areas for further research. Includes (clockwise from left): theca cell origins, hormone signaling, pathology, artificial ovary, and cell-type identification. Made using ©BioRender - biorender.com.

Key Areas for Further Research and Future Perspectives

Understanding the origins of the theca cells

The theca cell layer is divided into the theca interna, with cytoplasmic lipid droplets characteristic of its role in steroid production, and the theca externa, which is a mix of fibroblasts and smooth muscle cells that are more contiguous with the broader ovarian stroma (reviewed in Young and McNeilly, 2010; Richards *et al.*, 2018). The relationship between the supporting cells of the ovarian stroma and the theca cells has not been definitively established, although it is generally agreed that the theca cells originate at least in part from stromal cells (Young and McNeilly, 2010; Rotgers *et al.*, 2018).

Murine theca cells have been shown to arise from two types of progenitors: *Wt1*-positive cells in the fetal ovary and *Gli1*-positive cells migrating from the mesonephros adjacent to the ovary (Liu *et al.*, 2015). Near birth, desert hedgehog and Indian hedgehog paracrine signals from granulosa cells appear to prompt expression in undifferentiated stromal progenitor cells of the theca lineage marker *Gli1*. Microarray analysis suggested differences based on theca progenitor population, with increased steroidogenesis in the mesonephros-derived *Gli1*-positive cells (Liu *et al.*, 2015). The steroidogenic androgen-producing theca cells may arise from the mesonephros derived progenitors, while the theca fibroblasts, perivascular smooth muscle cells, and possibly the interstitial ovarian cells may arise from the ovarian WT1+ progenitors (Richards *et al.*, 2018).

Additional undifferentiated stromal cell progenitors (possibly positive for *Lhx9, Mafb, Coup-tfII, and Arx)* may yield a nonsteroidogenic stromal cell population, possibly expressing *Coup-tfII* and *Arx*. Overlapping expression of COUP-TFII and ARX in the same population of cells has not been established (Rotgers *et al.*, 2018). Sonic hedgehog signaling has been shown to regulate expression of COUP-TFII, which was identified in murine theca interna cells and in mesenchymal cells around the corpus luteum (Krishnan *et al.*, 1997; Takamoto *et al.*, 2005). COUP-TFII is likely expressed in steroidogenic cells, as haploinsufficient female mice demonstrated altered reproduction function, including reduced expression of steroidogenic enzymes needed for progesterone synthesis and reduced vascularization (Takamoto *et al.*, 2005). Three populations of somatic cell precursors have been demonstrated in murine fetal ovaries, marked by mutually exclusive expression of COUP-TFII and the granulosa cell markers FOXL2 and LGR5 (Rastetter *et al.*, 2014). Mutually exclusive FOXL2 and COUP-TFII expression was

also seen in early fetal human ovaries, with COUP-TFII expression in the stromal cell population. Several 46,XX *SRY*-negative children with mutations in the gene encoding COUP-TFII were virilized, with testicular tissue confirmed in one child, suggesting a "pro-ovary" and "anti-testis" role for COUP-TFII in developing human female gonads (Bashamboo *et al.*, 2018).

A transgenic mouse study suggests the presence of at least two steroidogenic cell types for ovarian theca and interstitial gland cells. In postnatal mouse ovaries, only a portion of the steroidogenic theca and interstitial gland cells expressed enhanced green fluorescent protein (EGFP) as a reporter of the fetal Leydig enhancer (FLE) of the *Nr5a1* gene (SF-1). SF-1 regulates expression of steroidogenic *CYP* genes. In testes, the FLE differentiates fetal from adult Leydig cells. In these ovaries only approximately 16% of the SF-1 postive cells were positive for EGFP, suggesting at least two cell populations (Miyabayashi *et al.*, 2015).

A transcriptome analysis of the bovine ovarian stroma found that populations isolated by laser microdissection were similar between general interstitial stroma and what they labeled as pre-theca cells (stroma adjacent to preantral follicles). They combined them for the purpose of analysis, and the subsequent stroma was found to be different from both the tunica albuginea and the theca interna (Hummitzsch *et al.*, 2019). The theca interna of small antral follicles had an upregulation of genes associated with steroid hormone and cholesterol synthesis as compared to the stroma (Hummitzsch *et al.*, 2019).

Of note, the concept of theca interstitial cells (TICs) has been used as a catch-all for the residual ovarian tissue husk once follicles had been punctured (Tingen *et al.*, 2011; Tian *et al.*,

2015). When cultured, theca interstitial cells from mouse ovaries take on a fibroblast-like appearance that is distinct from granulosa cells (Tian *et al.*, 2015). The heterogeneity of the TICs has been noted, with a reported shift in populations over a 12-day co-culture with follicles. At the beginning of the culture, the population contained predominantly lipid droplet-containing cells resembling theca cells as well as fibroblast-like cells, whereas the cells were mainly macrophages by day 12 (Tingen *et al.*, 2011). This transition in cell phenotype may be due to differential survival in culture of the different starting cell populations, emphasizing that TICs are not a homogenous grouping.

Further understanding the stromal compartment may aid in better identification of theca progenitors (Fig. 17). Additionally, studies using mixed populations of TICs may benefit from greater categorization of these non-follicular populations to aid in interpretation and reproducibility of findings.

Stromal cell hormone production and responsiveness

Some of the ovarian stromal cells are capable of steroid hormone production and contain hormone receptors. For instance, estrogen receptor alpha and beta have been identified in the cytoplasm and nucleus of bovine interstitial cells, which were described as oval cells with lipid droplets and vacuoles that were distinguishable from fibroblasts (Kenngott *et al.*, 2016). Progesterone receptor alpha has been identified in stromal cells and interstitial cells of pregnant and post-partum rabbit ovaries (Abd-Elkareem, 2017). Interstitial cells with features of steroid production have been documented in early gestation in the human fetal ovary (Konishi *et al.*, 1986). Postmenopausal ovarian stromal cells have been postulated to produce androgens,

although a study of *in vitro* isolated postmenopausal human stromal cells found that the predominant population had negligible expression of a key steroidogenic enzyme in the androgen biosynthesis pathway, *CYP17A1*, and did not appear to have significant steroidogenic potential (Jabara *et al.*, 2003). Additionally, they found that transcripts for certain steroidogenic enzymes (*STAR*, *CYP11A1*, and *HSD3B*) were much less abundant in the *in vitro* isolated stromal cells than in theca cells, with the exception of *STAR* which had more transcript abundance in stromal cells than in fibroblasts (Jabara *et al.*, 2003). In contrast, localization of CYP17A1 shifted from exclusively the theca interna in control mice to patches in the interstitial stroma in DHT-treated mice, supporting a potential role for the stroma in androgen production following certain perturbations (Candelaria *et al.*, 2019). Single-cell RNA sequencing studies have also demonstrated subpopulations of stromal cells expressing *CYP17A1* and *STAR* (Wagner *et al.*, 2020; Wang *et al.*, 2020). Although stromal cells have demonstrated varied hormone production and responsiveness, definitive characterization of these dynamics and their functional significance remains to be established (Fig. 17).

Pathological ovarian stromal changes: polycystic ovary syndrome as an example

Polycystic ovary syndrome (PCOS) has been defined by the Rotterdam Criteria (2004) as two of the three characteristics – hyperandrogenism, oligo or amenorrhea, and follicular cysts as noted on ultrasound (The Rotterdam ESHRE/ASRM-Sponsored PCOS consensus workshop group, 2004). Polycystic ovarian morphology includes the following features: thickening of the tunica albuginea, ovarian stromal hyperplasia, stromal cell luteinization, and large cystic antral follicles (Hughesdon, 1982). The thickness of the cortical stroma is increased by one third and the subcortical stroma by five-fold (Hughesdon, 1982). In detailed ultrasound assessment,

women with PCOS were found to have significantly increased ovarian volume, stromal volume, and stromal peak blood flow velocity as compared to controls (Buckett *et al.*, 1999). In contrast, no difference was found in ovarian stromal blood flow between women with PCOS and a control group explicitly excluding patients with low ovarian reserve (Younis *et al.*, 2011). The ratio of ovarian stromal area to total ovarian area (S/A) by ultrasound was a good predictor of hyperandrogenism in lean Italian women with PCOS, with increased ovarian vascularization and blood flow noted in PCOS patients as compared to controls (Battaglia *et al.*, 2012), and S/A ratio has been proposed as a method to refine the Rotterdam PCOS classification (Belosi *et al.*, 2006). In contrast, the S/A ratio was found to have limited predictive value as a PCOS diagnostic in reproductive-aged Thai women with PCOS (Leerasiri *et al.*, 2015). Another study found increased ovarian stromal area with PCOS, but was unable to demonstrate a relationship between stromal area and PCOS hormonal characteristics (Kaleli *et al.*, 1998). Ovarian angiogenesis dysfunction including increased ovarian stromal vascularization, lower impedance to flow (Alcázar and Kudla, 2012), and alterations in angiogenic factors levels in PCOS have been further reviewed elsewhere (Di Pietro *et al.*, 2018), with possible implications that restoration of appropriate vessel formation could improve folliculogenesis and ovulation. Inflammation-related gene expression was downregulated in the ovarian stroma and upregulated in granulosa cells for PCOS women as compared to controls, although the downregulation in the stroma may have been affected by a reduced abundance of leukocytes in the PCOS stroma as measured by *CD45* mRNA levels (Schmidt *et al.*, 2014). A reduction in theca-associated activated/memory T lymphocytes has also been seen in PCOS ovaries as compared to controls, without notable differences in macrophage or neutrophil levels across multiple ovarian compartments (Wu *et al.*, 2007). Broadly, PCOS may impact stromal volume, tunica albuginea thickness, stromal

luteinization, vascularization, blood flow, inflammation and immune cell distribution, although the causes and functional impacts of these stromal changes have not been fully elucidated.

Hyperandrogenism, one of the common aspects of PCOS, has been shown to drive certain stromal alterations. For instance, in transgender men given exogenous testosterone therapy, increases were noted in tunica albuginea collagenization, stromal hyperplasia, and stromal luteinization with clusters of luteinized stromal cells (Spinder *et al.*, 1989; Ikeda *et al.*, 2013), as well as increased stromal androgen receptor staining (Chadha *et al.*, 1994). Multiple cell types in polycystic ovaries may produce androgens, as immunohistochemistry revealed the presence of steroidogenic enzymes for androgen synthesis in follicular theca cells, luteinized stromal cells, hilar cells, and sporadic non-luteinized stromal cells (Kaaijk *et al.*, 2000). Mice treated with dihydrotestosterone (DHT) also demonstrated stromal changes, including less dense, hyperplastic, and lipid-filled stroma when compared to age-matched controls. These mice also had an overexpression of multiple genes in the mechanically-separated stroma between controls and DHT-treated mice (Candelaria *et al.*, 2019). This included increased *Vcam1* expression (which may impact vascular and immune responses) in thecal and stromal cells, while theca-specific androgen receptor knockout mice (ThARKO, *Cyp17a1*-iCre, $AR^{f/f}$ mice) demonstrated a lack of DHT-induced *Vcam1* elevation (Richards *et al.*, 2018; Candelaria *et al.*, 2019). ThARKO mice were also shown to retain much of their reproductive function, including cyclicity and fertility as compared to controls when treated with DHT (Ma *et al.*, 2017). For mice with DHT-induced stromal changes, superovulation rescued at least some of the abnormal stromal morphology (Candelaria *et al.*, 2019).

Several changes occur in the ovarian ECM in polycystic ovary syndrome. The cortex and basal laminas of follicles thicken and become more collagenous with reduced glycosaminoglycan content (Salvetti *et al.*, 2003). A comparison of human PCOS to control ovaries in both the follicular and luteal phases revealed significantly lower pro-collagen IV expression compared to control ovaries, and this decrease in collagen IV was postulated to contribute to premature luteinization (Oksjoki *et al.*, 2004). PCOS patients tend to have increased MMP-9 secretion as well, which may be related to the inability of follicles to undergo normal atresia (Dambala *et al.*, 2019).

Stromal contribution to artificial ovary technology

The term 'artificial ovary' typically references an ovary constructed using a combination of ovarian follicles (or hormone-producing cell types) within a supportive scaffold (Fig. 17). The creation of an artificial ovary as a means of fertility preservation and endocrine support has been a persistent challenge from biological and engineering perspectives, as follicle development requires a complex symphony of soluble signals and mechanical cues, some of which may derive from the ovarian stroma.

Co-culture of follicles with stromal feeder cells has shown promise for providing the key soluble factors to promote growth of early stage murine follicles *in vitro* (Tingen *et al.*, 2011). With regard to directly sourcing ovarian stromal cells, ideal collection strategies may differ between stromal cells and follicles. Human stromal cells have been shown to be better preserved after vitrification than slow freezing, with slow freezing increasing necrosis and collagen bundle disruption in the stromal cells, while follicles were similarly preserved in both vitrification and

slow freezing (Keros *et al.*, 2009). Isolating human stromal cells from fresh medullary tissue was shown to be superior to isolation from ovarian cortex in slow frozen and fresh samples, and led to increased cell yield, better viability, and improved vascularization when encapsulated in fibrin and implanted in the peritoneal pockets of nude mice (Soares *et al.*, 2015). For xenograft models, the importance of transplanting stromal endothelial cells has been demonstrated (Dath *et al.*, 2011). Isolated human ovarian cortical stromal cell suspensions containing stromal endothelial cells yielded well-vascularized and organized grafts after a 1-week implantation in mice, in contrast to grafts depleted of stromal endothelial cells, which were smaller, necrotic, and poorly vascularized (Dath *et al.*, 2011).

It is also challenging to develop a supportive scaffold that fully recapitulates the ovarian ECM. Multiple 3D hydrogel culture systems such as alginate, fibrin, and poly(ethylene glycol) (PEG) aim to recapitulate the mechanical properties of the ovarian environment to maintain the spherical structure of follicles and allow for their expansion; however, these systems are lacking the biological functionality of ECM and the ability to sequester growth factors (Luyckx *et al.*, 2014; Smith *et al.*, 2014b; Kniazeva *et al.*, 2015; Kim *et al.*, 2016; Chiti *et al.*, 2018; Rios *et al.*, 2018). Several groups have attempted to restore the biological function of ECM in these artificial ovaries by encapsulating follicles in ECM matrices such as Matrigel or decellularized tissues (Scott *et al.*, 2004; Laronda *et al.*, 2015). Unfortunately, these matrices do not include all of the components present in native ovarian ECM and also face challenges in translation in regard to availability of tissue and batch-to-batch variability.

While each of these systems incorporates key components necessary for follicle growth, there is yet to be a system that truly mimics the ovarian microenvironment in both complexity of cell populations and extracellular matrix composition which can be translated for clinical use. Part of this limitation relates to scarcity of knowledge as it pertains to the cell types and functions of the ovarian stroma.

Identification of ovarian stromal cells

The multiple populations of cells referred to as stromal cells are incompletely characterized and categorized, leading to confusion across studies that report findings about stromal cells without further identification (Fig. 17). Regional differences (e.g. cortex vs. medulla) likely influence the distribution and subtypes of stromal cells. Immunofluorescent imaging using known markers for follicular or stromal cells has advanced our understanding of the ovarian stroma, including the delineation of at least two distinct populations of steroidogenic theca and interstitial gland cells in postnatal murine ovaries, as well as the identification of at least three different somatic cell lineages in murine fetal ovaries (Rastetter *et al.*, 2014; Miyabayashi *et al.*, 2015). With developments in single-cell sequencing technologies to complement these detailed imaging studies, we may soon have the ability to better characterize the cells commonly called stromal cells and refer to them with more precise names as we understand their individual roles in physiologic and pathologic processes.

Single-cell RNA-sequencing experiments have already made progress in identifying major ovarian cell types, transition stages, and markers for cell identification. These studies have significantly contributed to mapping the signatures of human and murine oocytes and granulosa

cells from multiple follicular stages (Zhang *et al.*, 2018). Yet, data about the ovarian stroma remain elusive and comparatively scarce. An investigation of somatic cells only in the inner cortex was performed in women undergoing fertility preservation procedures, detecting five clusters of granulosa cells, five clusters of theca and stromal cells, two clusters of smooth muscle cells, three clusters of endothelial cells, and four clusters of immune cells (Fan *et al.*, 2019). They confirmed the presence of adaptive immune cells including T lymphocytes, Natural Killer cells, and B lymphocytes, as well as innate immune cells including monocytes and macrophages. This study also identified upregulation of the complement system (including C1R, C1S, and C7) by theca and stromal cells as a potential contributor to ovarian tissue remodeling (Fan *et al.*, 2019). A subsequent single-cell analysis of the human ovarian cortex reported six clusters, including oocytes, granulosa cells, immune cells, endothelial cells, perivascular cells, and stromal cells. They classified a majority of cells (83%) as stroma, noting shared expression of mesodermal lineage markers (*PDGFRA*, *DCN*), ECM proteins (*COL1A1, COL6A1*), as well as expression of *STAR* and *CYP17A1* by some cells in the stromal cluster. Although they isolated many stromal cells, their study mainly focused on discerning whether cells isolated using the Abcam DDX4 antibody were oogonial stem cells (Wagner *et al.*, 2020). A single-cell transcriptomic study of ovarian aging in nonhuman primate ovaries identified seven ovarian cell types, including oocytes, granulosa cells, stromal cells, smooth muscle cells, endothelial cells, Natural Killer T cells, and macrophages (Wang *et al.*, 2020). The stromal cell cluster specifically expressed *TCF21* and *COL1A2*, with some cells in the stromal cluster expressing high levels of *STAR* (Wang *et al.*, 2020). A time series single-cell RNA sequencing study was performed for cells labeled with the gonadal somatic cell marker *Nr5a1* (steroidogenic factor 1, SF-1) in the developing mouse ovary from E10.5 to postnatal day 6. Four distinct populations, including early

progenitors, stromal progenitors, pre-granulosa cells, and postnatal granulosa cells were identified from their sequencing. Using their time series, they analyzed cell conversion from early progenitors to both the stromal progenitor lineage (E13.5) and the granulosa cell lineages (E11.5-E12.5) (Stévant *et al.*, 2019). These studies are supported by precise immunofluorescent characterization of at least three somatic cell populations in fetal mouse ovaries, including COUP-TFII-positive possible pre-theca progenitors, LGR5-positive cortical granulosa cell progenitors, and FOXL2-positive medullary granulosa cell progenitors (Rastetter *et al.*, 2014). Although single-cell sequencing studies allow for greater granularity in understanding the nuance of different ovarian cellular populations, including the stroma, it remains important to continually reflect on the possible limitations of any starting cellular populations (e.g. inner cortex only), with the overall goal of broadening our understanding of the entire ovarian microenvironment.

Future perspectives

As the majority of ovarian research studies focus on the ovarian follicles, a thorough understanding of the components and functions of the ovarian stroma is an active area of current research. The support provided by the ovarian stroma is essential for 3D follicular maintenance and the integration of signals to support folliculogenesis. The stromal compartment is heterogeneous and analyses using bulk methods or gross dissection may lose the granularity that could be observed between low density specialized cellular populations. In addition to precise immunohistochemical and immunofluorescent studies for specific stromal cell population identification and lineage tracing, single-cell sequencing studies will continue to allow for more in-depth analysis of physiologic and pathologic changes occurring to specific cell types that

might otherwise be grouped together. These sequencing studies must be conducted with critical reflection on the specifics of the origin of the sequenced cells. Greater understanding and careful ontology of the different populations of stromal cells would reduce ambiguity between studies. Further study integrating phenotypic changes in specific stromal cellular populations with functional changes would also help determine how changes in the ovarian stroma occur over time and may interact with folliculogenesis, position, and hormone production.

Declaration of Interest

Vasantha Padmanabhan is an Associate Editor of *Reproduction.* Vasantha Padmanabhan was not involved in the review or editorial process for this paper, on which she is listed as an author. The other authors have nothing to disclose.

Funding

This work was supported by the National Institutes of Health (R01-EB022033 to A.S., R01-HD098233 to M.B.M., P01-HD044232 to V.P., F30-HD100163 and T32-HD079342 to H.M.K., F31-HD100069 and T32-DE007057 to C.E.T.); NSF CAREER (1552580 to A.S.), American Society for Reproductive Medicine/Society for Reproductive Endocrinology and Infertility Grant to M.B.M., Chan Zuckerberg Initiative Human Cell Atlas of the Female Reproductive System to A.S., University of Michigan Office of Research funding (U058227) to M.B.M.

Author Contribution Statement

H.M.K., A.S. and V.P. conceived and drafted the review. A.S. provided oversight. H.M.K. and C.E.T. wrote the review. F.L.C. revised the figures. M.B.M., M.X. and F.L.C. provided critical input and edits. All authors read and approved the final version.

Bibliography

Abbott DH, Barnett DK, Bruns CM, Dumesic DA. Androgen excess fetal programming of female reproduction: a developmental aetiology for polycystic ovary syndrome? *Hum Reprod Update* 2005;**11**:357–374.

Abd-Elkareem M. Cell-specific immuno-localization of progesterone receptor alpha in the rabbit ovary during pregnancy and after parturition. *Anim Reprod Sci* 2017;**180**:100–120.

Adeleye AJ, Cedars MI, Smith J, Mok-Lin E. Ovarian stimulation for fertility preservation or family building in a cohort of transgender men. *J Assist Reprod Genet* 2019;**36**:2155–2161.

Aflatounian A, Edwards MC, Rodriguez Paris V, Bertoldo MJ, Desai R, Gilchrist RB, Ledger WL, Handelsman DJ, Walters KA. Androgen signaling pathways driving reproductive and metabolic phenotypes in a PCOS mouse model. *J Endocrinol* 2020;**245**:381–395.

Alcázar JL, Kudla MJ. Ovarian stromal vessels assessed by spatiotemporal image correlation-high definition flow in women with polycystic ovary syndrome: a case-control study. *Ultrasound Obstet Gynecol* 2012;**40**:470–475.

Amir H, Yaish I, Samara N, Hasson J, Groutz A, Azem F. Ovarian stimulation outcomes among transgender men compared with fertile cisgender women. *J Assist Reprod Genet* 2020;**37**:2463–2472.

Amirikia H, Savoy-Moore RT, Sundareson AS, Moghissi KS. The effects of long-term androgen treatment on the ovary. *Fertil Steril* 1986;**45**:202–208.

Anderson WJ, Kolin DL, Neville G, Diamond DA, Crum CP, Hirsch MS, Vargas SO. Prostatic Metaplasia of the Vagina and Uterine Cervix. *Am J Surg Pathol* 2020;**44**:1040–1049.

Andrews S. FastQC: A quality control tool for high throughput sequence data. 2010;Available from: http://www.bioinformatics.babraham.ac.uk/projects/fastqc/.

Armuand G, Dhejne C, Olofsson JII, Rodriguez-Wallberg KAA. Transgender men's experiences of fertility preservation: a qualitative study. *Hum Reprod* 2017;**32**:383–390.

Arnold AP, Breedlove SM. Organizational and Activational Effects of Sex Steroids on Brain and Behavior: A Reanalysis. *Horm Behav* 1985;**19**:469–498.

Auer MK, Fuss J, Nieder TO, Briken P, Biedermann S V., Stalla GK, Beckmann MW, Hildebrandt T. Desire to Have Children Among Transgender People in Germany: A Cross-Sectional Multi-Center Study. *J Sex Med* 2018;**15**:757–767.

Auersperg N, Wong AST, Choi K-C, Kang SK, Leung PCK. Ovarian Surface Epithelium: Biology, Endocrinology, and Pathology. *Endocr Rev* 2001;**22**:255–288.

Baba T, Endo T, Honnma H, Kitajima Y, Hayashi T, Ikeda H, Masumori N, Kamiya H, Moriwaka O, Saito T. Association between polycystic ovary syndrome and female-to-male transsexuality. *Hum Reprod* 2007;**22**:1011–1016.

Baddela VS, Sharma A, Viergutz T, Koczan D, Vanselow J. Low Oxygen Levels Induce Early Luteinization Associated Changes in Bovine Granulosa Cells. *Front Physiol* 2018;**9**:1066.

Baram S, Myers SA, Yee S, Librach CL. Fertility preservation for transgender adolescents and young adults: a systematic review. *Hum Reprod Update* 2019;**25**:694–716.

Barria A, Leyton V, Ojeda SR, Lara HE. Ovarian steroidal response to gonadotropins and β-Adrenergic stimulation is enhanced in polycystic ovary syndrome: Role of sympathetic innervation. *Endocrinology* 1993;**133**:2696–2703.

Bartels CB, Uliasz TF, Lestz L, Mehlmann LM. Short-term testosterone use in female mice does not impair fertilizability of eggs: implications for the fertility care of transgender males. *Hum Reprod* 2020;1–10.

Bashamboo A, Eozenou C, Jorgensen A, Bignon-Topalovic J, Siffroi JP, Hyon C, Tar A, Nagy P, Sólyom J, Halász Z, *et al.* Loss of Function of the Nuclear Receptor NR2F2, Encoding COUP-TF2, Causes Testis Development and Cardiac Defects in 46,XX Children. *Am J Hum Genet* 2018;**102**:487–493.

Battaglia C, Battaglia B, Morotti E, Paradisi R, Zanetti I, Meriggiola MC, Venturoli S. Two- and Three-Dimensional Sonographic and Color Doppler Techniques for Diagnosis of Polycystic Ovary Syndrome. *J Ultrasound Med* 2012;**31**:1015–1024.

Becerra-Fernández A, Pérez-López G, Román MM, Martín-Lazaro JF, Pérez MJL, Araque NA, Rodríguez-Molina JM, Sertucha MCB, Vilas MVA. Prevalence of hyperandrogenism and polycystic ovary syndrome in female to male transsexuals. *Endocrinol Nutr* 2014;**61**:351–358.

Belosi C, Selvaggi L, Apa R, Guido M, Romualdi D, Fulghesu AM, Lanzone A. Is the PCOS diagnosis solved by ESHRE/ASRM 2003 consensus or could it include ultrasound examination of the ovarian stroma? *Hum Reprod* 2006;**21**:3108–3115.

Benten WPM, Ulrich P, Kühn-Velten WN, Vohr HW, Wunderlich F. Testosterone-induced susceptibility to Plasmodium chabaudi malaria: persistence after withdrawal of testosterone. *J Endocrinol* 1997;**153**:275–281.

Berkholtz CB, Shea LD, Woodruff TK. Extracellular matrix functions in follicle maturation. *Semin Reprod Med* 2006;**24**:262–269.

Briley SM, Jasti S, McCracken JM, Hornick JE, Fegley B, Pritchard MT, Duncan FE. Reproductive age-associated fibrosis in the stroma of the mammalian ovary. *Reproduction* 2016;**152**:245–260.

Broughton D, Omurtag K. Care of the transgender or gender-nonconforming patient undergoing in vitro fertilization. *Int J Transgenderism* 2017;**18**:372–375.

Brown HM, Robker RL, Russell DL. Development and hormonal regulation of the ovarian lymphatic vasculature. *Endocrinology* 2010;**151**:5446–5455.

Brown HM, Russell DL. Blood and lymphatic vasculature in the ovary: Development, function and disease. *Hum Reprod Update* 2014;**20**:29–39.

Buckett WM, Bouzayen R, Watkin KL, Tulandi T, Tan SL. Ovarian stromal echogenicity in women with normal and polycystic ovaries. *Hum Reprod* 1999;**14**:618–621.

Caanen MR, Schouten NE, Kuijper EAM, Rijswijk J van, Berg MH van den, Dulmen-den Broeder E van, Overbeek A, Leeuwen FE van, Trotsenburg M van, Lambalk CB. Effects of long-term exogenous testosterone administration on ovarian morphology, determined by transvaginal (3D) ultrasound in female-to-male transsexuals. *Hum Reprod* 2017;**32**:1457–1464.

Caanen MR, Soleman RS, Kuijper EAM, Kreukels BPC, Roo C De, Tilleman K, Sutter P De, Trotsenburg MAA van, Broekmans FJ, Lambalk CB. Antimüllerian hormone levels decrease in female-to-male transsexuals using testosterone as cross-sex therapy. *Fertil Steril* 2015;**103**:1340–1345.

Caldwell ASL, Middleton LJ, Jimenez M, Desai R, McMahon AC, Allan CM, Handelsman DJ, Walters KA. Characterization of Reproductive, Metabolic, and Endocrine Features of Polycystic Ovary Syndrome in Female Hyperandrogenic Mouse Models. *Endocrinology* 2014;**155**:3146–3159.

Candelaria NR, Padmanabhan A, Stossi F, Ljungberg MC, Shelly KE, Pew BK, Solis M, Rossano AM, McAllister JM, Wu S, *et al.* VCAM1 is induced in ovarian theca and stromal cells in a mouse model of androgen excess. *Endocrinology* 2019;**160**:1377–1393.

Care AS, Diener KR, Jasper MJ, Brown HM, Ingman W V., Robertson SA. Macrophages regulate corpus luteum development during embryo implantation in mice. *J Clin Invest* 2013;**123**:3472–3487.

Carlock C, Wu J, Zhou C, Ross A, Adams H, Lou Y. Ovarian phagocyte subsets and their distinct tissue distribution patterns. *Reproduction* 2013;**146**:491–500.

Chadha S, Pache TD, Huikeshoven FJM, Brinkmann AO, Kwast TH van der. Androgen Receptor Expression in Human Ovarian and Uterine Tissue of Long Term Androgen-Treated Transsexual Women. *Hum Pathol* 1994;**25**:1198–1204.

Chapin RE, Morrissey RE, Gulati DK, Hope E, Barnes L, Russell S, SR K. Are Mouse Strains Differentially Susceptible to the Reproductive Toxicity of Ethylene Glycol Monomethyl Ether? A Study of Three Strains. *Fundam Appl Toxicol* 1993;**21**:8–14.

Chistiakov DA, Killingsworth MC, Myasoedova VA, Orekhov AN, Bobryshev Y V. CD68/macrosialin: Not just a histochemical marker. *Lab Investig* 2017;**97**:4–13.

Chiti MC, Dolmans M-M, Mortiaux L, Zhuge F, Ouni E, Shahri PAK, Ruymbeke E Van, Champagne S-D, Donnez J, Amorim CA. A novel fibrin-based artificial ovary prototype resembling human ovarian tissue in terms of architecture and rigidity. *J Assist Reprod Genet* 2018;**35**:41–48.

Cho K, Harjee R, Roberts J, Dunne C. Fertility preservation in a transgender man without prolonged discontinuation of testosterone: a case report and literature review. *F&S Reports* 2020;**1**:43–47.

Coleman E, Bockting W, Botzer M, Cohen-Kettenis P, DeCuypere G, Feldman J, Fraser L, Green J, Knudson G, Meyer WJ, *et al.* Standards of Care for the Health of Transsexual, Transgender, and Gender-Nonconforming People, Version 7. *Int J Transgenderism* 2011;**13**:165–232.

Cora MC, Kooistra L, Travlos G. Vaginal Cytology of the Laboratory Rat and Mouse: Review and Criteria for the Staging of the Estrous Cycle Using Stained Vaginal Smears. *Toxicol Pathol* 2015;**43**:776–793.

Curry T, Smith M. Impact of Extracellular Matrix Remodeling on Ovulation and the Folliculo-Luteal Transition. *Semin Reprod Med* 2006;**24**:228–241.

Dambala K, Paschou SA, Michopoulos A, Siasos G, Goulis DG, Vavilis D, Tarlatzis BC. Biomarkers of Endothelial Dysfunction in Women With Polycystic Ovary Syndrome. *Angiology* 2019;**70**:797–801.

Dath C, Dethy A, Langendonckt A Van, Eyck AS Van, Amorim CA, Luyckx V, Donnez J, Dolmans MM. Endothelial cells are essential for ovarian stromal tissue restructuring after xenotransplantation of isolated ovarian stromal cells. *Hum Reprod* 2011;**26**:1431–1439.

Deanesly R, Parkes AS. Note on the subcutaneous absorption of oils by rats and mice, with special reference to the assay of œstrin. *J Physiol* 1933;**78**:155–160.

Delibasi T, Erdogan MF, Serinsöz E, Kaygusuz G, Erdogan G, Sertçelik A. Ovarian hilus-cell hyperplasia and high serum testosterone in a patient with postmenopausal virilization. *Endocr Pract* 2007;**13**:472–475.

Delić D, Gailus N, Vohr HW, Dkhil M, Al-Quraishy S, Wunderlich F. Testosterone-induced permanent changes of hepatic gene expression in female mice sustained during Plasmodium chabaudi malaria infection. *J Mol Endocrinol* 2010;**45**:379–390.

Ding X, Liu G, Xu B, Wu C, Hui N, Ni X, Wang J, Du M, Teng X, Wu J. Human GV oocytes generated by mitotically active germ cells obtained from follicular aspirates. *Sci Rep* 2016;**6**:1–17.

Dobin A, Davis CA, Schlesinger F, Drenkow J, Zaleski C, Jha S, Batut P, Chaisson M, Gingeras TR. STAR: ultrafast universal RNA-seq aligner. *Bioinformatics* 2013;**29**:15–21.

Dulohery K, Trottmann M, Bour S, Liedl B, Alba-Alejandre I, Reese S, Hughes B, Stief CG, Kölle S. How do elevated levels of testosterone affect the function of the human fallopian tube and fertility?—New insights. *Mol Reprod Dev* 2020;**87**:30–44.

Ellis SA, Wojnar DM, Pettinato M. Conception, Pregnancy, and Birth Experiences of Male and Gender Variant Gestational Parents: It's How We Could Have a Family. *J Midwifery Women's Heal* 2015;**60**:62–69.

Erickson GF, Magoffin DA, Dyer CA, Hofeditz C. The ovarian androgen producing cells: A review of structure/function relationships. *Endocr Rev* 1985;**6**:371–399.

Esparza LA, Terasaka T, Lawson MA, Kauffman AS. Androgen Suppresses In Vivo and In Vitro LH Pulse Secretion and Neural Kiss1 and Tac2 Gene Expression in Female Mice. *Endocrinology* 2020;**161**:1–16.

Ethics Committee of the American Society for Reproductive Medicine. Access to fertility services by transgender persons: an Ethics Committee opinion. *Fertil Steril* 2015;**104**:1111–1115. Elsevier.

Falck F, Frisén L, Dhejne C, Armuand G. Undergoing pregnancy and childbirth as trans masculine in Sweden: experiencing and dealing with structural discrimination, gender norms and microaggressions in antenatal care, delivery and gender clinics. *Int J Transgender Heal* 2020;**22**:42–53.

Fan X, Bialecka M, Moustakas I, Lam E, Torrens-Juaneda V, Borggreven N V., Trouw L, Louwe LA, Pilgram GSK, Mei H, *et al.* Single-cell reconstruction of follicular remodeling in the human adult ovary. *Nat Commun* 2019;**10**:1–13.

Flores AR, Herman JL, Gates GJ, Brown TNT. *How Many Adults Identify As Transgender in the United States?* [Internet]. *Williams Inst* [Internet] 2016; Los Angeles, CAAvailable from: https://williamsinstitute.law.ucla.edu/wp-content/uploads/How-Many-Adults-Identify-as-Transgender-in-the-United-States.pdf.

Flurkey K, Currer J, Harrison D. The Mouse in Aging Research. In Fox J, editor. *Mouse Biomed Res* 2007;, p. 637–672. American College Laboratory Animal Medicine (Elsevier):

Burlington, MA.

Futterweit W, Deligdisch L. Histopathological Effects of Exogenously Administered Testosterone in 19 Female to Male Transsexuals. *J Clin Endocrinol Metab* 1986;**62**:16–21.

Gafvels M, Selstam G, Damber JE. Influence of oxygen tension and substrates on basal and luteinizing hormone stimulated progesterone production and energy metabolism by isolated corpora lutea of adult pseudopregnant rats. *Acta Physiol Scand* 1987;**130**:475–482.

Goetz LG, Mamillapalli R, Devlin MJ, Robbins AE, Majidi-Zolbin M, Taylor HS. Cross-sex testosterone therapy in ovariectomized mice: addition of low-dose estrogen preserves bone architecture. *Am J Physiol - Endocrinol Metab* 2017;**313**:E540-E551.

Goetz LG, Mamillapalli R, Sahin C, Majidi-Zolbin M, Ge G, Mani A, Taylor HS. Addition of Estradiol to Cross-Sex Testosterone Therapy Reduces Atherosclerosis Plaque Formation in Female ApoE−/− Mice. *Endocrinology* 2018;**159**:754–762.

Gray H. *Anatomy of the Human Body*. In Lewis WH, editor. 1918; Lea & Febiger: Philadelphia and New York.

Greenwald P, Dubois B, Lekovich J, Pang JH, Safer J. Successful In Vitro Fertilization in a Cisgender Female Carrier Using Oocytes Retrieved From a Transgender Man Maintained on Testosterone. *AACE Clin Case Reports* 2021;7–9.

Grimstad FW, Fowler KG, New EP, Ferrando CA, Pollard RR, Chapman G, Gomez-Lobo V, Gray M. Uterine pathology in transmasculine persons on testosterone: a retrospective multicenter case series. *Am J Obstet Gynecol* 2019;**220**:257.e1-257.e7.

Grynberg M, Fanchin R, Dubost G, Colau JC, Brémont-Weil C, Frydman R, Ayoubi J-M. Histology of genital tract and breast tissue after long-term testosterone administration in a female-to-male transsexual population. *Reprod Biomed Online* 2010;**20**:553–558.

Hahn M, Sheran N, Weber S, Cohan D, Obedin-Maliver J. Providing Patient-Centered Perinatal Care for Transgender Men and Gender-Diverse Individuals. *Obstet Gynecol* 2019;**134**:959–963.

Hartanti MD, Hummitzsch K, Bonner WM, Bastian NA, Irving-Rodgers HF, Rodgers RJ. Formation of the Bovine Ovarian Surface Epithelium during Fetal Development. *J Histochem Cytochem* 2020;**68**:113–126.

Hawkins M, Deutsch MB, Obedin-Maliver J, Stark B, Grubman J, Jacoby A, Jacoby VL. Endometrial findings among transgender and gender nonbinary people using testosterone at the time of gender-affirming hysterectomy. *Fertil Steril* 2021;**115**:1312–1317.

Hembree WC, Cohen-Kettenis PT, Gooren L, Hannema SE, Meyer WJ, Murad MH, Rosenthal SM, Safer JD, Tangpricha V, T'Sjoen GG. Endocrine Treatment of Gender-

Dysphoric/Gender-Incongruent Persons: An Endocrine Society* Clinical Practice Guideline. *J Clin Endocrinol Metab* 2017;**102**:1–35.

Henning NF, LeDuc RD, Even KA, Laronda MM. Proteomic analyses of decellularized porcine ovaries identified new matrisome proteins and spatial differences across and within ovarian compartments. *Sci Rep* 2019;**9**:20001.

Herman JL, Flores AR, Brown TNT, Wilson BDM, Conron KJ. *Age of Individuals who Identify as Transgender in the United States* [Internet]. *Williams Inst* [Internet] 2017; Los Angeles, CAAvailable from: https://williamsinstitute.law.ucla.edu/wp-content/uploads/Age-Trans-Individuals-Jan-2017.pdf.

Hornick JE, Duncan FE, Shea LD, Woodruff TK. Isolated primate primordial follicles require a rigid physical environment to survive and grow in vitro. *Hum Reprod* 2012;**27**:1801–1810.

Houten ELAF van, Visser JA. Mouse models to study polycystic ovary syndrome: A possible link between metabolism and ovarian function? *Reprod Biol* 2014;**14**:32–43.

Hughesdon PE. Morphology and Morphogenesis of the Stein-Leventhal Ovary and of So-called "Hyperthecosis." *Obstet Gynecol Surv* 1982;**37**:59–77.

Hummitzsch K, Anderson RA, Wilhelm D, Wu J, Telfer EE, Russell DL, Robertson SA, Rodgers RJ. Stem cells, progenitor cells, and lineage decisions in the ovary. *Endocr Rev* 2015;**36**:65–91.

Hummitzsch K, Hatzirodos N, Macpherson AM, Schwartz J, Rodgers RJ, Irving-Rodgers HF. Transcriptome analyses of ovarian stroma: tunica albuginea, interstitium and theca interna. *Reproduction* 2019;**157**:545–565.

Hummitzsch K, Irving-Rodgers HF, Hatzirodos N, Bonner W, Sabatier L, Reinhardt DP, Sado Y, Ninomiya Y, Wilhelm D, Rodgers RJ. A New Model of Development of the Mammalian Ovary and Follicles. In Schmidt EE, editor. *PLoS One* 2013;**8**:e55578.

Ikeda K, Baba T, Noguchi H, Nagasawa K, Endo T, Kiya T, Saito T. Excessive androgen exposure in female-to-male transsexual persons of reproductive age induces hyperplasia of the ovarian cortex and stroma but not polycystic ovary morphology. *Hum Reprod* 2013;**28**:453–461.

Insogna IG, Ginsburg E, Srouji S. Fertility Preservation for Adolescent Transgender Male Patients: A Case Series. *J Adolesc Heal* 2020;**66**:750–753.

Irving-Rodgers HF, Rodgers RJ. Extracellular matrix of the developing ovarian follicle. *Semin Reprod Med* 2006;**24**:195–203.

Jabara S, Christenson LK, Wang CY, McAllister JM, Javitt NB, Dunaif A, Strauss JF. Stromal cells of the human postmenopausal ovary display a distinctive biochemical and molecular

phenotype. *J Clin Endocrinol Metab* 2003;**88**:484–492.

Jackson-Bey T, Colina J, Isenberg BC, Coppeta J, Urbanek M, Kim JJ, Woodruff TK, Burdette JE, Russo A. Exposure of human fallopian tube epithelium to elevated testosterone results in alteration of cilia gene expression and beating. *Hum Reprod* 2020;**35**:2086–2096.

Jiménez R. Ovarian Organogenesis in Mammals: Mice Cannot Tell Us Everything. *Sex Dev* 2009;**3**:291–301.

Johnson J, Canning J, Kaneko T, Pru JK, Tilly JL. Germline stem cells and follicular renewal in the postnatal mammalian ovary. *Nature* 2004;**428**:145–150.

Kaaijk EM, Sasano H, Suzuki T, Beek JF, Veen F van der. Distribution of steroidogenic enzymes involved in androgen synthesis in polycystic ovaries: an immunohistochemical study. *Mol Hum Reprod* 2000;**6**:443–447.

Kaleli S, Erel CT, Oral E, Elter K, Akman C, Colgar U. Ovarian stromal hypertrophy in polycystic ovary syndrome. *J Reprod Med Obstet Gynecol* 1998;**43**:893–897.

Kawamura K, Cheng Y, Suzuki N, Deguchi M, Sato Y, Takae S, Ho C, Kawamura N, Tamura M, Hashimoto S, *et al.* Hippo signaling disruption and Akt stimulation of ovarian follicles for infertility treatment. *Proc Natl Acad Sci* 2013;**110**:17474–17479.

Kenngott RAM, Scholz W, Sinowatz F. Ultrastructural Aspects of the Prenatal Bovine Ovary Differentiation with a Special Focus on the Interstitial Cells. *Anat Histol Embryol* 2016;**45**:357–366.

Keros V, Xella S, Hultenby K, Pettersson K, Sheikhi M, Volpe A, Hreinsson J, Hovatta O. Vitrification versus controlled-rate freezing in cryopreservation of human ovarian tissue. *Hum Reprod* 2009;**24**:1670–1683.

Khalifa MA, Toyama A, Klein ME, Santiago V. Histologic Features of Hysterectomy Specimens From Female-Male Transgender Individuals. *Int J Gynecol Pathol* 2019;**38**:520–527.

Kim J, Perez AS, Claflin J, David A, Zhou H, Shikanov A. Synthetic hydrogel supports the function and regeneration of artificial ovarian tissue in mice. *npj Regen Med* 2016;**1**:16010.

Kim JH, Karnovsky A, Mahavisno V, Weymouth T, Pande M, Dolinoy DC, Rozek LS, Sartor MA. LRpath analysis reveals common pathways dysregulated via DNA methylation across cancer types. *BMC Genomics* 2012;**13**:526.

Kinnear HM, Constance ES, David A, Marsh EE, Padmanabhan V, Shikanov A, Moravek MB. A mouse model to investigate the impact of testosterone therapy on reproduction in transgender men. *Hum Reprod* 2019;**34**:2009–2017.

Kinnear HM, Hashim PH, Cruz C Dela, Rubenstein G, Chang FL, Nimmagadda L, Brunette

MA, Padmanabhan V, Shikanov A, Moravek MB. Reversibility of testosterone-induced acyclicity after testosterone cessation in a transgender mouse model. *F&S Sci* 2021;**2**:116–123.

Kinnear HM, Tomaszewski CE, Chang FL, Moravek MB, Xu M, Padmanabhan V, Shikanov A. The ovarian stroma as a new frontier. *Reproduction* 2020;**160**:R25–R39.

Kizuka-Shibuya F, Tokuda N, Takagi K, Adachi Y, Lee L, Tamura I, Maekawa R, Tamura H, Suzuki T, Owada Y, *et al.* Locally existing endothelial cells and pericytes in ovarian stroma, but not bone marrow-derived vascular progenitor cells, play a central role in neovascularization during follicular development in mice. *J Ovarian Res* 2014;**7**:10.

Kniazeva E, Hardy AN, Boukaidi SA, Woodruff TK, Jeruss JS, Shea LD. Primordial Follicle Transplantation within Designer Biomaterial Grafts Produce Live Births in a Mouse Infertility Model. *Sci Rep* 2015;**5**:1–11.

Kong L-L, Yang N-Z, Shi L-H, Zhao G-H, Zhou W, Ding Q, Wang M-H, Zhang Y-S. The optimum marker for the detection of lymphatic vessels. *Mol Clin Oncol* 2017;**7**:515–520.

Konishi I, Fujii S, Okamura H, Parmley T, Mori T. Development of interstitial cells and ovigerous cords in the human fetal ovary: an ultrastructural study. *J Anat* 1986;**148**:121–135.

Krishnan V, Pereira FA, Qiu Y, Chen C-H, Beachy PA, Tsai SY, Tsai M-J. Mediation of Sonic Hedgehog-Induced Expression of COUP-TFII by a Protein Phosphatase. *Science (80-)* 1997;**278**:1947–1950.

Laronda MM, Jakus AE, Whelan KA, Wertheim JA, Shah RN, Woodruff TK. Initiation of puberty in mice following decellularized ovary transplant. *Biomaterials* 2015;**50**:20–29.

Leerasiri P, Wongwananuruk T, Rattanachaiyanont M, Indhavivadhana S, Techatraisak K, Angsuwathana S. Ratio of ovarian stroma and total ovarian area by ultrasound in prediction of hyperandrogenemia in reproductive-aged Thai women with polycystic ovary syndrome: A diagnostic test. *J Obstet Gynaecol Res* 2015;**41**:248–253.

Lei L, Spradling AC. Female mice lack adult germ-line stem cells but sustain oogenesis using stable primordial follicles. *Proc Natl Acad Sci U S A* 2013;**110**:8585–8590.

Leung A, Sakkas D, Pang S, Thornton K, Resetkova N. Assisted reproductive technology outcomes in female-to-male transgender patients compared with cisgender patients: a new frontier in reproductive medicine. *Fertil Steril* 2019;**112**:858–865.

Li B, Dewey CN. RSEM: accurate transcript quantification from RNA-Seq data with or without a reference genome. *BMC Bioinformatics* 2011;**12**:323.

Lierman S, Tilleman K, Braeckmans K, Peynshaert K, Weyers S, T'Sjoen G, Sutter P De.

Fertility preservation for trans men: frozen-thawed in vitro matured oocytes collected at the time of ovarian tissue processing exhibit normal meiotic spindles. *J Assist Reprod Genet* 2017;**34**:1449–1456.

Lierman S, Tolpe A, Croo I De, Gheselle S De, Defreyne J, Baetens M, Dheedene A, Colman R, Menten B, T'Sjoen G, *et al.* Low feasibility of in vitro matured oocytes originating from cumulus complexes found during ovarian tissue preparation at the moment of gender confirmation surgery and during testosterone treatment for fertility preservation in transgender men. *Fertil Steril* 2021;**116**:1068–1076.

Light A, Wang LF, Zeymo A, Gomez-Lobo V. Family planning and contraception use in transgender men. *Contraception* 2018;**98**:266–269.

Light AD, Obedin-Maliver J, Sevelius JM, Kerns JL. Transgender Men Who Experienced Pregnancy After Female-to-Male Gender Transitioning. *Obstet Gynecol* 2014;**124**:1120–1127.

Lin LH, Hernandez A, Marcus A, Deng F-M, Adler E. Histologic Findings in Gynecologic Tissue From Transmasculine Individuals Undergoing Gender-Affirming Surgery. *Arch Pathology Lab Med* 2021;

Lind A-K, Weijdegård B, Dahm-Kähler P, Mölne J, Sundfeldt K, Brännström M. Collagens in the human ovary and their changes in the perifollicular stroma during ovulation. *Acta Obstet Gynecol Scand* 2006;**85**:1476–1484.

Liu C, Peng J, Matzuk MM, Yao HHC. Lineage specification of ovarian theca cells requires multicellular interactions via oocyte and granulosa cells. *Nat Commun* 2015;**6**:6934.

Liu R, Zhang X, Fan Z, Wang Y, Yao G, Wan X, Liu Z, Yang B, Yu L. Human amniotic mesenchymal stem cells improve the follicular microenvironment to recover ovarian function in premature ovarian failure mice. *Stem Cell Res Ther* 2019;**10**:1–14.

Lliberos C, Liew SH, Zareie P, Gruta NL La, Mansell A, Hutt K. Evaluation of inflammation and follicle depletion during ovarian ageing in mice. *Sci Rep* 2021;**11**:278.

Logan A, Hill DJ. Bioavailability: Is this a key event in regulating the actions of peptide growth factors? *J Endocrinol* 1992;**134**:157–161.

Love MI, Huber W, Anders S. Moderated estimation of fold change and dispersion for RNA-seq data with DESeq2. *Genome Biol* 2014;**15**:550.

Loverro G, Resta L, Dellino M, Edoardo DN, Cascarano MA, Loverro M, Mastrolia SA. Uterine and ovarian changes during testosterone administration in young female-to-male transsexuals. *Taiwan J Obstet Gynecol* 2016;**55**:686–691.

Luyckx V, Dolmans M-M, Vanacker J, Legat C, Fortuño Moya C, Donnez J, Amorim CA. A

new step toward the artificial ovary: Survival and proliferation of isolated murine follicles after autologous transplantation in a fibrin scaffold. *Fertil Steril* 2014;**101**:1149–1156.

Ma Y, Andrisse S, Chen Y, Childress S, Xue P, Wang Z, Jones D, Ko C, Divall S, Wu S. Androgen Receptor in the Ovary Theca Cells Plays a Critical Role in Androgen-Induced Reproductive Dysfunction. *Endocrinology* 2017;**158**:98–108.

Martin M. Cutadapt removes adapter sequences from high-throughput sequencing reads. *EMBnet.journal* 2011;**17**:10–12.

Matousek M, Carati C, Gannon B, Brännström M. Novel method for intrafollicular pressure measurements in the rat ovary: increased intrafollicular pressure after hCG stimulation. *Reproduction* 2001;**121**:307–314.

McArthur ME, Irving-Rodgers HF, Byers S, Rodgers RJ. Identification and Immunolocalization of Decorin, Versican, Perlecan, Nidogen, and Chondroitin Sulfate Proteoglycans in Bovine Small-Antral Ovarian Follicles1. *Biol Reprod* 2000;**63**:913–924.

McIntush EW, Smith MF. Matrix metalloproteinases and tissue inhibitors of metalloproteinases in ovarian function. *Rev Reprod* 1998;**3**:23–30.

McKey J, Bunce C, Batchvarov IS, Ornitz DM, Capel B. Neural crest-derived neurons invade the ovary but not the testis during mouse gonad development. *Proc Natl Acad Sci* 2019;**116**:5570–5575.

Mescher AL. *Epithelial Tissue*. In Weitz M, Kearns B, Boyle P, editors. *Junqueira's Basic Histol Text Atlas* 2018; McGraw-Hill Education: New York, NY.

Meyer WJ, Webb A, Stuart CA, Finkelstein JW, Lawrence B, Walker PA. Physical and Hormonal Evaluation of Transsexual Patients : A Longitudinal Study. *Arch Sex Behav* 1986;**15**:121–138.

Miller N, Bédard YC, Cooter NB, Shaul DL. Histological changes in the genital tract in transsexual women following androgen therapy. *Histopathology* 1986;**10**:661–669.

Miyabayashi K, Tokunaga K, Otake H, Baba T, Shima Y, Morohashi K. Heterogeneity of ovarian theca and interstitial gland cells in mice. *PLoS One* 2015;**10**:e0128352.

Monniaux D, Huet-Calderwood C, Bellego F Le, Fabre S, Monget P, Calderwood DA. Integrins in the Ovary. *Semin Reprod Med* 2006;**24**:251–261.

Moravek MB, Kinnear HM, George J, Batchelor J, Shikanov A, Padmanabhan V, Randolph JF. Impact of Exogenous Testosterone on Reproduction in Transgender Men. *Endocrinology* 2020;**161**:1–13.

Morrissey RE, Lamb JC, Morris RW, Chapin RE, Gulati DK, Heindel JJ. Results and

Evaluations of 48 Continuous Breeding Reproduction Studies Conducted in Mice. *Fundam Appl Toxicol* 1989;**13**:747–777.

Moseson H, Fix L, Hastings J, Stoeffler A, Lunn MR, Flentje A, Lubensky ME, Capriotti MR, Ragosta S, Forsberg H, *et al.* Pregnancy intentions and outcomes among transgender, nonbinary, and gender-expansive people assigned female or intersex at birth in the United States: Results from a national, quantitative survey. *Int J Transgender Heal* 2021;**22**:30–41.

Mueller A, Gooren LJ, Naton-Schötz S, Cupisti S, Beckmann MW, Dittrich R. Prevalence of Polycystic Ovary Syndrome and Hyperandrogenemia in Female-to-Male Transsexuals. *J Clin Endocrinol Metab* 2008;**93**:1408–1411.

Neilson D, Seegar Jones G, Woodruff JD, Goldberg B. The innervation of the ovary. *Obstet Gynecol Surv* 1970;**25**:889–904.

Nelson JF, Karelus K, Felicio LS, Johnson TE. Genetic influences on the timing of puberty in mice. *Biol Reprod* 1990;**42**:649–655.

Norman RJ, Brannstrom M. White cells and the ovary – incidental invaders or essential effectors? *J Endocrinol* 1994;**140**:333–336.

Okamura H, Takenaka A, Yajima Y, Nishimura T. Ovulatory changes in the wall at the apex of the human Graafian follicle. *J Reprod Fert* 1980;**58**:153–155.

Oksjoki S, Rahkonen O, Haarala M, Vuorio E, Anttila L. Differences in connective tissue gene expression between normally functioning, polycystic and post-menopausal ovaries. *Mol Hum Reprod* 2004;**10**:7–14.

Ouni E, Vertommen D, Chiti MC, Dolmans M-M, Amorim CA. A Draft Map of the Human Ovarian Proteome for Tissue Engineering and Clinical Applications. *Mol Cell Proteomics* 2019;**18**:S159–S173.

Pache TD, Chadha S, Gooren LJG, Hop WCJ, Jaarsma KW, Dommerholt HBR, Fauser BCJM. Ovarian morphology in long-term androgen-treated female to male transsexuals. A human model for the study of polycystic ovarian syndrome? *Histopathology* 1991;**19**:445–452.

Padmanabhan V, Veiga-Lopez A. Animal models of the polycystic ovary syndrome phenotype. *Steroids* 2013;**78**:734–740.

Patek E, Nilsson L, Johannisson E, Hellema M, Bout J. Scanning Electron Microscopic Study of the Human Fallopian Tube. Report III. The Effect of Midpregnancy and of Various Steroids. *Fertil Steril* 1973;**24**:31–43.

Pepe G, Locati M, Torre S Della, Mornata F, Cignarella A, Maggi A, Vegeto E. The estrogen-macrophage interplay in the homeostasis of the female reproductive tract. *Hum Reprod Update* 2018;**24**:652–672.

Perrone AM, Cerpolini S, Maria Salfi NC, Ceccarelli C, Giorgi LB De, Formelli G, Casadio P, Ghi T, Pelusi G, Pelusi C, *et al.* Effect of Long-Term Testosterone Administration on the Endometrium of Female-to-Male (FtM) Transsexuals. *J Sex Med* 2009;**6**:3193–3200.

Pietro M Di, Pascuali N, Parborell F, Abramovich D. Ovarian angiogenesis in polycystic ovary syndrome. *Reproduction* 2018;**155**:R199–R209.

Rastetter RH, Bernard P, Palmer JS, Chassot A-A, Chen H, Western PS, Ramsay RG, Chaboissier M-C, Wilhelm D. Marker genes identify three somatic cell types in the fetal mouse ovary. *Dev Biol* 2014;**394**:242–252.

Reeves G. Specific Stroma in the Cortex and Medulla of the Ovary. *Obstet Gynecol* 1971;**37**:832–844.

Rensen SSM, Doevendans PAFM, Eys GJJM van. Regulation and characteristics of vascular smooth muscle cell phenotypic diversity. *Netherlands Hear J* 2007;**15**:100–108.

Richards JS, Ren YA, Candelaria N, Adams JE, Rajkovic A. Ovarian Follicular Theca Cell Recruitment, Differentiation, and Impact on Fertility: 2017 Update. *Endocr Rev* 2018;**39**:1–20.

Rios PD, Kniazeva E, Lee HC, Xiao S, Oakes RS, Saito E, Jeruss JS, Shikanov A, Woodruff TK, Shea LD. Retrievable hydrogels for ovarian follicle transplantation and oocyte collection. *Biotechnol Bioeng* 2018;**115**:2075–2086.

Rodgers RJ, Lavranos TC, Wezel IL van, Irving-Rodgers HF. Development of the ovarian follicular epithelium. *Mol Cell Endocrinol* 1999;**151**:171–179.

Rolaki A, Drakakis P, Millingos S, Loutradis D, Makrigiannakis A. Novel trends in follicular development, atresia and corpus luteum regression: A role for apoptosis. *Reprod Biomed Online* 2005;**11**:93–103.

Roo C De, Lierman S, Tilleman K, Peynshaert K, Braeckmans K, Caanen M, Lambalk CB, Weyers S, T'Sjoen G, Cornelissen R, *et al.* Ovarian tissue cryopreservation in female-to-male transgender people: insights into ovarian histology and physiology after prolonged androgen treatment. *Reprod Biomed Online* 2017;**34**:557–566.

Roo C De, Tilleman K, Tsjoen G, Sutter P De. Fertility options in transgender people. *Int Rev Psychiatry* 2016;**28**:112–119.

Rotgers E, Jørgensen A, Yao HH-C. At the crossroads of fate - somatic cell lineage specification in the fetal gonad. *Endocr Rev* 2018;**39**:739–759.

Rowley JE, Amargant F, Zhou LT, Galligos A, Simon LE, Pritchard MT, Duncan FE. Low molecular weight hyaluronan induces an inflammatory response in ovarian stromal cells and impairs gamete development in vitro. *Int J Mol Sci* 2020;**21**:1036.

Russo L, Woolmough E, Heatley MK. Structural and cell surface antigen expression in the rete ovarii and epoophoron differs from that in the Fallopian tube and in endometriosis. *Histopathology* 2000;**37**:64–69.

Salvetti NR, Gimeno EJ, Canal AM, Lorente JA, Ortega HH. Histochemical Study of the Extracellular Matrix Components in the Follicular Wall of Induced Polycystic Ovaries. *Braz J morphol Sci* 2003;**20**:93–100.

Schmidt J, Weijdegård B, Mikkelsen AL, Lindenberg S, Nilsson L, Brännström M. Differential expression of inflammation-related genes in the ovarian stroma and granulosa cells of PCOS women. *Mol Hum Reprod* 2014;**20**:49–58.

Scott JE, Carlsson IB, Bavister BD, Hovatta O. Human ovarian tissue cultures: extracellular matrix composition, coating density and tissue dimensions. *Reprod Biomed Online* 2004;**9**:287–293.

Shi D, Vine DF. Animal models of polycystic ovary syndrome: a focused review of rodent models in relationship to clinical phenotypes and cardiometabolic risk. *Fertil Steril* 2012;**98**:185–193.

Singh K, Sung CJ, Lawrence WD, Quddus MR. Testosterone-induced "Virilization" of Mesonephric Duct Remnants and Cervical Squamous Epithelium in Female-to-Male Transgenders: A Report of 3 Cases. *Int J Gynecol Pathol* 2017;**36**:328–333.

Siu MKY, Cheng CY. The blood-follicle barrier (BFB) in disease and in ovarian function. *Adv Exp Med Biol* 2012;**763**:186–192.

Smith P, Wilhelm D, Rodgers RJ. Development of mammalian ovary. *J Endocrinol* 2014a;**221**:R145–R161.

Smith RM, Shikanov A, Kniazeva E, Ramadurai D, Woodruff TK, Shea LD. Fibrin-mediated delivery of an ovarian follicle pool in a mouse model of infertility. *Tissue Eng - Part A* 2014b;**20**:3021–3030.

Soares M, Sahrari K, Chiti MC, Amorim CA, Ambroise J, Donnez J, Dolmans MM. The best source of isolated stromal cells for the artificial ovary: medulla or cortex, cryopreserved or fresh? *Hum Reprod* 2015;**30**:1589–1598.

Sousa Resende S de, Kussumoto VH, Arima FHC, Krul PC, Rodovalho NCM, Jesus Sampaio MR de, Alves MM. A transgender man, a cisgender woman, and assisted reproductive technologies: A Brazilian case report. *J Bras Reprod Assist* 2020;**24**:513–516.

Spinder T, Spijkstra JJ, Tweel JG van den, Burger CW, Kessel H van, Hompes PGA, Gooren LJG. The Effects of Long Term Testosterone Administration on Pulsatile Luteinizing Hormone Secretion and on Ovarian Histology in Eugonadal Female to Male Transsexual Subjects. *J Clin Endocrinol Metab* 1989;**69**:151–157.

Stévant I, Kühne F, Greenfield A, Chaboissier MC, Dermitzakis ET, Nef S. Dissecting Cell Lineage Specification and Sex Fate Determination in Gonadal Somatic Cells Using Single-Cell Transcriptomics. *Cell Rep* 2019;**26**:3272-3283.e3.

Stroumsa D, Roberts EF, Kinnear H, Harris LH. The Power and Limits of Classification – A 32-Year-Old Man with Abdominal Pain. *N Engl J Med* 2019;**380**:1885–1888.

Sun L-F, Yang Y-L, Xiao T-X, Li M-X, Zhang J V. Removal of DHT can relieve polycystic ovarian but not metabolic abnormalities in DHT-induced hyperandrogenism in mice. *Reprod Fertil Dev* 2019;**31**:1597–1606.

Suzuki T, Sasano H, Takaya R, Fukaya T, Yajima A, Date F, Nagura H. Leukocytes in normal-cycling human ovaries: immunohistochemical distribution and characterization. *Hum Reprod* 1998;**13**:2186–2191.

Svingen T, François M, Wilhelm D, Koopman P. Three-Dimensional Imaging of Prox1-EGFP Transgenic Mouse Gonads Reveals Divergent Modes of Lymphangiogenesis in the Testis and Ovary. *PLoS One* 2012;**7**:e52620.

T'Sjoen G, Arcelus J, Gooren L, Klink DT, Tangpricha V. Endocrinology of Transgender Medicine. *Endocr Rev* 2019;**40**:97–117.

Tack LJW, Craen M, Dhondt K, Bossche H Vanden, Laridaen J, Cools M. Consecutive lynestrenol and cross-sex hormone treatment in biological female adolescents with gender dysphoria: a retrospective analysis. *Biol Sex Differ* 2016;**7**:14.

Taipale J, Keski-Oja J. Growth factors in the extracellular matrix. *FASEB J* 1997;**11**:51–59.

Takamoto N, Kurihara I, Lee K, DeMayo FJ, Tsai MJ, Tsai SY. Haploinsufficiency of chicken ovalbumin upstream promoter transcription factor II in female reproduction. *Mol Endocrinol* 2005;**19**:2299–2308.

Taub RL, Ellis SA, Neal-Perry G, Magaret AS, Prager SW, Micks EA. The effect of testosterone on ovulatory function in transmasculine individuals. *Am J Obstet Gynecol* 2020;**223**:229.e1-229.e8.

The Rotterdam ESHRE/ASRM-Sponsored PCOS consensus workshop group. Revised 2003 consensus on diagnostic criteria and long-term health risks related to polycystic ovary syndrome (PCOS). *Hum Reprod* 2004;**19**:41–47.

Theocharis AD, Skandalis SS, Gialeli C, Karamanos NK. Extracellular matrix structure. *Adv Drug Deliv Rev* 2016;**97**:4–27.

Tian Y, Shen W, Lai Z, Shi L, Yang S, Ding T, Wang S, Luo A. Isolation and identification of ovarian theca-interstitial cells and granulose cells of immature female mice. *Cell Biol Int* 2015;**39**:584–590.

Tingen CM, Kiesewetter SE, Jozefik J, Thomas C, Tagler D, Shea L, Woodruff TK. A macrophage and theca cell-enriched stromal cell population influences growth and survival of immature murine follicles in vitro. *Reproduction* 2011;**141**:809–820.

Turner EC, Hughes J, Wilson H, Clay M, Mylonas KJ, Kipari T, Duncan WC, Fraser HM. Conditional ablation of macrophages disrupts ovarian vasculature. *Reproduction* 2011;**141**:821–831.

Uchida S. Sympathetic regulation of estradiol secretion from the ovary. *Auton Neurosci Basic Clin* 2015;**187**:27–35.

Wagner M, Yoshihara M, Douagi I, Damdimopoulos A, Panula S, Petropoulos S, Lu H, Pettersson K, Palm K, Katayama S, *et al.* Single-cell analysis of human ovarian cortex identifies distinct cell populations but no oogonial stem cells. *Nat Commun* 2020;**11**:1–15.

Walters KA. Role of androgens in normal and pathological ovarian function. *Reproduction* 2015;**149**:R193–R218.

Walters KA, Allan CM, Handelsman DJ. Rodent Models for Human Polycystic Ovary Syndrome. *Biol Reprod* 2012;**86**:1–12.

Walters KA, Paris VR, Aflatounian A, Handelsman DJ. Androgens and ovarian function: translation from basic discovery research to clinical impact. *J Endocrinol* 2019;**242**:R23–R50.

Wang S, Zheng Y, Li J, Yu Y, Zhang W, Song M, Liu Z, Min Z, Hu H, Jing Y, *et al.* Single-Cell Transcriptomic Atlas of Primate Ovarian Aging. *Cell* 2020;**180**:585-600.e19.

Wenzel JGW, Odend'hal S. The mammalian rete ovarii: a literature review. *Cornell Vet* 1985;**75**:411–425.

West-Farrell ER, Xu M, Gomberg MA, Chow YH, Woodruff TK, Shea LD. The Mouse Follicle Microenvironment Regulates Antrum Formation and Steroid Production: Alterations in Gene Expression Profiles1. *Biol Reprod* 2009;**80**:432–439.

West ER, Xu M, Woodruff TK, Shea LD. Physical properties of alginate hydrogels and their effects on in vitro follicle development. *Biomaterials* 2007;**28**:4439–4448.

Wierckx K, Caenegem E Van, Pennings G, Elaut E, Dedecker D, Peer F Van de, Weyers S, Sutter P De, T'Sjoen G. Reproductive wish in transsexual men. *Hum Reprod* 2012;**27**:483–487.

Wierckx K, Caenegem E Van, Schreiner T, Haraldsen I, Fisher A, Toye K, Kaufman JM, T'Sjoen G. Cross-Sex Hormone Therapy in Trans Persons is Safe and Effective at Short-Time Follow-Up: Results from the European Network for the Investigation of Gender Incongruence. *J Sex Med* 2014;**11**:1999–2011.

Wilson BDM, Meyer IH. *Nonbinary LGBTQ Adults in the United States* [Internet]. *Williams Inst* [Internet] 2021; Los Angeles, CAAvailable from: https://williamsinstitute.law.ucla.edu/wp-content/uploads/Nonbinary-LGBTQ-Adults-Jun-2021.pdf.

Wingett SW, Andrews S. FastQ Screen: A tool for multi-genome mapping and quality control. *F1000Research* 2018;**7**:1338.

Wolf CJ, Hotchkiss A, Ostby JS, LeBlanc GA, Gray Jr. LE. Effects of Prenatal Testosterone Propionate on the Sexual Development of Male and Female Rats: A Dose-Response Study. *Toxicol Sci* 2002;**65**:71–86.

Wu C, Xu B, Li X, Ma W, Zhang P, Chen X, Wu J. Tracing and Characterizing the Development of Transplanted Female Germline Stem Cells In Vivo. *Mol Ther* 2017;**25**:1408–1419.

Wu R, Fujii S, Ryan NK, Hoek KH Van der, Jasper MJ, Sini I, Robertson SA, Robker RL, Norman RJ. Ovarian leukocyte distribution and cytokine/chemokine mRNA expression in follicular fluid cells in women with polycystic ovary syndrome. *Hum Reprod* 2007;**22**:527–535.

Wu R, Hoek KH Van der, Ryan NK, Norman RJ, Robker RL. Macrophage contributions to ovarian function. *Hum Reprod Update* 2004;**10**:119–133.

Xu J, Zheng T, Hong W, Ye H, Hu C, Zheng Y. Mechanism for the Decision of Ovarian Surface Epithelial Stem Cells to Undergo Neo-Oogenesis or Ovarian Tumorigenesis. *Cell Physiol Biochem* 2018;**50**:214–232.

Yaish I, Tordjman K, Amir H, Malinger G, Salemnick Y, Shefer G, Serebro M, Azem F, Golani N, Sofer Y, *et al.* Functional ovarian reserve in transgender men receiving testosterone therapy: evidence for preserved anti-Müllerian hormone and antral follicle count under prolonged treatment. *Hum Reprod* 2021;**36**:2753–2760.

Yang M, Li J, An Y, Zhang S. Effects of androgen on immunohistochemical localization of androgen receptor and Connexin 43 in mouse ovary. *Tissue Cell* 2015;**47**:526–532.

Young B, O'Dowd G, Woodford P. *Cell structure and function*. In Hall A, editor. *Wheater's Funct Histol A Text Colour Atlas* 2014; Churchill Livingstone: Philadephia.

Young JM, McNeilly AS. Theca: the forgotten cell of the ovarian follicle. *Reproduction* 2010;**140**:489–504.

Younis JS, Jadaon JE, Haddad S, Izhaki I, Ben-Ami M. Prospective evaluation of basal stromal Doppler studies in women with good ovarian reserve and infertility undergoing in vitro fertilization-embryo transfer treatment: patients with polycystic ovary syndrome versus ovulatory patients. *Fertil Steril* 2011;**95**:1754–1758.

Zarate-Garcia L, Lane SIR, Merriman JA, Jones KT. FACS-sorted putative oogonial stem cells

from the ovary are neither DDX4-positive nor germ cells. *Sci Rep* 2016;**6**:27991.

Zhang H, Zheng W, Shen Y, Adhikari D, Ueno H, Liu K. Experimental evidence showing that no mitotically active female germline progenitors exist in postnatal mouse ovaries. *Proc Natl Acad Sci U S A* 2012;**109**:12580–12585.

Zhang Y, Yan Z, Qin Q, Nisenblat V, Chang HM, Yu Y, Wang T, Lu C, Yang M, Yang S, *et al.* Transcriptome Landscape of Human Folliculogenesis Reveals Oocyte and Granulosa Cell Interactions. *Mol Cell* 2018;**72**:1021-1034.e4.

Zhang Z, Schlamp F, Huang L, Clark H, Brayboy L. Inflammaging is associated with shifted macrophage ontogeny and polarization in the aging mouse ovary. *Reproduction* 2020;**159**:325–337.